

CHALMERS



Evaluation of transcutaneous Bone Conduction Implant with a capsuled transducer

-Full scale investigation on skull simulator, dry skull and cadaver heads

Master of Science Thesis

Johannes Adler
John Gabrielsson

Department of Signals and System
Division of Biomedical Engineering
CHALMERS UNIVERSITY OF TECHNOLOGY
Göteborg, Sweden, 2009
Report No. EX018/2009

Abstract

People suffering from conductive or mixed hearing loss cannot benefit from traditional air conducted hearing aids. For these patients, bone anchored hearing aids becomes an important rehabilitation alternative. Conventional bone anchored hearing aids, BAHA, has been available in clinical practice for a long time, but still, this is not an area without need for improvements. Complications have been reported, mainly originating from the percutaneous anchoring of the transducer, implying permanent perforation of the skin.

A new type of bone conducted hearing aid has been proposed as an alternative to the percutaneous BAHA. Utilizing a modified BEST transducer incorporated into a housing, the so-called C-BEST becomes an implantable transcutaneous alternative to the conventional bone anchored hearing aids. The C-BEST transducer is implanted into a recess in the temporal bone simply by applying pressure. By combining the implantation of the transducer with an inductive electromagnetic energy transfer across the skin, the possibility of a transcutaneous solution is given. The transcutaneous solution leaves the skin intact, hence reducing the risk of complications.

The aim of this Master Thesis is to investigate the possibility to abandon the traditional titanium screw anchoring of bone conduction transducers in favor for a flat bottom design, intended for implantation in the temporal bone. To evaluate the C-BEST, three reference transducers have been used, the BEST90, the BAHA Classic 300 and the BAHA Intenso. Measurements have been conducted utilizing a skull simulator and a dry skull, performed in a laboratory environment. Also a cadaver head investigation was performed, involving measurements conducted on three subjects in total.

The results from the skull simulator measurements show an improved output force response for the C-BEST compared to its previous design, the BEST90. The ipsilateral frequency responses from the cadaver investigation, from acoustical stimulation, show a 5 – 10 dB increase in promontory acceleration response, between 600 and 7000 Hz, in favor for the C-BEST compared to the BAHA Classic 300. The same comparison to the BAHA Intenso does also indicate a 0-5 dB increase in ipsilateral promontory acceleration response. It is also apparent that by anchoring the transducer closer to the cochlea, the sensitivity to anti resonances in the skull, as well as the variation in frequency response among patients, is reduced. However, the contralateral response is significantly lower for the C-BEST compared to both the BAHA Classic and the BAHA Intenso.

Acknowledgements

First and foremost we would like to thank our supervisor Professor Bo Håkansson for giving us the opportunity to do this Master thesis as well as the good support and feedback. Further we would like to thank Måns Eeg Olofsson for his participation during the cadaver head measurements at Sahlgrenska University Hospital. Finally we would like to give a special thanks to Hamidreza Taghavi, Sabine Reinfeldt and Per Östli for helpful advices and participation during the cadaver investigations.

Table of contents

1	INTRODUCTION	1
1.1	BACKGROUND	2
1.2	OBJECTIVE.....	3
2	THEORY	4
2.1	HEARING PHYSIOLOGY	4
2.1.1	<i>Air conducted hearing</i>	4
2.1.2	<i>Bone conduction</i>	6
2.2	BINAURAL AND BILATERAL HEARING	6
2.3	BONE CONDUCTION TRANSDUCERS.....	7
2.3.1	<i>The BEST transducers</i>	7
2.3.2	<i>MED-EL inductive link</i>	9
2.3.3	<i>BAHA Classic 300 and BAHA Intenso</i>	10
3	EQUIPMENT	12
3.1	AGILENT FFT DYNAMIC SIGNAL ANALYZER	12
3.2	AGILENT 82357A GPIB/USB INTERFACE	13
3.3	SKULL SIMULATOR	13
3.4	POLYTEC HLV-1000 LASER DOPPLER VIBROMETER.....	14
3.5	CONDENSER MICROPHONE AND FILTER.....	14
3.6	DRY SKULL.....	16
4	METHOD	17
4.1	SKULL SIMULATOR MEASUREMENTS.....	17
4.1.1	<i>Electrical impedance</i>	18
4.1.2	<i>Frequency response</i>	19
4.2	DRY SKULL SURGERY	19
4.3	DRY SKULL MEASUREMENTS	21
4.3.1	<i>Acceleration from electrical stimulation</i>	21
4.3.2	<i>Acceleration from acoustical stimulation</i>	22
4.3.3	<i>High-pass filtering and amplification</i>	24
4.4	CADAVER HEAD MEASUREMENTS	25
5	RESULTS	28
5.1	ELECTRICAL IMPEDANCE MEASUREMENTS	28
5.2	FREQUENCY RESPONSE FUNCTIONS.....	31
5.2.1	<i>Voltage to force frequency response from Skull simulator</i>	31
5.2.2	<i>Acceleration on dry skull</i>	32
5.2.3	<i>Cadaver head investigation</i>	41
6	DISCUSSION	68
6.1	ELECTRICAL IMPEDANCE MEASUREMENTS	68
6.2	FORCE OUTPUT FROM SKULL SIMULATOR.....	68
6.3	FREQUENCY RESPONSE FROM ELECTRICAL STIMULATION ON DRY SKULL.....	70
6.4	FREQUENCY RESPONSE FROM ACOUSTICAL STIMULATION ON DRY SKULL	71
6.5	FREQUENCY RESPONSE FROM ELECTRICAL STIMULATION ON CADAVER	73
6.6	FREQUENCY RESPONSE FROM ACOUSTICAL STIMULATION ON CADAVER	75
7	CONCLUSION	80
8	REFERENCES	81
	APPENDIX A	83
	APPENDIX A	83
8.1	DATA ACQUISITION USING LABVIEW	83
9	APPENDIX B	88

1 Introduction

Hearing, or to perceive sound, is the ability to transduce vibrations of the cochlea, the auditory portion of the inner ear, into nerve impulses transmitted to the brain to be interpreted as sound. The cochlea vibrations can origin from two different mechanisms, air conducted and bone conducted stimulation of the cochlea. Traditional external hearing aids utilize amplification and modulation of sound to increase this stimulation, but in some cases a better way to improve a patient's hearing is by the use of implantable hearing devices, such as middle air implants or bone conducted hearing aids.

Middle ear implants work by having a sound processor picking up the sound, transferring it across the skin electromagnetically to an implanted receiver. The receiver transmits a signal to a floating mass transducer stimulating the ossicles, the middle ear bones. Both traditional external hearing aids and middle ear implants are classified as air conducted hearing aids. However, for patients suffering from a diseased middle ear, the use of air conducted hearing aids are no longer applicable. By utilizing the mechanism of cochlea stimulation rising from vibrations of the skull bone, patients with a damaged middle ear or damaged or absent ear canals, can instead benefit from bone conduction hearing aids.

Today's bone conduction hearing aids are either entirely external devices, contacting the mastoid area behind the ear using a steal-spring headband to induce vibrations in the skull bone, or as in the case of the Bone Anchored Hearing Aid (BAHA) where the transducer is attached to the skull bone percutaneously using a titanium screw, permanently perforating the skin. The latter implies the risk of certain complications, such as the risk of inflammation in the vicinity of the screw. The bone anchored hearing aids on the other hand has an advantage over the middle ear implants regarding the process of surgically implanting the aid. The surgery involved with middle ear implants is both complicated and expensive and involves a risk of damaging the facial nerve.

A combination of the two techniques, utilizing the electromagnetic energy transfer across the skin applied in the middle ear implants, with bone conducted stimulation of the cochlea associated the bone anchored hearing aids, would possibly result in a system benefiting from the separate advantages of both systems. A possible solution can be seen in Figure 1.

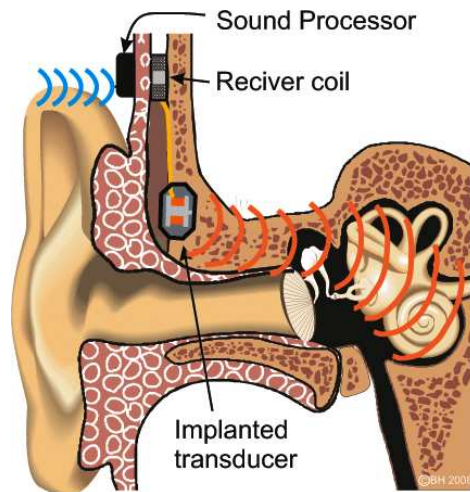


Figure 1: Illustration showing the transcutaneous BCI system with the implanted C-BEST transducer.

1.1 Background

The use of bone conduction hearing aids has increased over the past decades. However, this is not an area without need for improvements. The conventional bone conduction transducers still suffer from for example relatively poor performance at low frequencies. Hence, a new type of transducer, the Balanced Electromagnetic Separation Transducer (BEST) has been developed, with improved performance in terms of frequency response and total harmonic distortion compared to conventional transducers. Also the size of the BEST transducer could be decreased, making it suitable for future implantation of the device.

Several studies have been made covering sub tasks on the way to eventually determine the design for the first implantable bone anchored hearing aid. From earlier investigations, the technique to combine the BEST transducer, intended for bone conducted stimulation of the cochlea, with the inductive energy transfer link used in middle ear implants, by MED-EL Vibrant Soundbridge, has shown promising results. During these earlier studies, the evaluation was based on a provisional solution using a naked BEST transducer anchored to the temporal bone using the titanium screw snap coupling used in the BAHA system, making it a transcutaneous solution, but still not well suited for implantation. For this thesis, the BEST transducer design was slightly modified for further improvement and also incorporated into a housing. The idea is now to anchor the C-BEST transducer to the temporal bone simply by applying pressure, with no need for titanium implants.

1.2 Objective

The aim of this master thesis is to conduct a full scale investigation of a newly developed bone conduction transducer, the C-BEST, intended for implantation in osseous tissue. The investigation aims to evaluate the possibility of abandoning the traditional percutaneous anchoring of bone conduction transducers, using an ossiintegrated titanium screw, in favour for an implantable alternative allowing the possibility of a transcutaneous solution.

2 Theory

The underlying principles for the development of bone conducting hearing aids are essentially based on the theory of the human hearing. Sound can be perceived in two different ways, by air conducted- or bone conducted hearing. In this section the physiology of the human hearing is described as well as a technical description of the transducers used in the evaluation process. The following section, 2.1, is a summary of Reinfeldt S. thesis “Bone conducted soundtransmission for communication systems” [1].

2.1 Hearing physiology

To understand the basic concepts motivating bone conducted hearing aids, a fundamental understanding of the human hearing is essential. As mentioned earlier, sound can be perceived both by air conducted and bone conducted hearing. Figure 2 below illustrates the different conduction paths involved with these two concepts.

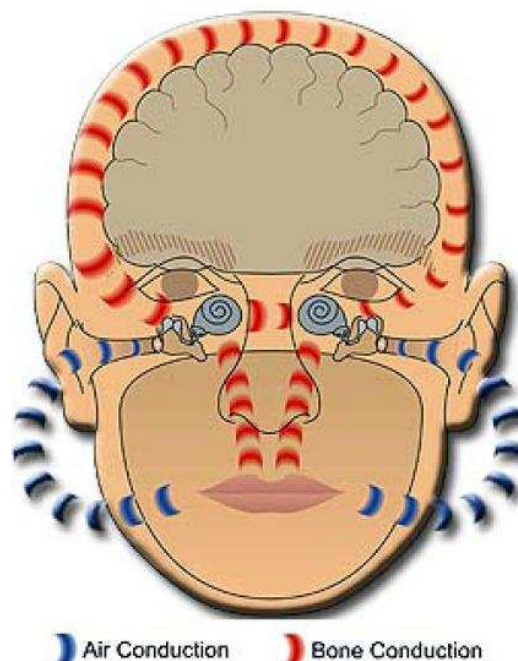


Figure 2: Sound conduction paths for air conducted- and bone conducted hearing.

2.1.1 Air conducted hearing

Air conducted (ac) hearing involves sound being captured by the ears and further conducted through the auditory canal to reach the cochlea. For easier understanding of the physiology behind ac hearing, the ear is considered as three parts; the outer-, middle- and inner ear. The outer ear consists of the pinna and the ear canal with the main function to enhance high

frequency sounds and to determine the direction of its source. The anatomy of the human ear is illustrated in Figure 3. At the end of the ear canal, at the border between the outer and the middle ear, the tympanic membrane is found with the purpose to transform sound energy into vibrations.

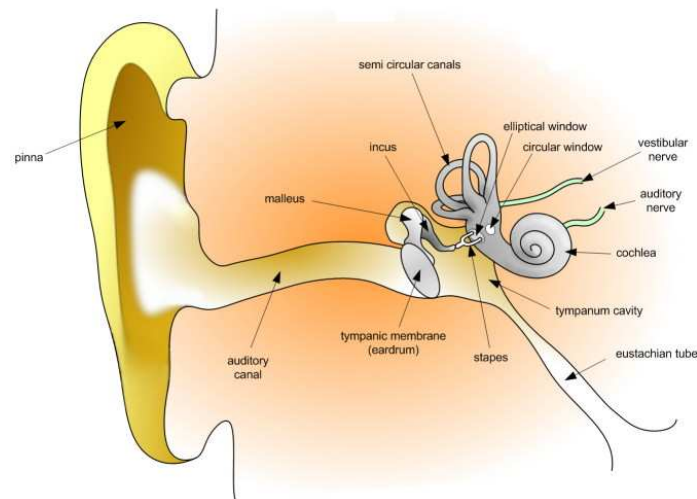


Figure 3: Illustration of the human ear showing the outer-, middle- and inner ear.

The vibrations are transferred to the three joined ossicles located in the middle ear, the malleus, the incus and the stapes. These bones connect the middle ear to the inner ear with the malleus contacting the tympanic membrane and the stapes contacting the oval window located in the inner ear. The ossicles are attached with several ligaments and two muscle tendons, the tensor tympani and the stapedius muscle. By contracting the stapedius muscle, the middle ear work as a damping function for incoming vibrations. In the case of loud sound exposure, the middle ear will damp the incoming sound with about 10 dB before transmitting the vibrations to the sensitive inner ear. Another important purpose of the middle ear is to act as a sound transformer, transforming the air conducted sound into fluid wave vibrations in the cochlea. Absence of this connection would result in loss of sound energy corresponding to approximately 25 dB. A malfunctioned middle ear outrules the possibility of improved hearing from middle ear implants and is one of the main reasons motivating bone conducted hearing aids.

The third part of the ear is the inner ear, containing three fluid filled systems; the cochlea, the semicircular canals and the vestibule; the latter two being contributors to the balance system of the human body. When the stapes attached to the oval window vibrates also, the fluid in the cochlea is set into motion and then the auditory sensory cells in the organ of corti, located in the basilar membrane are excited. The wave length of the vibrations depends on the frequency of the incoming sound and determines where along the basilar membrane the cochlea is stimulated. For low frequency sounds, the wave is transmitted to the apical end of the cochlea, whereas a higher frequency sound has a shorter traveling distance, near the base of the cochlea. When the auditory sensory cells are stimulated, a generated signal is transmitted to the auditory cortex of the brain to be interpreted as sound.

2.1.2 Bone conduction

Bone conducted (bc) hearing refers to sound perception rising from sound energy transmitted to the cochlea through vibrations in the bones and cavities of the skull. In contrast to ac hearing, bone conducted sound is not transmitted via the ear canal and middle ear to reach the inner ear and finally the cochlea. The fact that sound can be perceived both through ac and bc hearing explains why a sound recording of your own voice seems unfamiliar to how you normally recognize it. While the recording equipment captures only what is here referred to as air conducted sound, the cochlea is also sensitive to the bc transmission part of the own voice i.e. the vibrations propagating from the oral cavity through the skull bone as sound, making the voice on recording appear differently.

Bc sound can be transmitted to the cochlea both by pure bone conduction, but also through what is called body conduction, referring to sound conducted through soft tissue and fluids. Due to the fact that it is difficult to distinguish between these two phenomena, the general definition of bone conducted sound covers both of them.

2.2 Binaural and bilateral hearing

Binaural hearing is often referred to the ability to localize the origin of sounds. This function relies on the brain's ability to compare information from two separate auditory inputs, the ears. For patients suffering from a hearing loss in both ears, binaural amplification provides

the most benefit, but requires the left and the right ear independently supply the brain with information.

Bilateral hearing on the other hand, gives amplification of sounds to both ears, hence supplying both ears with the same information. Since the ears are not connected in any way and work independently of each other, bilateral hearing lacks the possibility to distinguish the location of the sound source.

The two concepts can both be applied within the area of hearing aids, and they have both advantages and disadvantages dependent on type of hearing loss [2].

2.3 Bone conduction transducers

In this thesis four transducers have been investigated: the capsuled Balanced Electromagnetic Separation Transducer (C-BEST), the BEST, the transducers in BAHA Classic 300 and the BAHA Intenso. The latter three are used as reference transducers for evaluating the C-BEST. To obtain the transcutaneous energy transfer across the skin when evaluating the BEST transducers acoustically, some components from MEL-EL's middle ear implants are utilized.

2.3.1 The BEST transducers

Two different BEST transducers are used in this thesis, the C-BEST for evaluation purpose and a BEST, used as a reference transducer. The two have the same basic design, but with the C-BEST having a completely new approach in how to transfer vibrations from the transducer to the skull bone. This section describes the basic idea behind the BEST transducers, covering both the BEST and the C-BEST.

The purpose of a bone conduction transducer is to transform electrical signal energy into mechanical vibration energy without loss of information. To achieve this, low distortion is needed. For conventional transducers, of variable reluctance type, low distortion is achieved by having a high static flux, with the consequence of requiring a stiff suspension. A stiffer suspension brings the requirement of using a heavier counterweight to preserve a good low-frequency response. Consequently, to achieve an acceptable distortion level, conventional transducers often suffer from poor low-frequency response.

The basic idea behind the design of the BEST transducers is to eliminate the static forces, enabling the use of softer suspension, hence minimizing the counterweight. This enables a lighter and more compact construction, well suited for implantation purpose. It is achieved by utilizing a construction having four air gaps instead of one, resulting in that the static forces of the upper and lower air gaps counterbalance each other. In Figure 4 the schematic design of the BEST transducer is illustrated.

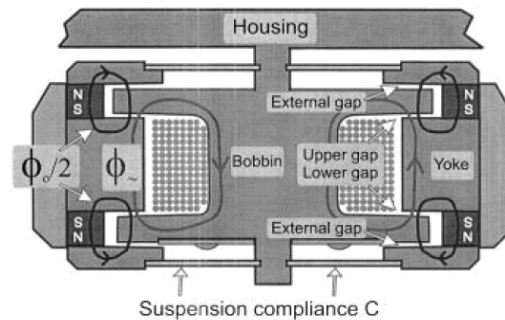


Figure 4: *The schematic design of the BEST transducer.*

The innermost part of the BEST transducer consists of a paramagnetic body with a surrounding coil. This is the part attached to the load, transferring the mechanical vibration energy to the skull bone. The outer part of the transducer contains ferromagnetic material and permanent magnets to create and conduct a constant magnetic flux. This part also serves as a counterweight. The separate parts are connected to each other using four blade springs, with the main purpose to keep the construction in place and to balance the position of the inner part to obtain equal air gaps [3], [4].

By driving a current in the coil, an electromagnetic field is generated. This field interacts with the magnetic field created by the magnets and will give rise to a force vibrating the inner part of the transducer. These vibrations are transferred to the load, i.e. the Skull simulator, the dry skull, the cadaver head or eventually the skull bone of a patient. Depending on which BEST transducer is used, the BEST or the C-BEST, the transferring of the vibrations differs. The BEST transducer is connected to the titanium implant using a snap coupling, whereas the C-BEST transducer is implanted in the skull bone making connection simply by applying pressure to the transducer against a flat surface. The transducers used in this thesis can be seen in Figure 5, [4].

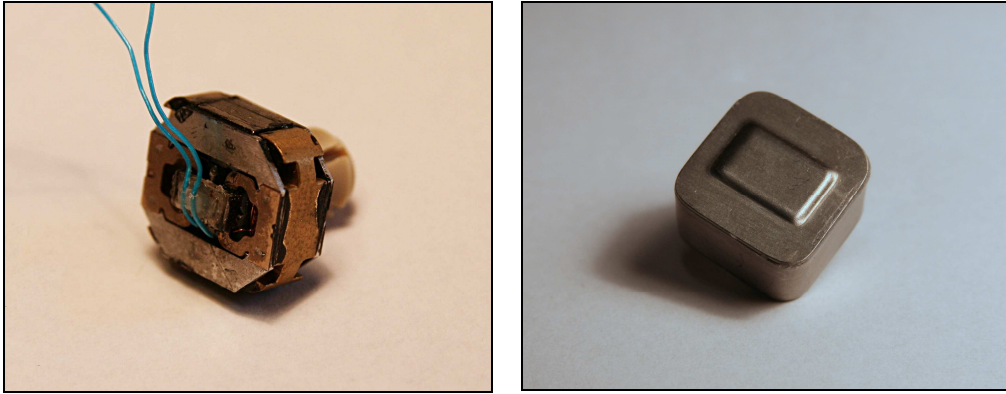


Figure 5: Photos showing both of the BEST transducers, the BEST to the left and the C-BEST to the right.

2.3.2 MED-EL inductive link

To evaluate the BEST transducers acoustically, the inductive energy transfer applied in middle ear implants by MED-EL Vibrant® Soundbridge® is used. The MED-EL system utilizes transcutaneous energy transmission across the skin by use of an inductive link. The complete middle ear implant system from MED-EL consists of one external component called an audio processor, AP, containing a microphone, a sound processing system and an AM-modulator circuit. The internal component of the MED-EL system consists of an implanted coil, a conductor link and a floating mass transducer. By excluding the floating mass transducer from the system, this equipment can be used to drive any electromagnetic transducer, in this case the BEST transducers. One of the setups involving the MED-EL inductive link is shown in Figure 6, in this case driving the BEST transducer.

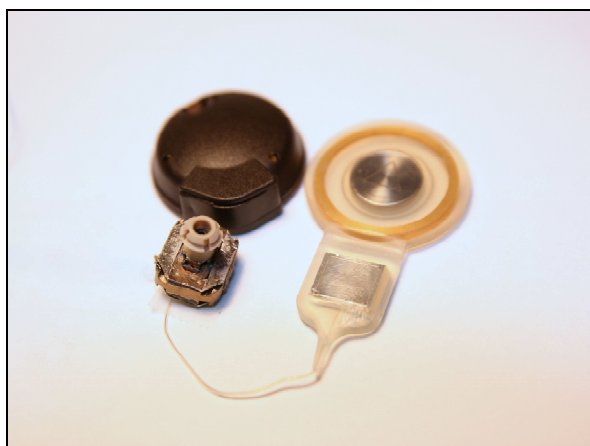


Figure 6: The MED-EL inductive link supplying the BEST transducer. To the upper left the AP, containing the microphone, the sound processing system and the modulator circuit, is shown. To the right the internal coil and the demodulator circuit are shown.

The system works by letting the externally worn receiver, the AP, pick up the sound and transform it into corresponding electrical signals supplying the sound processing system. The sound processing system adapts the signal according to the user's specific requirements in terms of hearing loss and dynamic range. The modulator circuit then modulates the signal of the output of the sound processor, to prevent potential noise and the signal is then transferred across the skin to the internal coil where a demodulator circuit converts it to the appropriate electrical drive signal supplying the transducer, the floating mass transducer or in this case the BEST [5].

2.3.3 BAHA Classic 300 and BAHA Intenso

To compare the performance of the C-BEST which is combined with the MED-EL driving circuit, referred to as the Bone Conducted Implant (BCI), with products already existing on the market, the BAHA Classic 300 and the BAHA Intenso were chosen as reference devices, see Figure 7. The new BAHA Intenso is the most powerful among the devices in the BAHA family and has some additional features compared to its foregoer, the BAHA Classic 300. One of them is the Automatic Gain Control Output compression, AGCO, a circuit designed to limit sound distortions. This circuit has a “dual time-constant system” to improve the sound quality in loud environments.



Figure 7: Photos of the both reference BAHA devices, the BAHA Classic 300 to the left and the BAHA Intenso to the right.

Both of these BAHA models consist of a microphone, an amplifier and a transducer encapsulated into an external housing. The microphone picks up sounds from its surroundings. The resulting signal is amplified before transmitted to the transducer, inducing vibrations in the skull bone. The vibrations are transferred to the skull bone via an abutment

connecting the hearing aid to an implanted titanium screw, fixated in the parietal bone behind the ear, see Figure 8. The titanium implant is integrated into the living bone tissue of the skull through the process of osseointegration [6], [7].

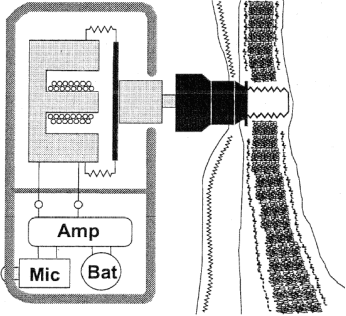


Figure 8: Schematic figure showing the basic construction of the BAHA systems, from the microphone to the titanium screw attachment the skull bone.

3 Equipment

In this study, a set of equipment has been used to be able to evaluate the different devices of the BEST transducer. In this section a description of the most important equipment is presented.

3.1 Agilent FFT Dynamic Signal Analyzer

The Agilent 35670A is a 2 to 4-Channel FFT Dynamic Signal Analyzer, and is the main component in the signal analysis process of the evaluated devices in this thesis. An image of this device can be seen in Figure 9. The instrument is used not only for measurement of signals, but it also acts as a signal generator. The Agilent 35670A was used in two different modes, FFT- and Swept-sine mode.

The FFT mode presents an almost instant frequency analysis of the desired measuring setup using the Fast Fourier Transform. This mode has the advantage of being fast, but has few possibilities to control the instrument's excitation signal. Therefore, this mode is only applicable for measurements with no demands on keeping a constant signal level at one of the input channel. For these measurements, e.g. measurements requiring a constant sound pressure level, instead the Swept-sine mode is used allowing more control over the instrument's source level [8].



Figure 9: The Agilent 35670A FFT Dynamic Signal Analyser.

3.2 Agilent 82357A GPIB/USB Interface

Due to that that the Agilent 35670A in its standard set-up handles data transfer between instrument and computer using a floppy drive, a subtask for this thesis was to implement the possibility of easier measurement data transfer using the instrument's available GPIB connection. Using a GPIB/USB interface, in this case the Agilent 82357A data cable, the Agilent 35670A can be connected directly to the computer, but there is no available software handling the actual transfer of measured data. For this purpose Labview was used to develop an application handling the communication. The programming structure and a description of the Labview application can be found in Appendix [9].

3.3 Skull simulator

The Skull simulator TU-1000, see Figure 10, is used to mimic the load characteristics of the human skull. Its dynamic behavior can be looked upon as a rigid mass body with a weight about 10 times higher than the counterweight of the transducer. The output signal from the Skull simulator is proportional to the force output generated by the transducer under test, obtained by measuring the motions of mass body using an accelerometer. The force is converted into a voltage, which can be measured with the Agilent Signal Analyzer. The output force level can be measured with high reliability in the frequency range within 100Hz to 10kHz [11].



Figure 10: The TU-1000 Skull simulator to the left and its power supply to the right.

3.4 Polytec HVL-1000 Laser Doppler Vibrometer

The Polytec HVL-1000 Laser Doppler Vibrometer is used to measure skull vibrations induced by a vibrating transducer. This instrument is specifically designed for use in hearing studies and the principle of the measuring technique is based on the Doppler effect. By directing the laser beam at a spot on the skull and measure the shift in frequency between the transmitted and the reflected beam, the velocity of the skull vibrations can be calculated. The frequency shift is known as the Doppler shift and is proportional to the velocity of the skull vibrations. At the measuring point of interest, a reflector is placed in order to get a sufficient reflecting beam and a high signal to noise ratio. The output from the Laser Doppler Vibrometer is a voltage proportional to the velocity of the skull vibrations, which is measured by the Agilent Signal Analyzer [4].



Figure 11: The Polytec HVL-1000 Laser Doppler Vibrometer.

3.5 Condenser microphone and filter

To be able to measure the frequency response at a constant sound pressure level, SPL, a condenser microphone, Brüel & Kjær Type 4134, was used, shown in Figure 12. By calibrating the equipment, measuring the voltage level for a reference SPL, 94dB at 1000 Hz, a relation between voltage and SPL is obtained. This relation is used to calculate the voltage levels corresponding to a set of predetermined SPL levels.



Figure 12: *The condenser microphone and its power supply.*

A condenser microphone requires a certain DC-voltage level applied over the capacitor to bias the plates with a fixed charge, Q . The distance between the capacitor plates slightly changes when exposed to sound vibrations, thus affecting the capacitance inversely proportional to the separation distance. Due to that the charge is kept constant while the capacitance varies, the voltage over the capacitor will fluctuate around the bias DC-voltage level according to Eq.(1) [10].

$$C = Q \cdot V \tag{1}$$

When measuring the voltage level from the microphone, it is desirable to remove the bias DC-component. Also the Agilent sets constraints on the minimum input signal to the instrument, which requires an amplification of the filtered microphone signal. For this purpose the circuit shown in Figure 13 was used, containing an high-pass filter and an operational amplifier, amplifying the signal ten times.

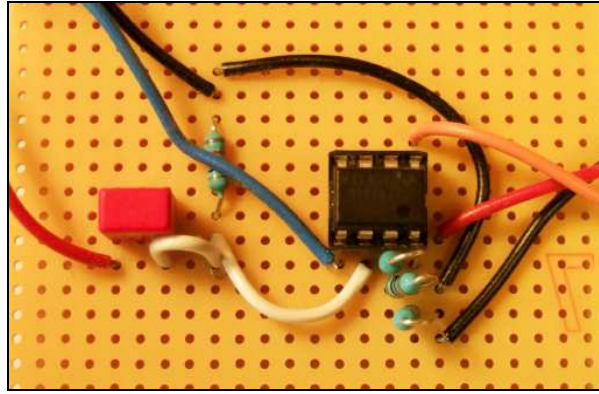


Figure 13: *The amplification and filtering circuit used to remove the condenser microphone's bias DC-component.*

3.6 Dry Skull

For one part of the evaluation process, comparing the new BEST transducer to its previous design as well as comparing it to the BAHA system, an intact dry skull, a cranium, was used. The cranium has been equipped with all the necessary abutments for connection of the different transducer systems. The positions for the different systems can be seen in Figure 14 below. For this thesis one additional location was chosen for the C-BEST transducer. Due to that the C-BEST design requires no titanium abutment, its location is simply a recess in the mastoid portion of the temporal bone corresponding to position B in the leftmost illustration presented in Figure 14.

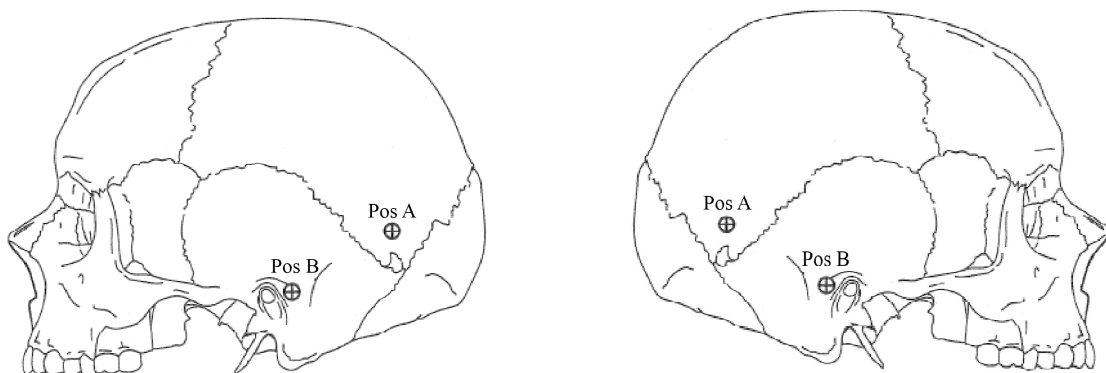


Figure 14: Illustration of the dry skull with its transducer attachment positions. The leftmost picture shows the left side of the skull, where Pos B corresponds to the attachment position for the C-BEST and Pos A is the position for the reference transducer, the BEST or the BAHA. The right side of the skull has no attachment possibility for the C-BEST, only for the reference transducers.

4 Method

The following section describes the methods applied for the evaluation of the transducers. It is divided into three main areas describing the measurement approaches involved with the Skull simulator-, the dry skull- and the cadaver head measurements. These methods account for the data acquisition of the transducers' respective electrical impedance, their force output level and their promontory acceleration levels. In Table 1 below, the settings used for the Agilent data acquisition can be seen.

	Frequency range	Resolution:	Windowing
FFT	100 – 12.6k Hz	400 lines	Hanning
Swept sine	100 – 10k Hz	400 lines	-

Table 1: Agilent settings.

4.1 Skull simulator measurements

The measuring setup involving the Skull simulator is illustrated in Figure 15 below. This setup allows for measurement of all quantities needed for calculation of both the electrical impedance and frequency response to be carried during the same sequence.

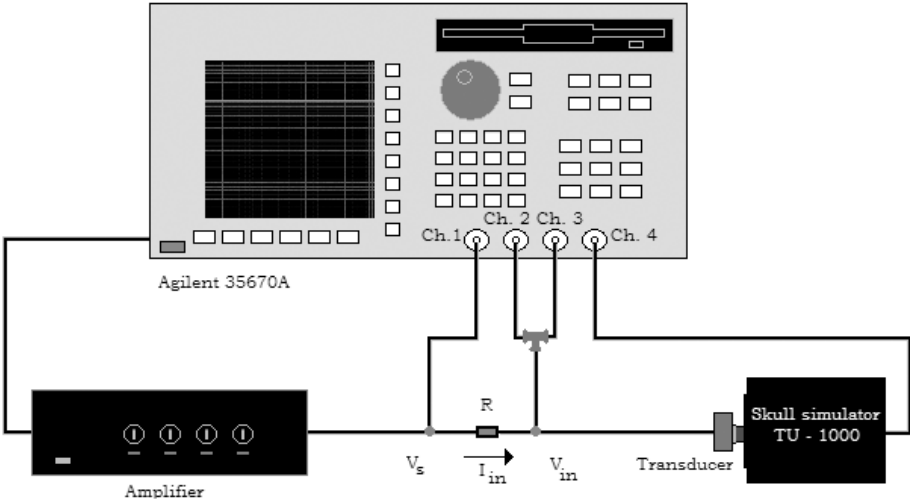


Figure 15: Measurement setup for calculating the transducers' electrical impedance and frequency response using the Skull simulator.

The transducer, mounted on the Skull simulator, is supplied with an amplified excitation signal, generated by the Agilent. The output signal from the Agilent is 50 mV peak-to-peak and the amplification is set to 20 dB. To protect the circuit, and to be able to measure the current, a 10 Ω resistor is connected in series. The amplified source voltage, the voltage supplying the transducer and the force output from the Skull simulator are measured using the Agilent set to FFT mode.

4.1.1 Electrical impedance

The electrical impedance is a complex quantity, in polar form described in Eq.(2).

$$\vec{Z}_{in} = Z_{in} \cdot e^{j\theta} \quad (2)$$

To calculate the electrical impedance, the equivalent circuit diagram, shown in Figure 16, was used. This circuit corresponds to the measuring setup illustrated above, where V_s refers to the source voltage, V_{in} and I_{in} to the voltage and current supplying the transducer and Z_{in} the transducer's electrical impedance.

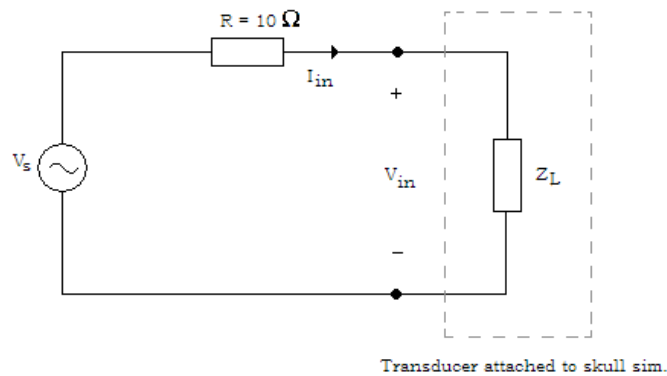


Figure 16: Equivalent circuit for electrical impedance calculations.

Starting from the expression for Ohm's law, Eq.(3), the electrical impedance, Z_{in} , can be calculated according to:

$$V_{in} = Z_{in} \cdot I_{in} \quad (3)$$

I_{in} is obtained by measuring the source- and input-voltage to the transducer, Eq.(4).

$$I_{in} = \frac{V_s - V_{in}}{R} \quad (4)$$

By rearranging the two expressions above, the electrical impedance is calculated using Eq.(5).

$$Z_{in} = \frac{V_{in}}{V_s - V_{in}} \cdot R = \frac{V_{in}/V_s}{1 - V_{in}/V_s} \cdot R \quad (5)$$

4.1.2 Frequency response

Using the same measuring setup as for the electrical impedance measurements, the frequency response can be simultaneously measured using the signal analyzer's two remaining channels.

The frequency response is calculated by dividing the output signal from the Skull simulator, a voltage proportional to the force output generated by the transducer, with the input voltage to the transducer. In order to present the frequency response in terms of output force, a conversion factor k_F has to be applied, converting the measured voltage into force. The expression used for calculating the frequency response is presented in Eq.(6).

$$FR = \frac{F_{skull}}{U_{in}} = k_F \cdot \frac{U_{skull}}{U_{in}} \quad (6)$$

4.2 Dry skull surgery

Since the idea of how to transfer the vibration energy from the C-BEST transducer to the skull bone differs from previous approaches, a minor surgery of the dry skull was needed. Both the BEST and the BAHA system require titanium anchoring of the transducer, whereas the C-BEST has a flat bottom, instead requiring a smooth attachment surface. Hence, a custom recess was drilled in the temporal bone of the dry skull to fit the transducer. The rightmost image in Figure 17 shows the different approaches for the anchoring of the transducers, the titanium snap on coupling used to attach the BEST and the BAHA as well as the recess used for the C-BEST transducer.

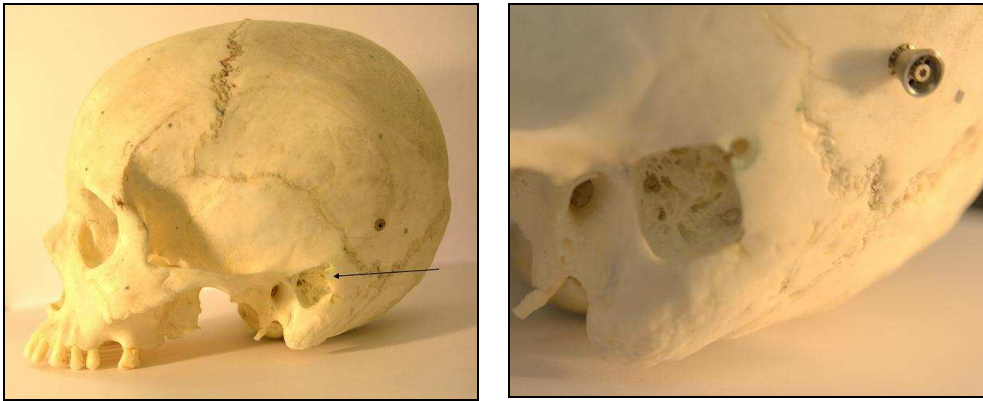


Figure 17: Photo of the dry skull showing the recess made for the C-BEST as well as the titanium screw attachment for the reference transducers.

Since the bottom of the recess was somewhat ruff, bone cement was used assuring the transducer to rest on a flat surface. By using bone cement, a material resembling the characteristics of bone, a flat bed was created, allowing the transducer to be pressed against a flat surface to assure good contact.

The product used for this purpose, Surgical Simplex (Stryker) which consists of two components, one powder part and one liquid part. By mixing the two ingredients, a soft substance is achieved. This soft substance hardens within minutes, to become a material resembling the characteristics of bone. The substance was applied to the bottom of the recess, after which the transducer was aligned. The transducer was fixated using a metal bar, attached using two titanium screws, holding the transducer in place. The resulting attachment of the C-BEST transducer is shown in Figure 18. To separate the transducer from its fixation bar, a small silicone tube is placed between the two metal surfaces.

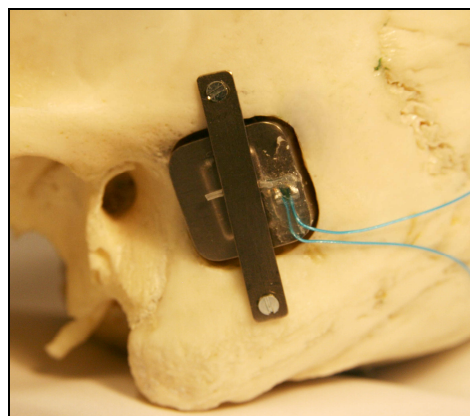


Figure 18: Close-up of the mastoid area of the dry skull with the C-BEST implanted.

4.3 Dry skull measurements

To mimic to the load characteristics of a future patient more realistically than when utilizing the Skull simulator, measurements were also carried out using the dry skull shown in Figure 17. The same cranium has been used in several prior studies, making it possible to compare acquired data with earlier measurements.

The fact that the skull is not perfectly symmetric implies that the conduction of sound through bone vibrations differs between the left and the right side of the skull. Measurements made on one side of the skull can therefore not be compared with the ones carried out on the other side.

Measurements involving the dry skull are carried out for both of the BEST transducers as well as the BAHA transducers. The transducers are both electrically stimulated and also stimulated acoustically by applying a constant sound pressure level. The frequency response is measured both on the right and the left side of the dry skull and both the ipsilateral and contralateral frequency responses are studied. The contralateral frequency response can be especially of significance for patients suffering from single sided deafness, by transferring the captured sound from the deaf side of the skull to the opposite healthy cochlea.

4.3.1 Acceleration from electrical stimulation

The first measuring setup, shown in Figure 19, looks similar to the setup involving the Skull simulator. The difference is that the Skull simulator now has been replaced by the dry skull in combination the laser doppler vibrometer. The transducer under test is mounted on the dry skull and is electrically stimulated using the signal analyzer. The excitation signal is set to 50 mV peak-to-peak. This signal is amplified by 20 dB, giving a decent signal to noise ratio.

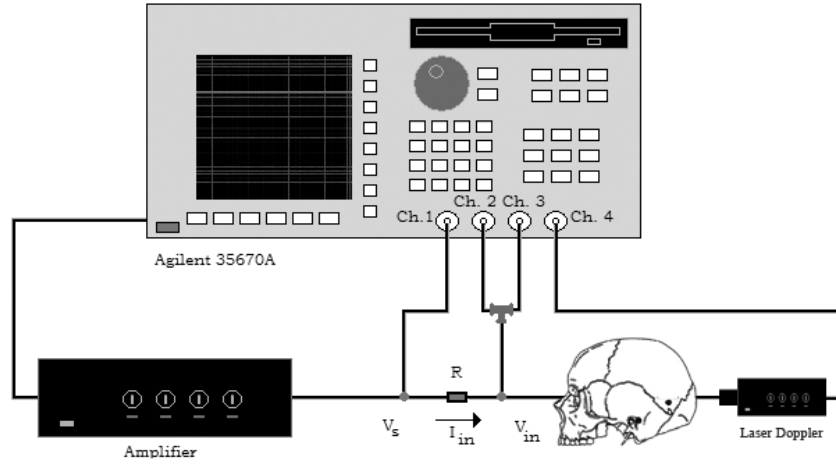


Figure 19: Measurement setup for calculating the transducers' electrical impedance and frequency response using the dry skull and the laser doppler vibrometer.

The laser doppler vibrometer measures the velocity of the vibrations induced at the promontory of the skull. The frequency response is presented as the acceleration (a_{skull}) of the vibrations divided by the voltage, u_{in} , supplying the transducer, see Eq.(7). The electrical impedance is also acquired during these measurements, in the same way as when the Skull simulator was used as load.

$$FR = \frac{a_{skull}}{u_{in}} = \{a_{rms}(j\omega) = j\omega v_{rms}\} = \frac{j\omega v_{rms}}{u_{in}} \quad (7)$$

4.3.2 Acceleration from acoustical stimulation

The acceleration measurements with acoustical stimulation are measured using the full hearing aid systems. Here, both the transducers' and the audio processors are taken into account, completing the procedure to transform captured sound vibration at the microphone into skull vibrations induced by the transducer.

Concerning the reference full devices, the BAHA Classic 300 and the BAHA Intenso are evaluated in their standard design, anchored to their designated position using a titanium snap coupling. When it comes to evaluating the C-BEST transducer an interesting factor is the inductive energy transfer across the skin. For investigating this MED-EL inductive link is used as its driving unit. To mimic the influence of the skin separating the transmitting and receiving coil, a set of silicone plates are used, forming a 5 mm distance between the coils.

Measurements were performed with the C-BEST transducer anchored to position B on the left side of the skull and the BAHA in position A on the same side. Both ipsilateral and contralateral measurements were conducted. Measurements were also carried out with the BEST transducer anchored to both position A and B on the right side of the skull for comparison of the anchoring positions.

All measurements were conducted in a soundproof environment to reduce the influence of acoustic noise. The setup can be seen in Figure 20 below, showing how the dry skull is placed on foam rubber bed to minimize vibrations from the surroundings. Also, the speaker is wired from the ceiling of the room to further minimize disturbances on the measuring system. The acceleration is measured using a laser doppler vibrometer, directed into the ear canal of the cranium, measuring the vibrations at the promontory in the same manner as for the measurements using electrical stimulations. The transducers are stimulated using three different SPL levels, 60, 70, and 90 dB. 60 dB corresponds to the approximate level of normal speech whereas the 90 dB response corresponds to the saturated response of the hearing aid.



Figure 20: Photos showing the laboratory setup used for conducting the acoustical measurements.

In order to keeping the SPL constant at the position of the BCI and BAHA's microphones during the measurements a condenser microphone, connected to the Agilent, is placed close to this position. By measuring the SPL at the condenser microphone, with the Agilent set to Swept sine mode, and specify an alternation tolerance level, the output signal supplying the speaker can be regulated to keep a constant SPL. The tolerance level was set to ± 1 dB, meaning that the SPL is kept within this deviation from the desirable SPL. As stated before, it is desirable to both remove the bias DC-component as well as amplify the signal level from

the condenser microphone. For this purpose the circuit shown in Figure 13 was connected in series with the condenser microphone.

4.3.3 High-pass filtering and amplification

The filter and amplification circuit, shown in Figure 21, has the purpose of removing the bias DC-component from the microphone signal, as well as amplifying the measuring signal supplying the signal analyzer. The circuit consists of a high-pass filter and an operational amplifier.

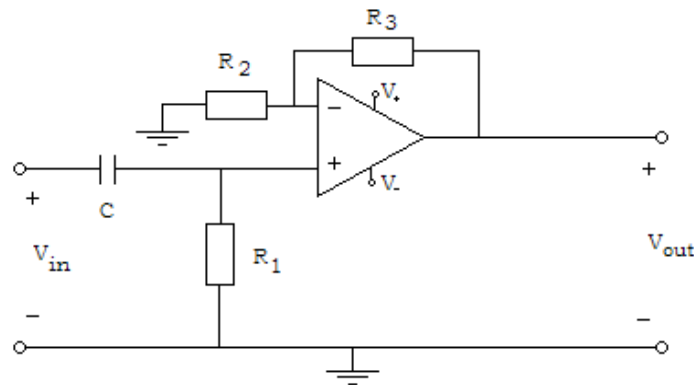


Figure 21: Circuit diagram for the amplification and filtering circuit.

The high-pass filter is designed to remove the DC-component from the microphone signal without interfering with the measurement interval, between 100 Hz-10 kHz. By choosing the resistor R_1 to 10 k Ω and the capacitor C to 0.47 μ F, a cut off frequency of 33.86 Hz is obtained, satisfying this requirement. The cut off frequency is calculated according to Eq.(8).

$$f_{3dB} = \frac{1}{2\pi R_1 C} = \frac{1}{2\pi \cdot (1 \cdot 10^4) \cdot (0.47 \cdot 10^{-6})} = 33.86 \text{ Hz} \quad (8)$$

The circuit's total gain is calculated using node analysis, resulting in Eq.(9). To obtain a total amplification of approximately 10 times within the measuring interval of interest, appropriate values for R_2 and R_3 are chosen.

$$\left| \frac{U_{out}}{U_{in}} \right| = \left| \frac{j\omega R_1 C (R_2 + R_3)}{R_2 \cdot (1 + j\omega R_1 C)} \right| \quad (9)$$

By selecting R_2 to 11 k Ω and R_3 to 100 k Ω , the amplification for high frequencies becomes 10.1 times. The Bode-diagram describing the total amplification of the circuit can be seen in Figure 22 below.

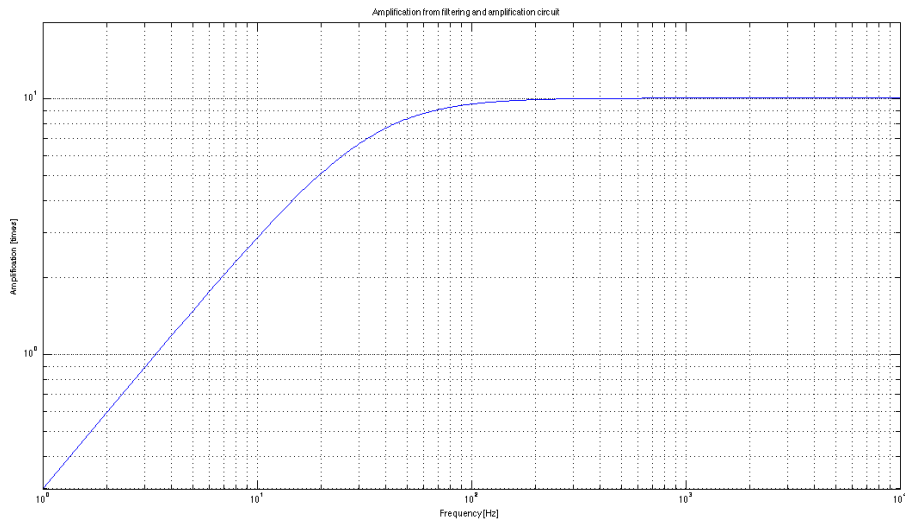


Figure 22: Amplification and filtering properties the circuit, with the component values presented above.

4.4 Cadaver head measurements

As a final part of this master thesis, measurements were also conducted on three human cadavers, performed at two different occasions at Sahlgrenska University Hospital. These measurements were performed utilizing both electrical and acoustical stimulation of the evaluated devices and transducers, similar to the dry skull measurements. This investigation on the other hand, gives more realistic results by adding the influence of soft tissue and also to be able to the study the actual energy loss in the inductive energy transfer through skin. The skin thickness of the subjects used in this study was between 4.1 and 5 mm. The ipsilateral and contralateral responses for the C-BEST, the BEST, the BAHA Classic 300 and the BAHA Intenso with their respective driving units, are studied.

Prior to the measurements, a few preparations were required. To anchor the C-BEST to the skull a minor surgical procedure was needed, similar to the one performed on the dry skull. The size of the customized recess was here chosen to 16 x 16 x 8 mm (hight x length x depth). The 8 mm depth is 1 mm less than the actual transducer height. The reason is to allow the transducer to be pressed against the contact surface in the bottom when the metal bar is applied to the external side, hence achieving better contact between transducer and skull bone.

To be able to anchor the BEST, the BAHA Classic 300 and the BAHA Intenso, also a titanium screw with a snap coupling was mounted on the subject. To determine the stability of this implant, a resonance frequency analysis instrument from Ostell was used. By attaching a Smartpeg with a magnet tip to the implant and apply a signal with varying frequency, a resonance frequency is generated. This resonance frequency is measured using a probe, giving a measure of stability. The measure of stability is presented as an ISQ value, Implant Stability Quotient, ranging from 1 up to 100, where a higher value corresponds to better stability [12], [13].

The setup for the cadaver head measurements is in principal the same as for the dry skull investigations, considering measuring equipment and measurement approach. With the Agilent Signal Analyzer set to Swept Sine mode, the velocity of the vibrations induced at the promontory of the subject is measured using the Laser Doppler Vibrometer (LDV). The LDV was configured with its sensitivity set to 1mm/s/V, the low pass filter with cut-off frequency 15kHz and the high pass filter on. To acquire a sufficient signal level from the reflected laser beam, small reflectors were glued to the promontory of the subject using a gel-based glue, Loctite 454. The excitation signal level from the Agilent was set to 50mVrms for the electrically stimulated measurements, somewhat higher than for the dry skull measurements. For the acoustical measurements the sound pressure levels were chosen to 60, 70 and 90 dB for the BCI and the BAHA Classic 300. For the BAHA Intenso measurements, the sound pressure levels used were 60, 70 and 100 dB for subject one and two, to assure the transducer to be working in saturation. Also the volume control for the BAHA Intenso was increased from 1.5 to 2 for subject one and two for same reason.

Regarding the acoustically stimulated measurements, the sound pressure level is regulated using the same condenser microphone and amplification circuit used for the dry skull measurements. To maintain a constant sound pressure level during the cadaver head measurements becomes more demanding than regulating the sound pressure level in a sound proof environment, due to the complexity of the acoustical environment at the hospital. To avoid interfering reflective sound to influence the measurements, the subject was placed on a soft foam bed. The hard surfaces surrounding the subject were also covered with the same material to improve the acoustic properties of the room.

Prior to the actual measurements on the subject, two measurements were performed to determine the room acoustics, and to assure that the background noise was not interfering with the lowest sound pressure level used during the test. Also, the equipment was calibrated both before and after the subject measurements, to assure that all measurements had been performed under the same circumstances.

5 Results

In the following section, acquired measurement data is presented. The section is divided into two parts, the transducers' electrical impedance and their respective frequency responses.

Results from measurements conducted using the Skull simulator, the dry skull as well as data from the cadaver head investigations are presented. All results in this section are smoothed using matlab and the command “smooth”, a five element moving averaging filter.

5.1 Electrical impedance measurements

The transducers' electrical impedance is of interest when later comparing their respective frequency responses. Due to the fact that a transducers' electrical impedance is dependent on the object it is anchored to, impedance measurements were conducted both on the Skull simulator and the dry skull. The results from both cases are presented in Figure 23 to 26 below. The impedance magnitude, phase, real and imaginary part for the C-BEST, the BEST, the transducers in BAHA Classic 300 and the BAHA Intenso are plotted, with the solid line representing the result from the Skull simulator measurements and the dashed line representing the measurements conducted on the dry skull. Also a comparison of the transducers' respective impedance magnitudes can be seen in Figure 27.

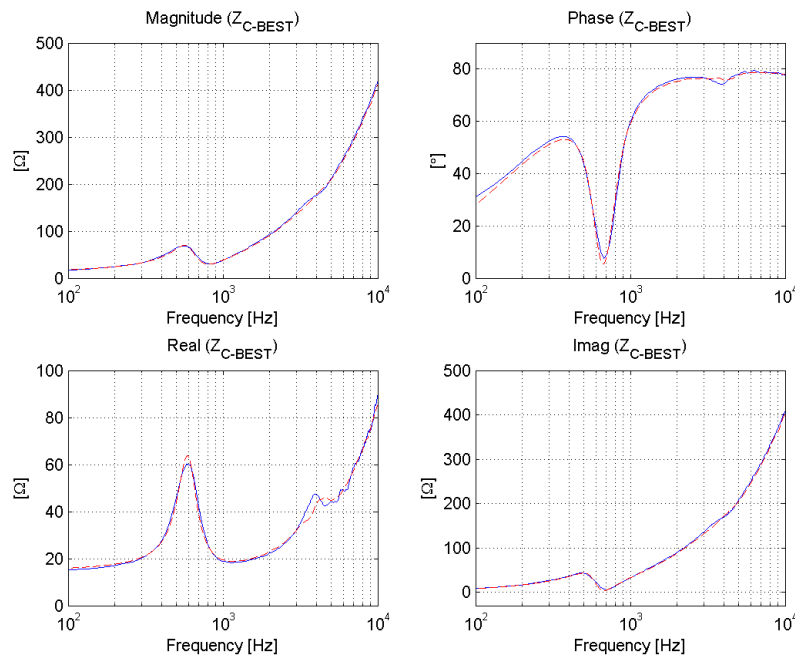


Figure 23: Electrical impedance for the C-BEST, presented as magnitude, phase, real- and imaginary part. The load was Skull simulator (solid line) and dry skull (dashed line.)

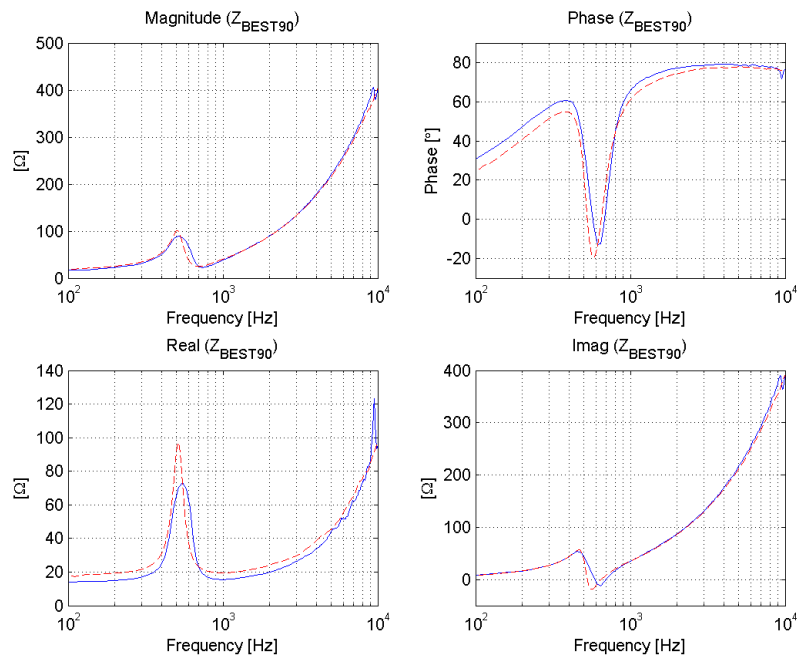


Figure 24: Electrical impedance for the BEST, presented as magnitude, phase, real- and imaginary part. The load was Skull simulator (solid line) and dry skull (dashed line.)

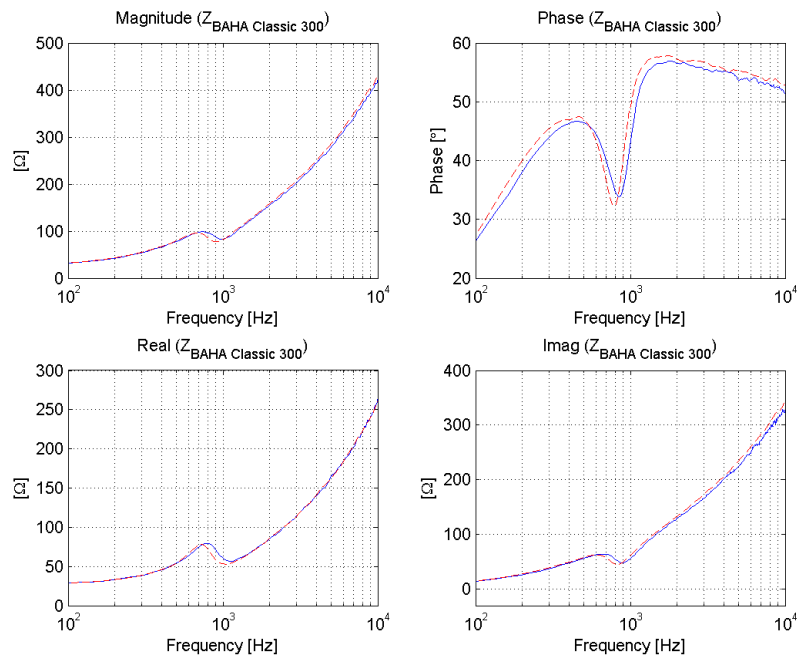


Figure 25: Electrical impedance for the BAHA Classic 300, presented as magnitude, phase, real- and imaginary part. The load was Skull simulator (solid line) and dry skull (dashed line.)

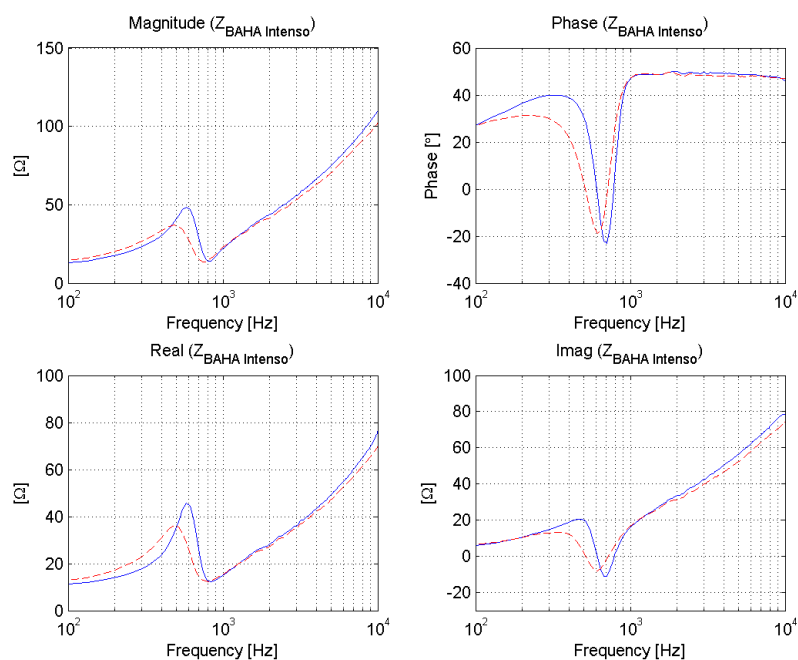


Figure 26: Electrical impedance for the BAHA Intenso, presented as magnitude, phase, real- and imaginary part. The load was Skull simulator (solid line) and dry skull (dashed line.)

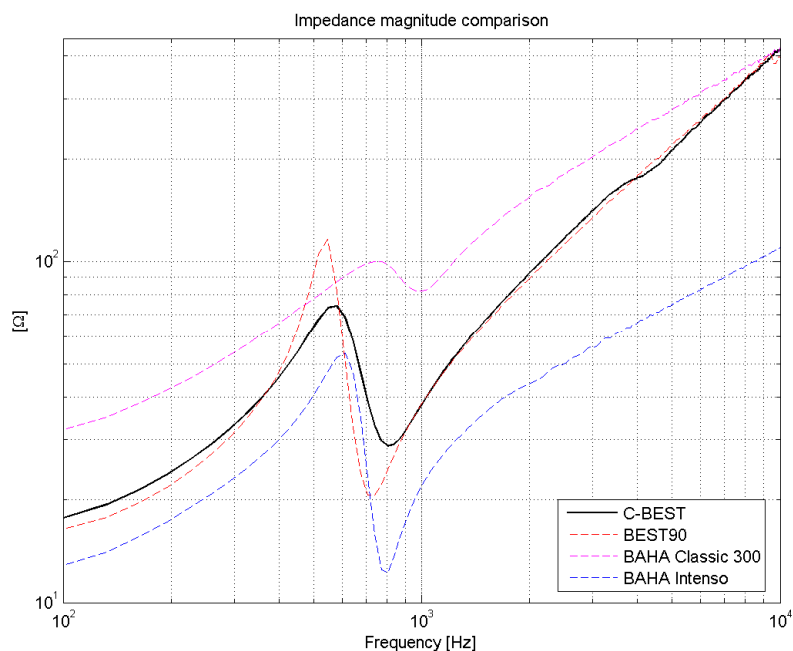


Figure 27: The transducers' respective impedance magnitudes presented in the same plot to give a better overview. Note the "BAHA Classic 300" and "BAHA Intenso" here only referred to the transducer incorporated in these devices

5.2 Frequency response functions

In this subsection the frequency response functions for the different transducers, with and without their respective driving units, are presented. It covers the voltage to force frequency response from the Skull simulator and electrical and acoustical frequency responses from both the dry skull and the cadaver head investigations. The evaluated transducers are the C-BEST, the BEST, the BAHA Classic 300 and the BAHA Intenso. The usage of the C-BEST in combination with the MED-EL inductive link, used in all acoustical measurements, is referred to as BCI.

5.2.1 Voltage to force frequency response from Skull simulator

The frequency response functions acquired from the Skull simulator measurements are presented as the force output from the Skull simulator divided by the input voltage over the transducers, representing the voltage to force frequency response function, $FRF_u(j\omega)$, see Figure 28.

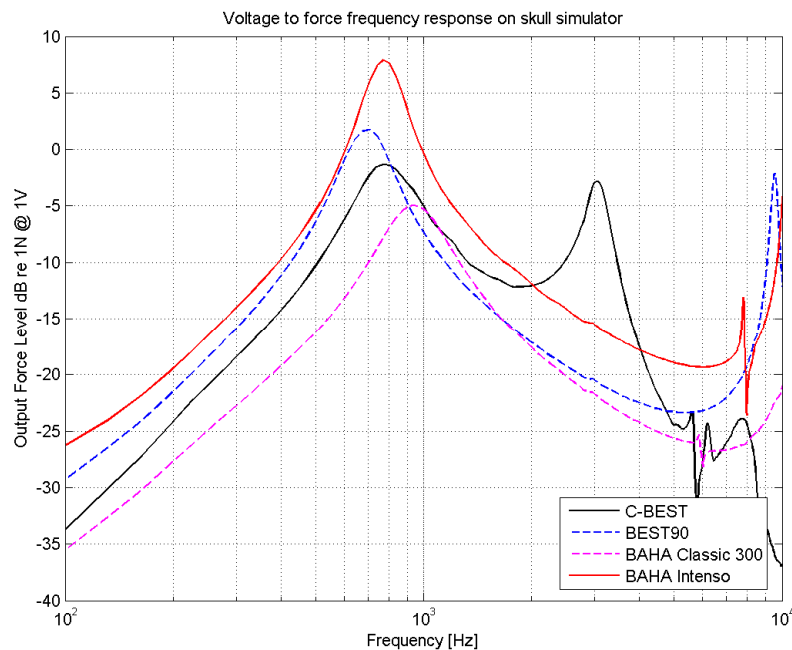


Figure 28: Skull simulator measurements presenting the voltage to force frequency response for all of the transducers. Note the “BAHA Classic 300” and “BAHA Intenso” here only referred to the transducer incorporated in these devices

The improved performance of the C-BEST, in terms of output force, compared to the BEST can be seen in Figure 29, where the difference between the two transducers is plotted.

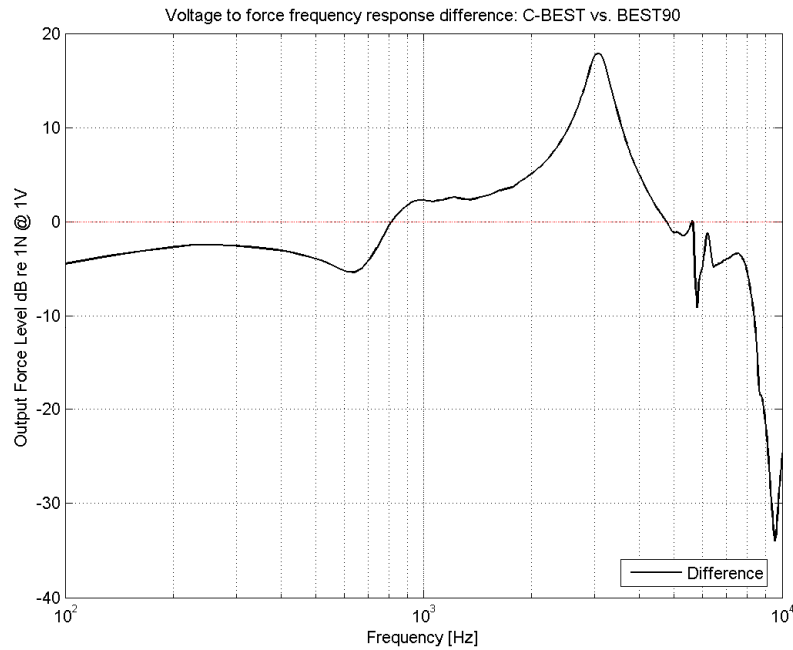


Figure 29: Difference in output force level between the C-BEST and the BEST, for the same electrical input.

5.2.2 Acceleration on dry skull

The promontory acceleration response measurements, utilizing the dry skull, were conducted in controlled laboratory environment. The ipsilateral and contralateral acceleration responses, from electrical stimulation of the transducers, can be found below for all four transducers, the C-BEST, the BEST-90, the transducers incorporated in BAHA Classic 300 and the BAHA Intenso. Acceleration responses from acoustical stimulation were conducted comparing the C-BEST to the conventional BAHA Classic 300 transducer. Additional comparison plots, covering the issue of anchoring position as well as the maximum power output for the acoustically stimulated transducers, are also found in the section below.

5.2.2.1 Frequency response from electrical stimulation

The ipsilateral and contralateral frequency responses for the C-BEST in pos B, the BEST, the transducers BAHA Classic 300 and the BAHA Intenso in pos A can be seen in Figure 30 to 31.

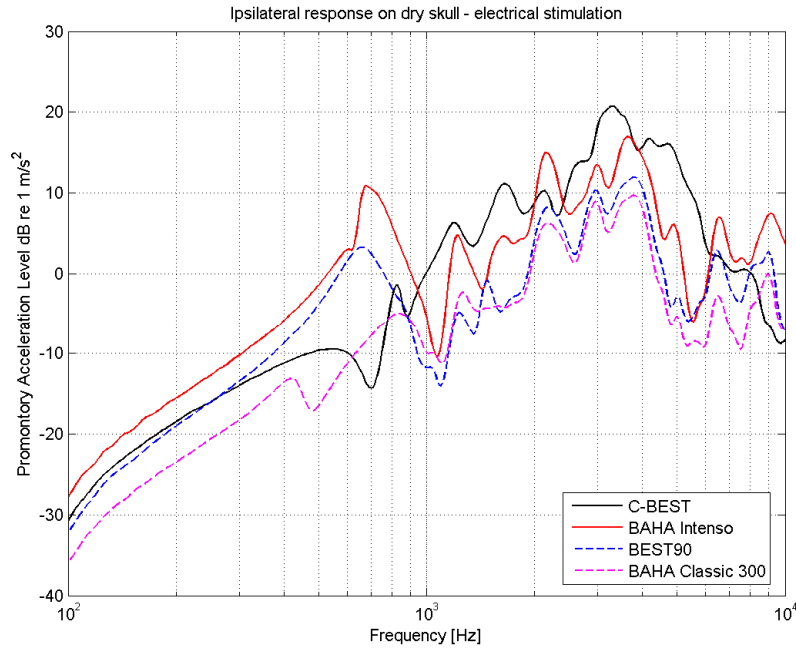


Figure 30: Ipsilateral frequency response from electrical stimulation on dry skull comparing all of the four transducers. Note the “BAHA Classic 300” and “BAHA Intenso” here only referred to the transducer incorporated in these devices

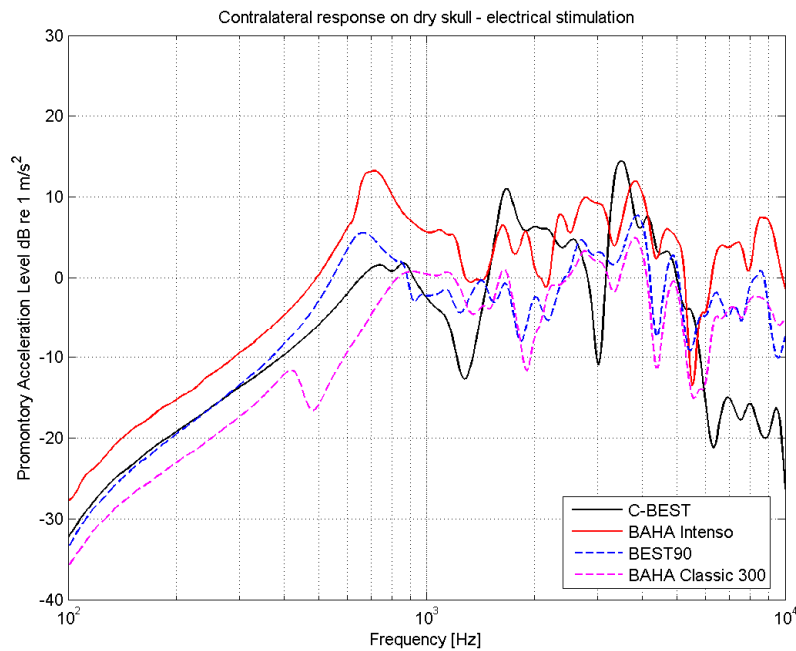


Figure 31: Contralateral frequency response from electrical stimulation on dry skull comparing all of the four transducers. Note the “BAHA Classic 300” and “BAHA Intenso” here only referred to the transducer incorporated in these devices

In Figure 32 and 33, the ipsilateral and contralateral frequency response differences between the C-BEST and the BEST, the BAHA Intenso and the BAHA Classic 300 are collected, with the C-BEST used as the reference transducer.

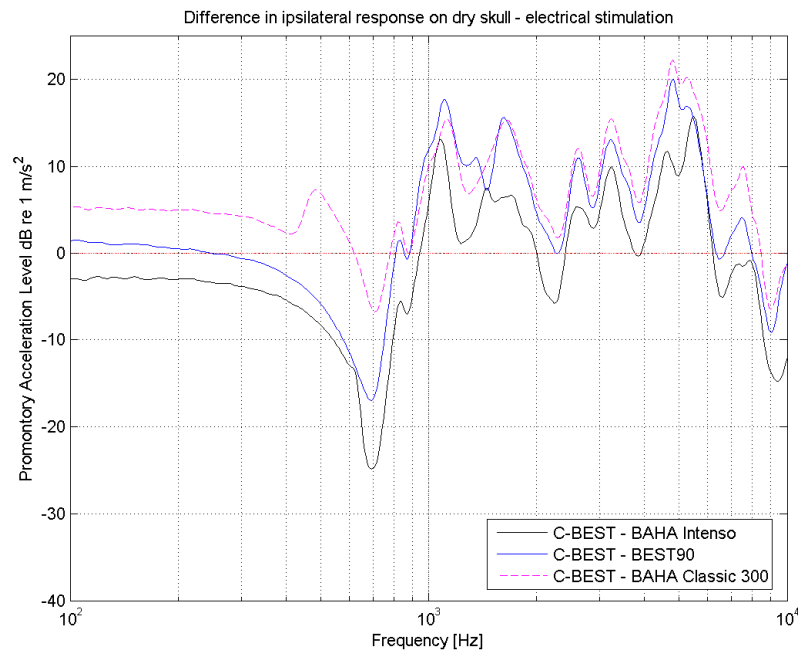


Figure 32: Comparison plot showing the difference in ipsilateral frequency response on the dry skull, with the C-BEST as reference transducer. Note the “BAHA Classic 300” and “BAHA Intenso” here only referred to the transducer incorporated in these devices

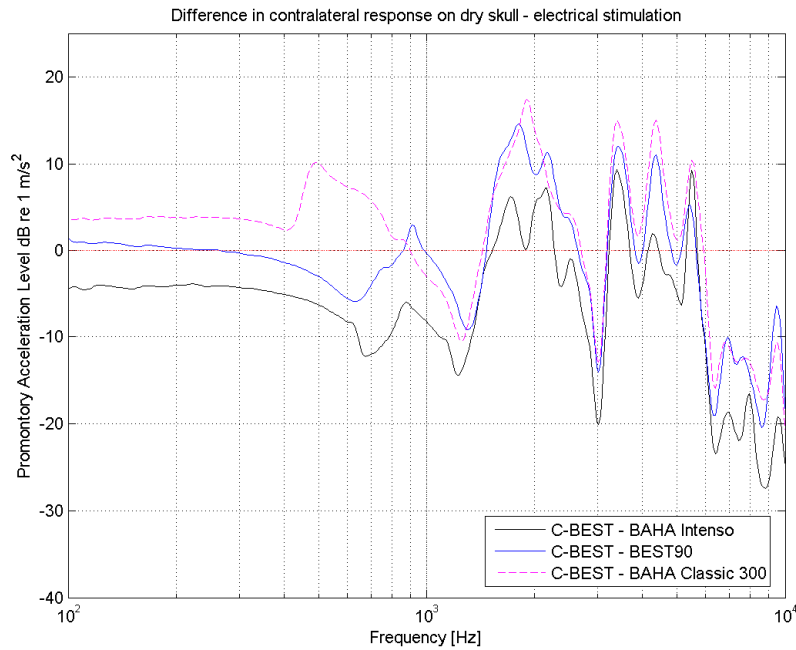


Figure 33: Comparison plot showing the difference in contralateral frequency response on the dry skull, with the C-BEST as reference transducer. Note the “BAHA Classic 300” and “BAHA Intenso” here only referred to the transducer incorporated in these devices

To visualize the issue of anchoring position, the ipsilateral and contralateral frequency responses functions for the BEST transducer, attached to both position A and B on the dry skull, are presented in Figure 34 and 35. It should be noted that this is the opposite side (right side) to the side where the C-BEST and BCI was evaluated, see also Figure 14.

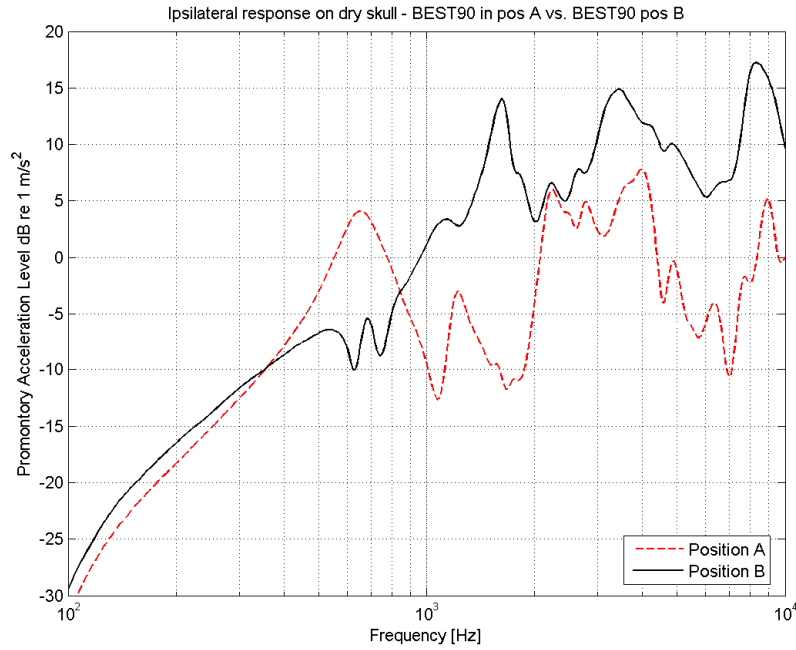


Figure 34: Ipsilateral frequency response on dry skull from electrical stimulation with the same transducer, the BEST, attached to both position A and B on the right side of the dry skull, to study the possible benefit of stimulating closer to the cochlea.

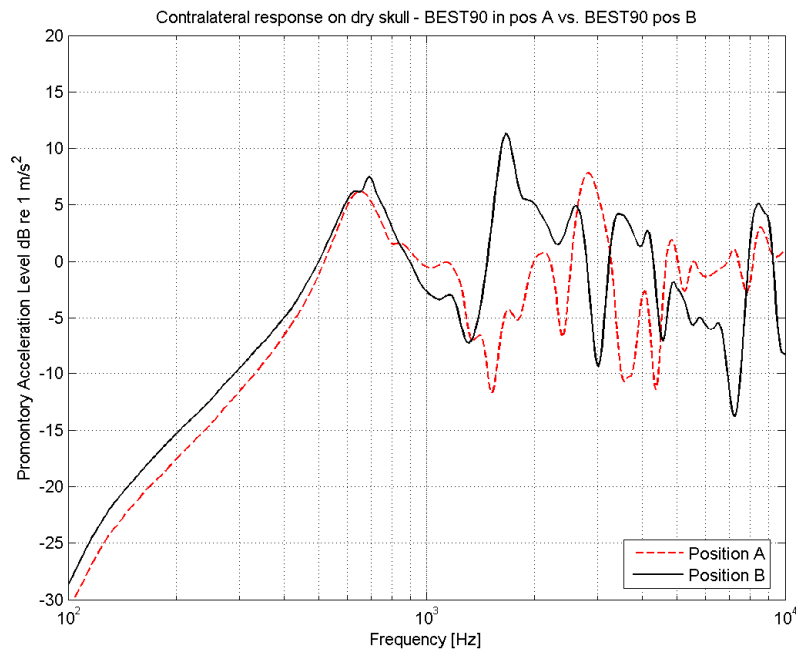


Figure 35: Contralateral frequency response on dry skull from electrical stimulation with the BEST attached to position A and B on the right side of the dry skull.

5.2.2.2 Frequency response from acoustical stimulation

Frequency responses obtained from acoustical stimulation of the BCI and BAHA Classic 300 are plotted in Figure 36 to 39 below. The acceleration responses at the promontory of the dry skull are presented for both ipsilateral and contralateral measurements.

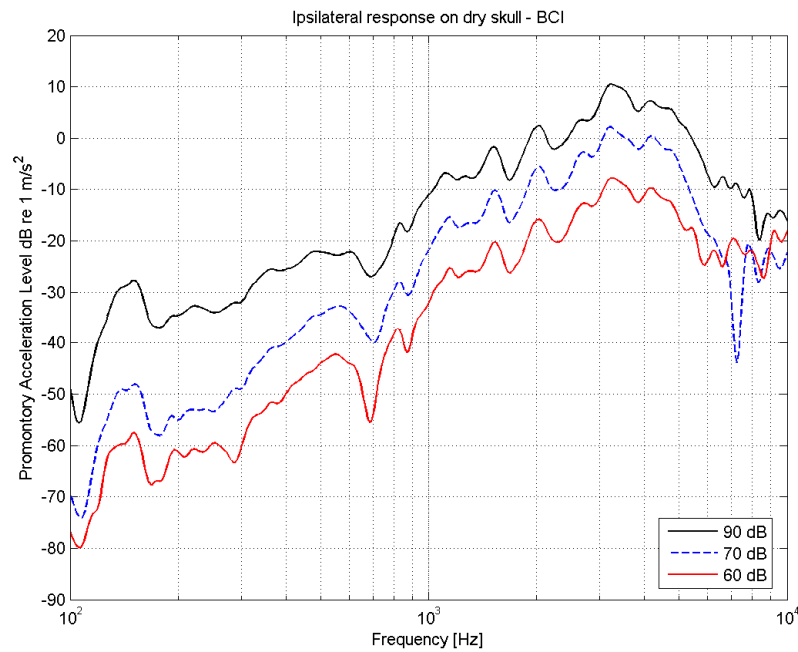


Figure 36: Ipsilateral frequency response on dry skull from acoustical stimulation showing the 60, 70 and 90 dB response for the BCI.

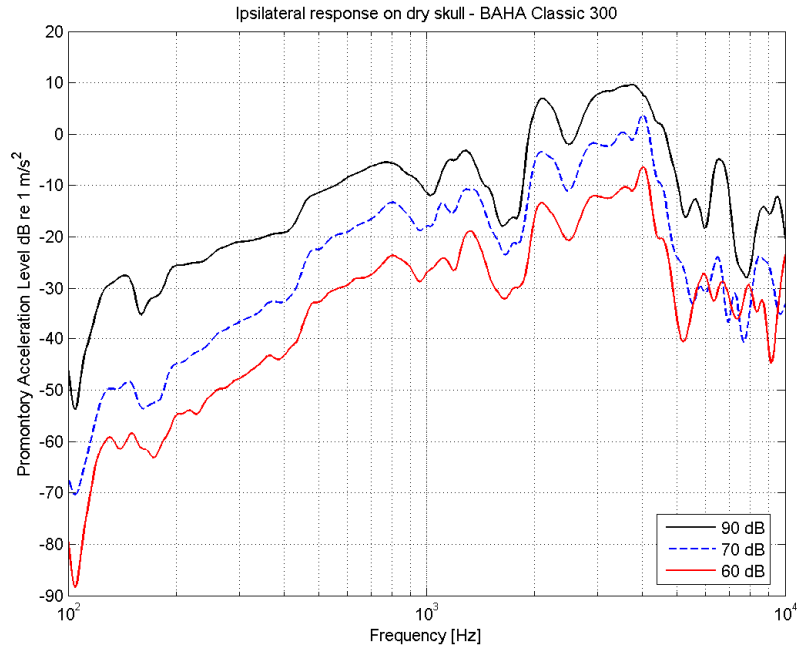


Figure 37: Ipsilateral frequency response on dry skull from acoustical stimulation showing the 60, 70 and 90 dB response for the BAHA Classic 300.

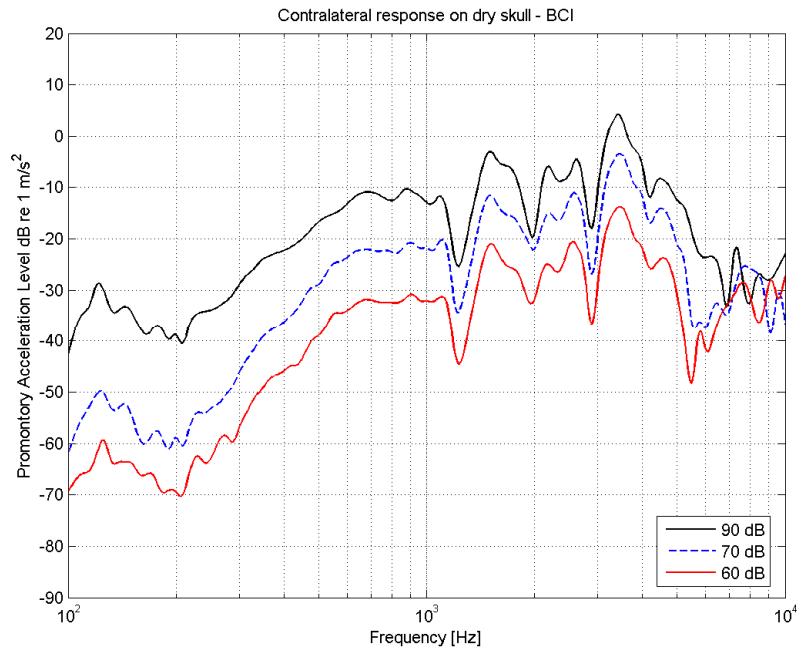


Figure 38: Contralateral frequency response on dry skull from acoustical stimulation showing the 60, 70 and 90 dB response for the BCI.

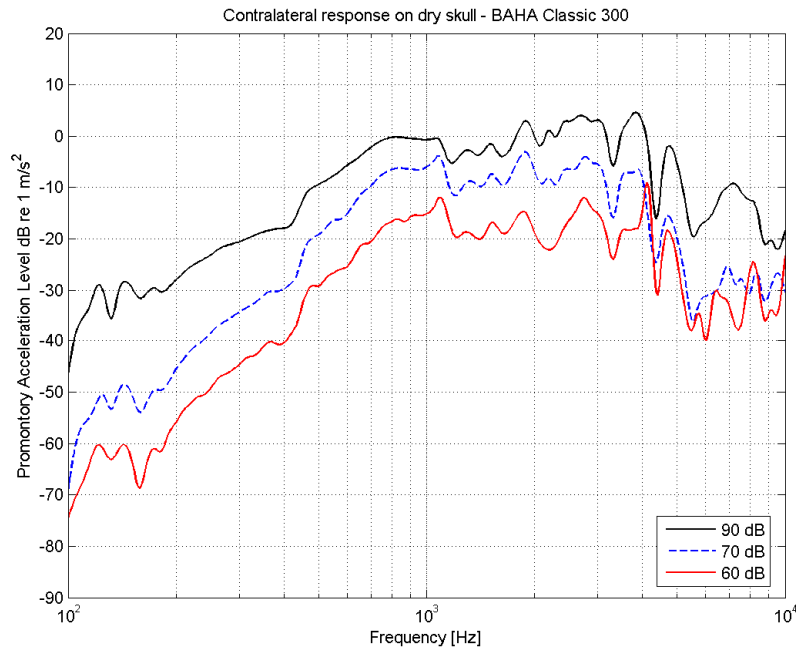


Figure 39: *Contralateral frequency response on dry skull from acoustical showing the 60, 70 and 90 dB response for the BAHA Classic 300.*

To compare the transducers' maximum power output level (MPO), the transducers' respective saturation curves, the acceleration responses obtained at 90 dB SPL, are arranged separately in Figure 40 and 41.

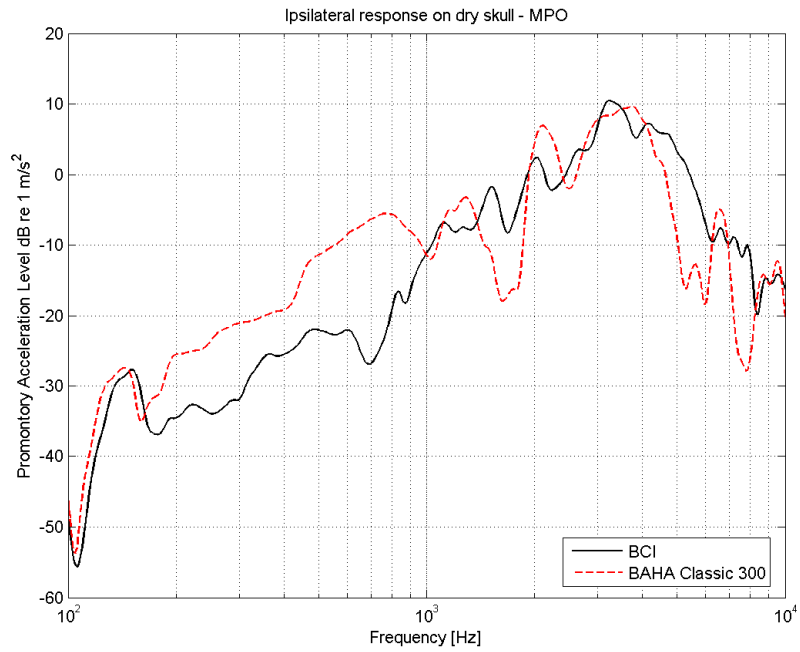


Figure 40: Ipsilateral MPO response on dry skull for the BCI and the BAHA Classic 300.

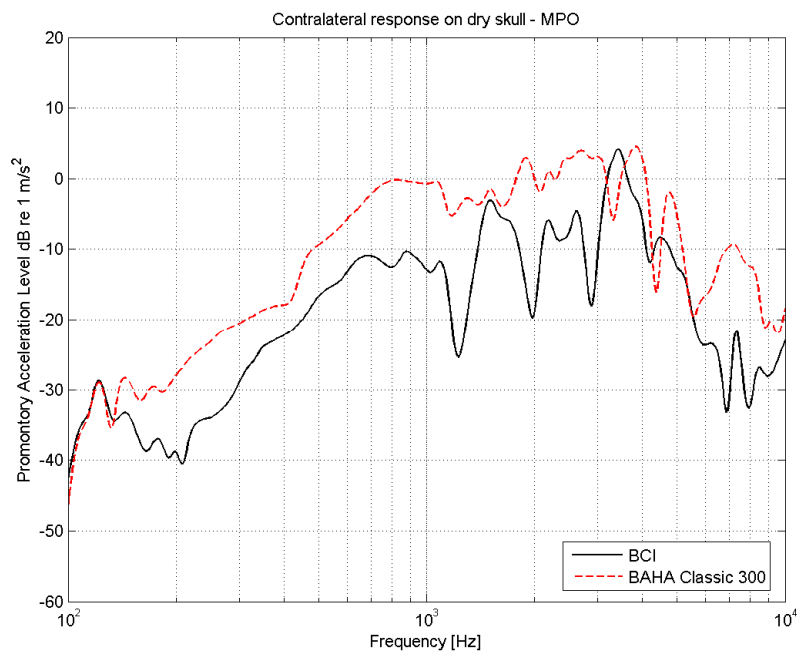


Figure 41: Contralateral MPO response on dry skull for the BCI and the BAHA Classic 300.

5.2.3 Cadaver head investigation

Prior to the frequency response measurements, the Implant Stability Quotient, ISQ, for the titanium snap coupling was measured. The result can be seen in Table 2.

Measuring direction	ISQ _{SUBJECT1}	ISQ _{SUBJECT2}	ISQ _{SUBJECT3}
Front to back	79	79	72
Back to front	81	78	74
Up and down	79	77	76

Table 2: Implant Stability Quotient

5.2.3.1 Frequency response from electrical stimulation

The ipsilateral and contralateral frequency responses obtained from electrical stimulation of the C-BEST and the BEST can be seen in Figure 42 to 45. Each figure includes data from three different cadaver measurements to show the variation among subjects.

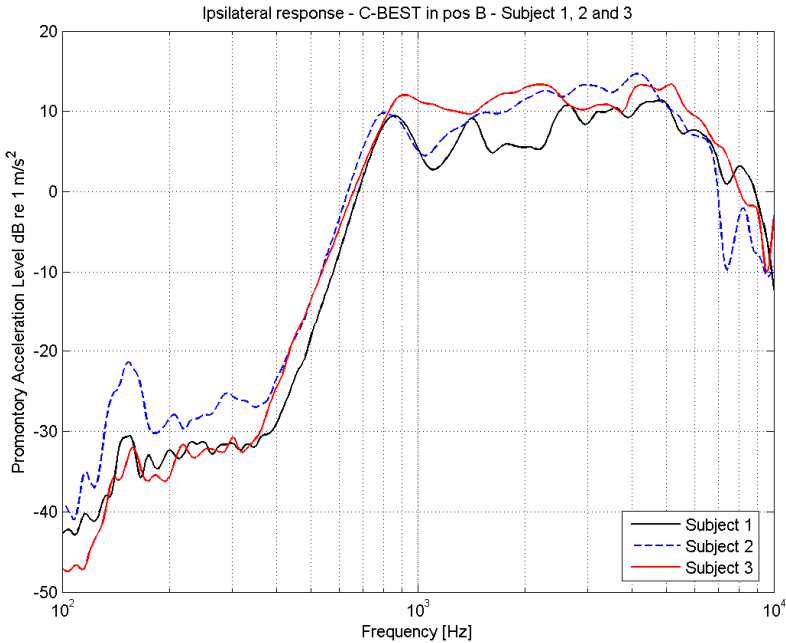


Figure 42: ipsilateral frequency response from electrical stimulation of the C-BEST.

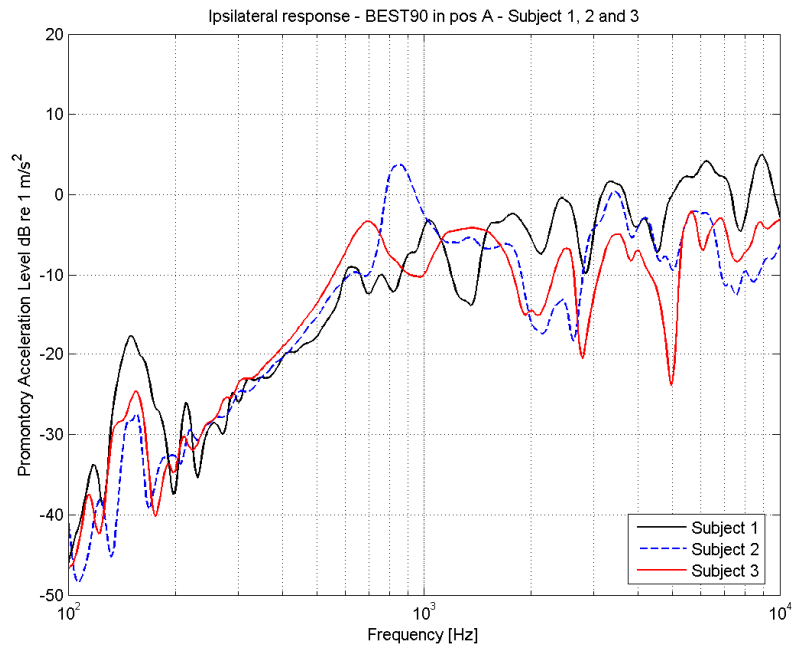


Figure 43: Ipsilateral frequency response from electrical stimulation of the BEST.

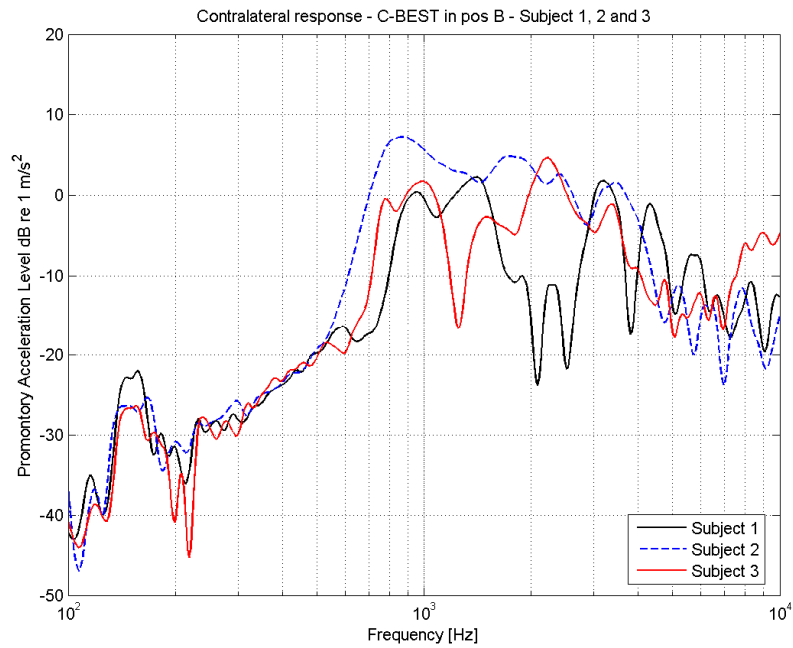


Figure 44: Contralateral frequency response from electrical stimulation of the C-BEST for the three subjects.

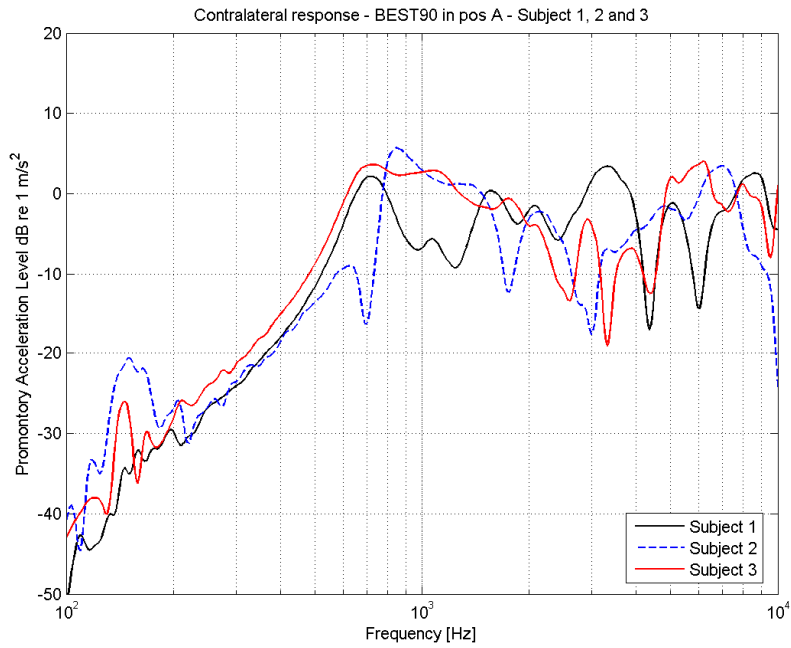


Figure 45: *Contralateral frequency response from electrical stimulation of the BEST for the three subjects.*

To visualize the difference between the two BEST transducers when attached to their designated positions, the C-BEST in position B and the BEST in position A, their respective frequency response functions for each of the three subjects are compared in Figure 46 to 51 below.

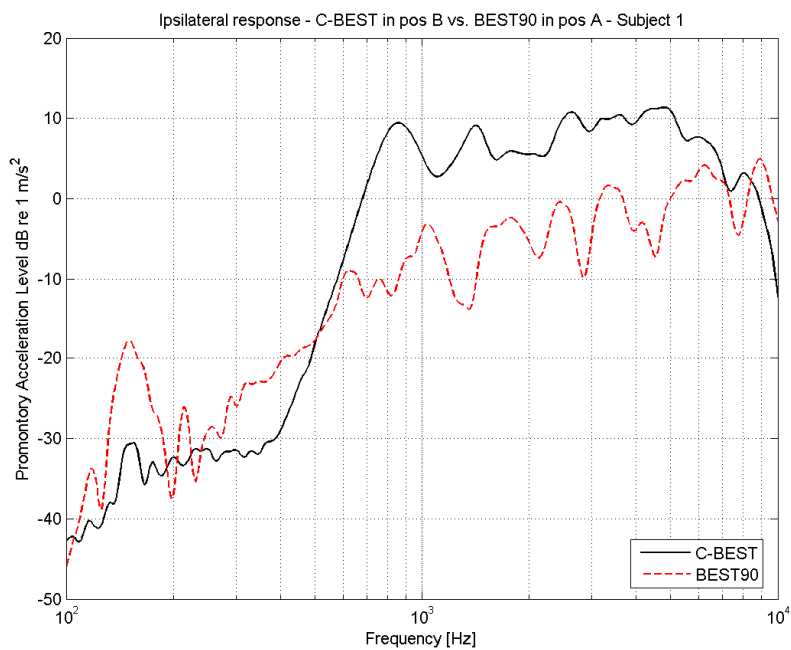


Figure 46: *Comparison of the ipsilateral frequency responses from electrical stimulation of the C-BEST and the BEST on subject 1.*

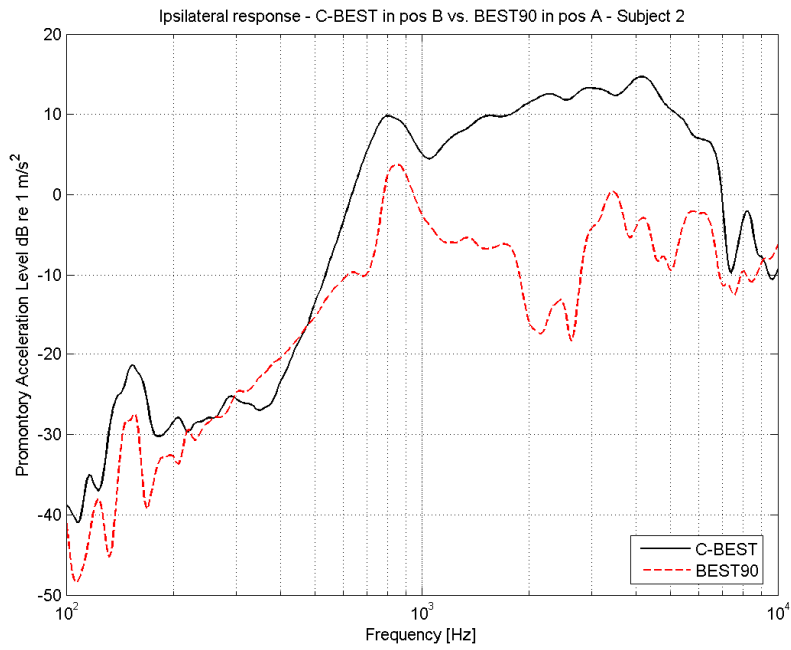


Figure 47: Comparison of the ipsilateral frequency responses from electrical stimulation of the C-BEST and the BEST on subject 2

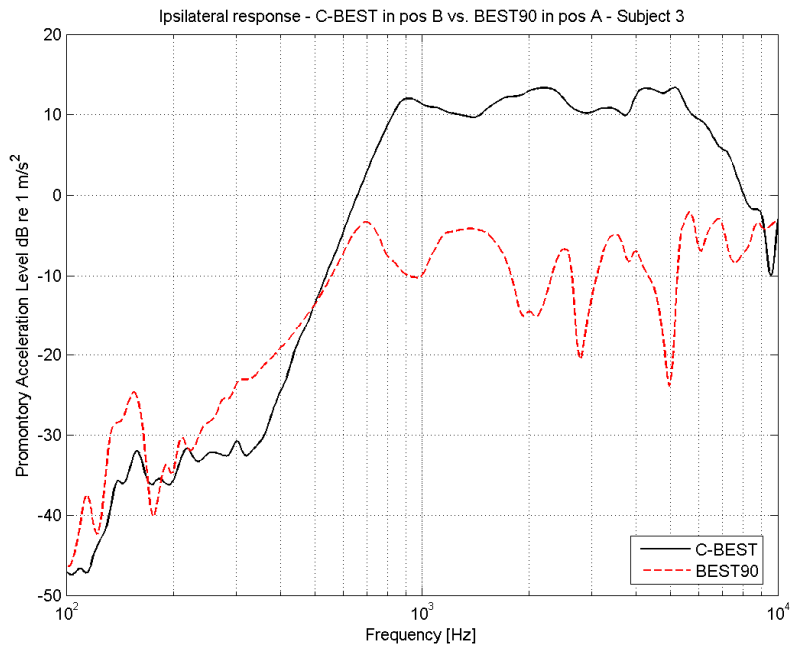


Figure 48: Comparison of the ipsilateral frequency responses from electrical stimulation of the C-BEST and the BEST on subject 3.

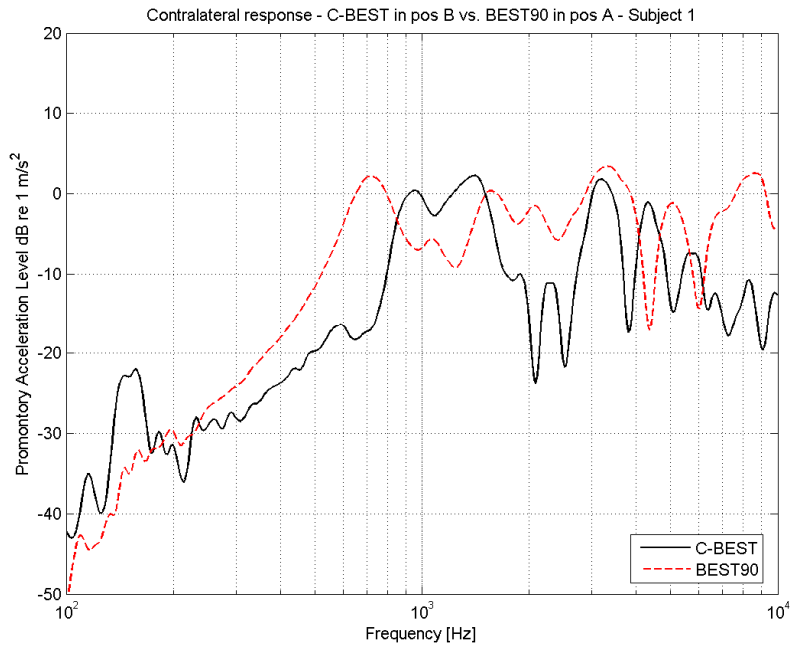


Figure 49: Comparison of the contralateral frequency responses from electrical stimulation of the C-BEST and the BEST on subject 1.

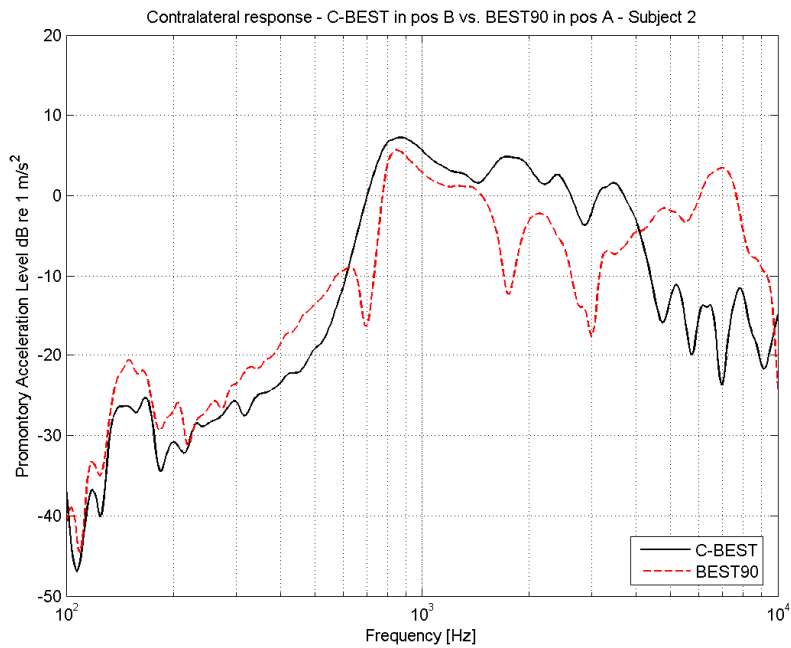


Figure 50: Comparison of the contralateral frequency responses from electrical stimulation of the C-BEST and the BEST on subject 2.

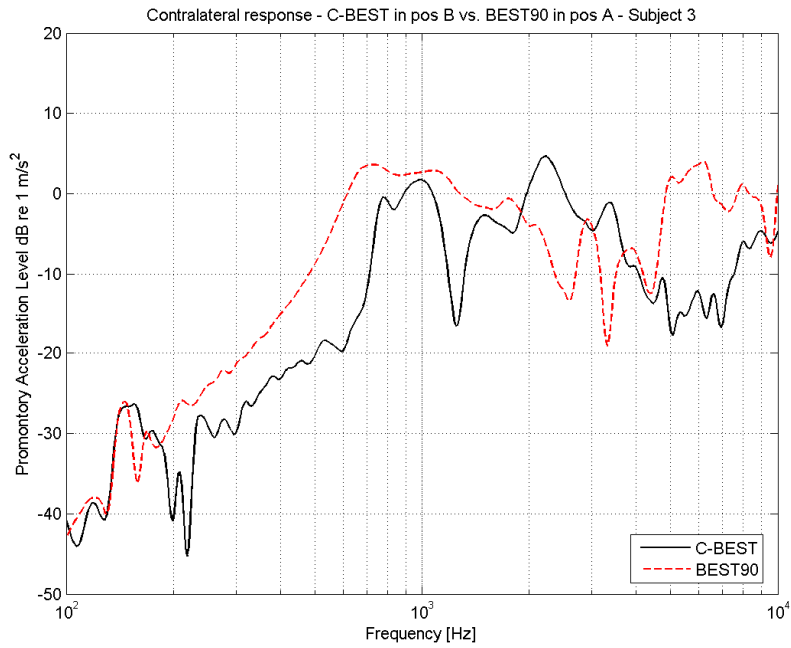


Figure 51: Comparison of the contralateral frequency responses from electrical stimulation of the C-BEST and the BEST on subject 3.

5.2.3.2 Frequency response from acoustical stimulation

The ipsilateral and contralateral frequency response functions from acoustical stimulation of the BCI, the BAHA Classic 300 and BAHA Intenso are presented in Figure 52 to 69. The sound pressure levels used for stimulation of the BCI and BAHA Classic 300 are 60, 70 and 90 dB. For the BAHA Intenso, 100 dB SPL instead of 90 dB SPL was used to assure saturation in the maximum power output measurement

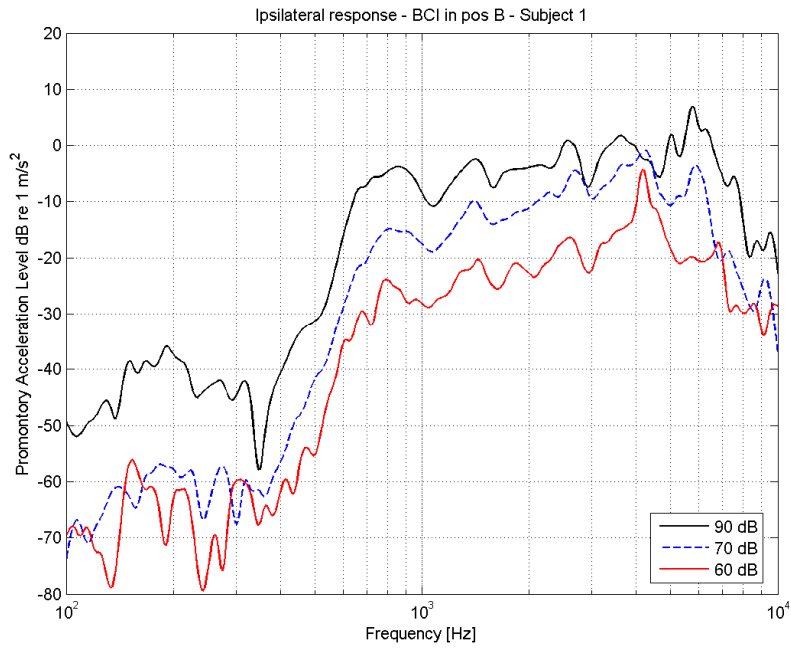


Figure 52: Ipsilateral promontory acceleration response for the BCI at 60, 70 and 90 dB SPL on subject 1.

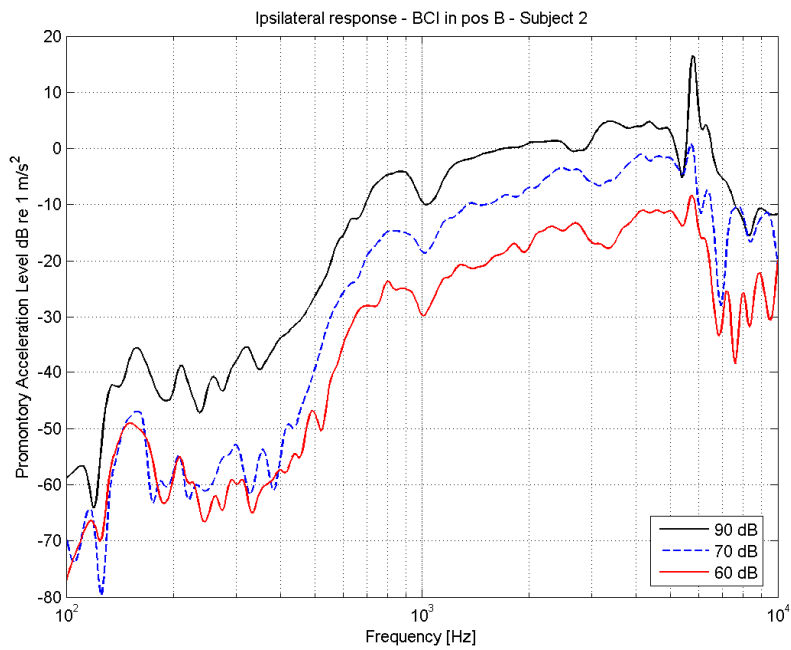


Figure 53: Ipsilateral promontory acceleration response for the BCI at 60, 70 and 90 dB SPL on subject 2.

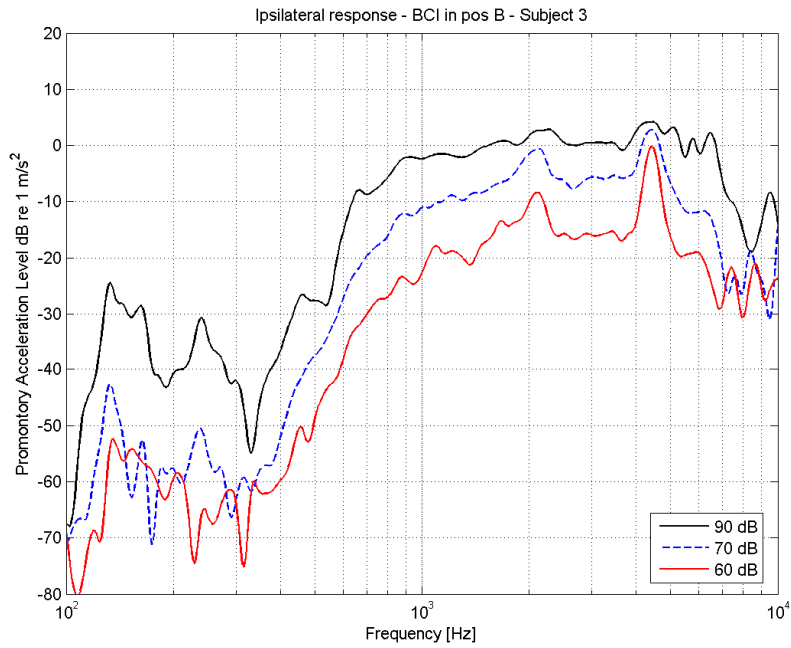


Figure 54: *Ipsilateral promontory acceleration response for the BCI at 60, 70 and 90 dB SPL on subject 3.*

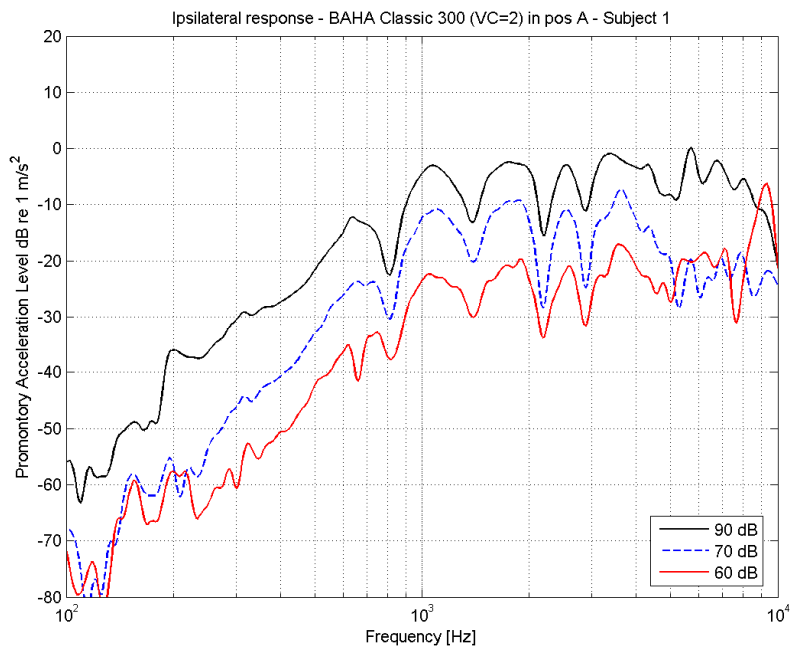


Figure 55: *Ipsilateral promontory acceleration response for the BAHA Classic 300 at 60, 70 and 90 dB SPL on subject 1.*

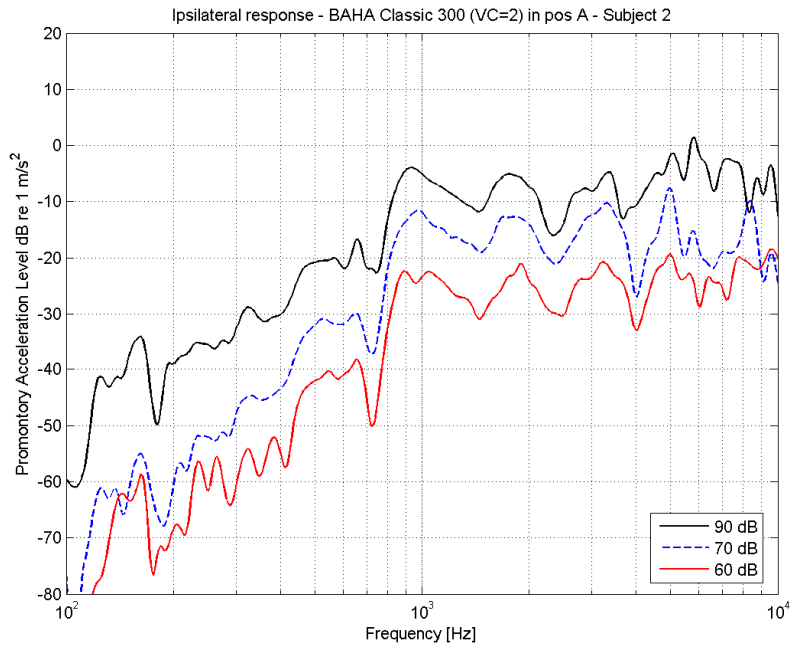


Figure 56: Ipsilateral promontory acceleration response for the BAHA Classic 300 at 60, 70 and 90 dB SPL on subject 2.

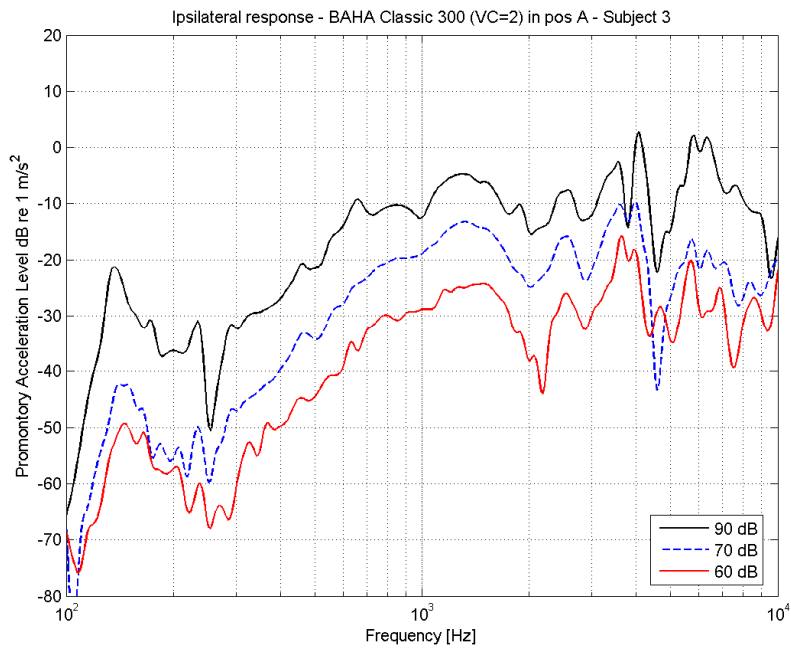


Figure 57: Ipsilateral promontory acceleration response for the BAHA Classic 300 at 60, 70 and 90 dB SPL on subject 3.

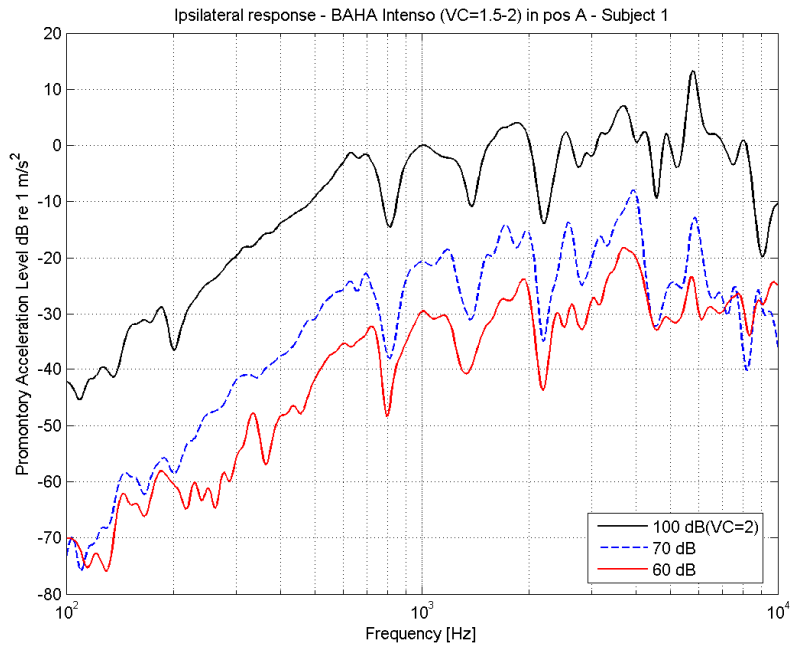


Figure 58: Ipsilateral promontory acceleration response for the BAHA Intenso at 60, 70 and 100 dB SPL on subject 1.

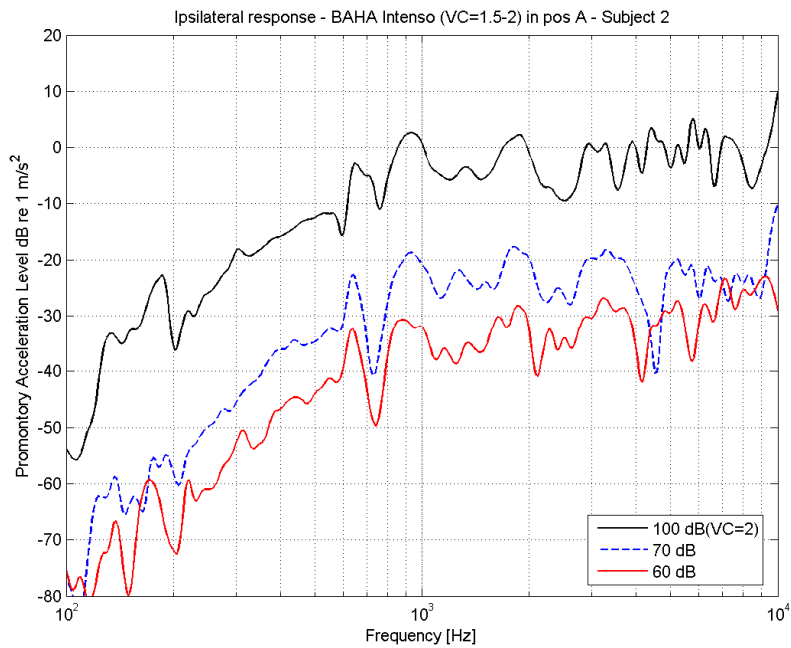


Figure 59: Ipsilateral promontory acceleration response for the BAHA Intenso at 60, 70 and 100 dB SPL on subject 2.

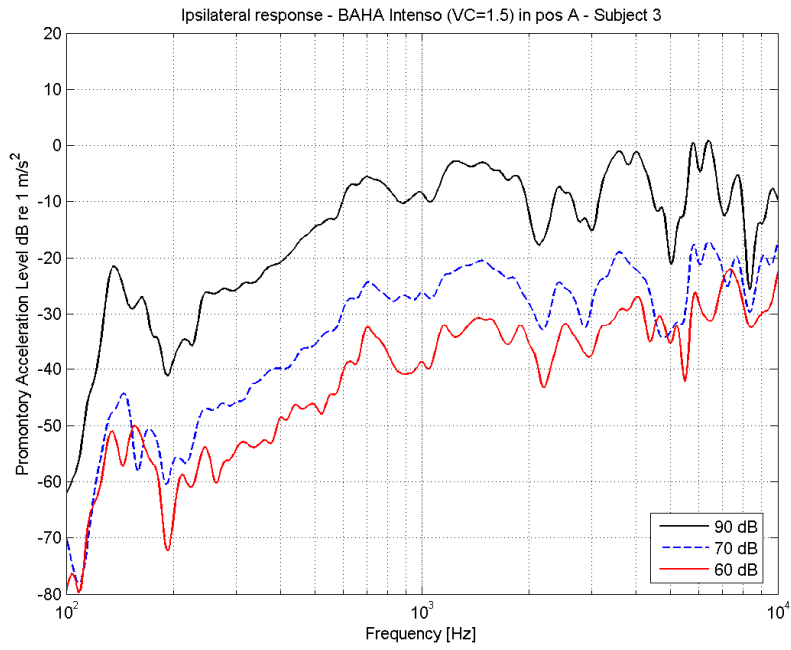


Figure 60: Ipsilateral promontory acceleration response for the BAHA Intenso at 60, 70 and 100 dB SPL on subject 3.

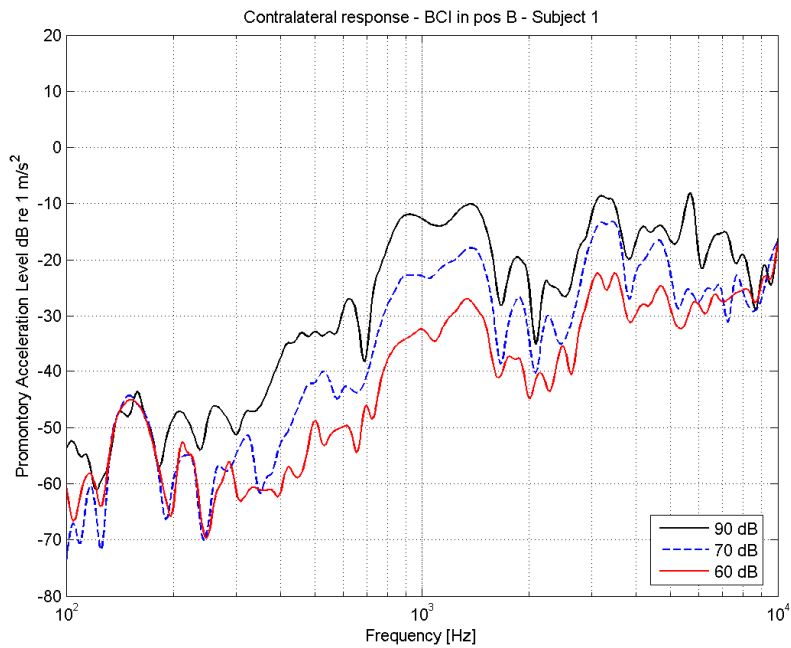


Figure 61: Contralateral promontory acceleration response for the BCI at 60, 70 and 90 dB SPL on subject 1.

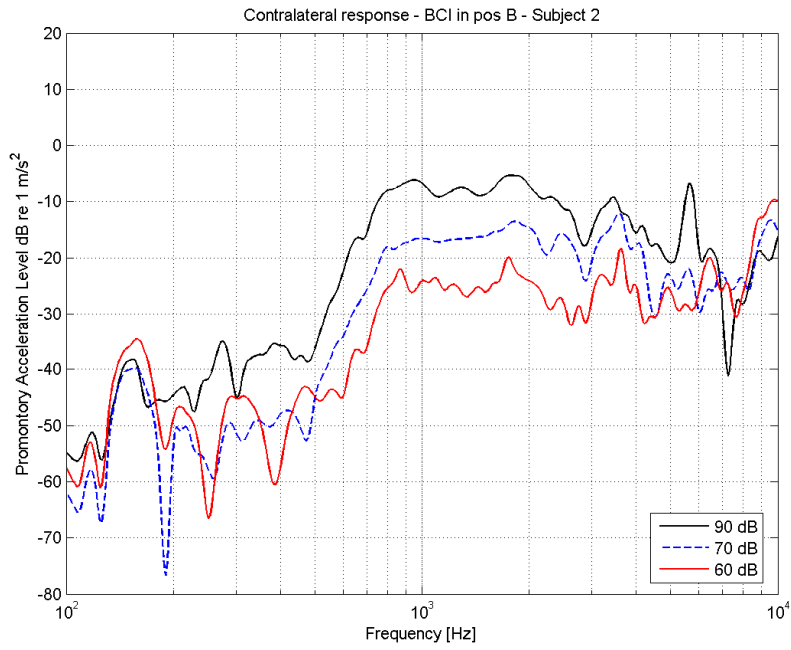


Figure 62: *Contralateral promontory acceleration response for the BCI at 60, 70 and 90 dB SPL on subject 2.*

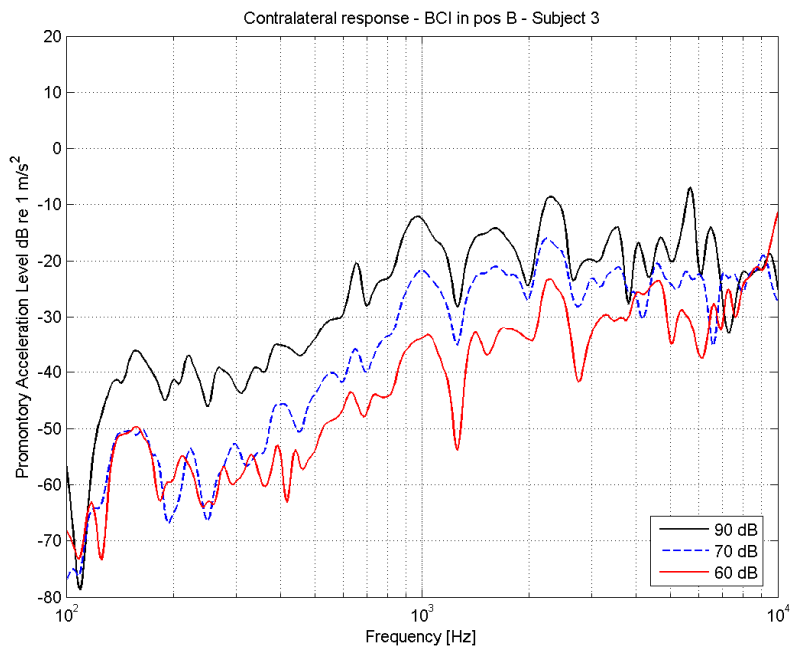


Figure 63: *Contralateral promontory acceleration response for the BCI at 60, 70 and 90 dB SPL on subject 2.*

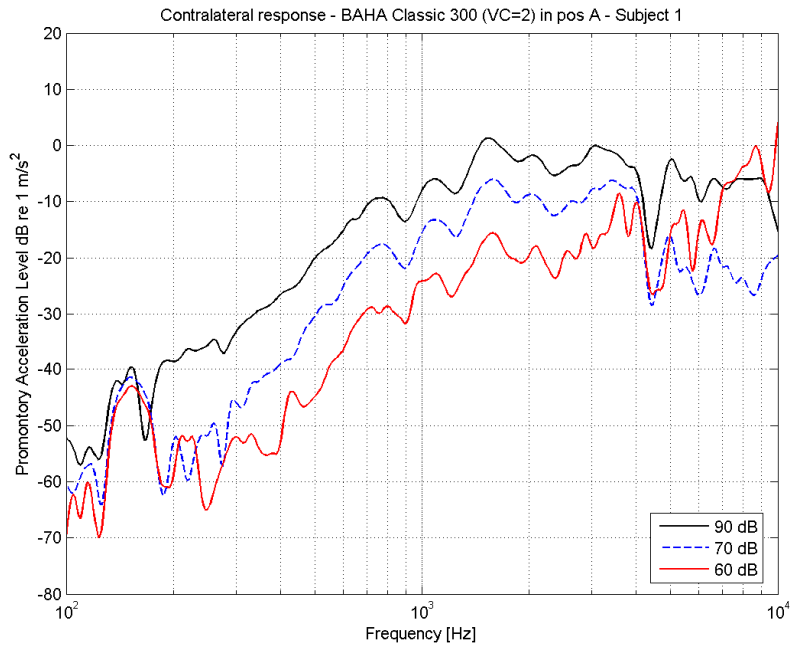


Figure 64: *Contralateral promontory acceleration response for the BAHA Classic 300 at 60, 70 and 90 dB SPL on subject 1.*

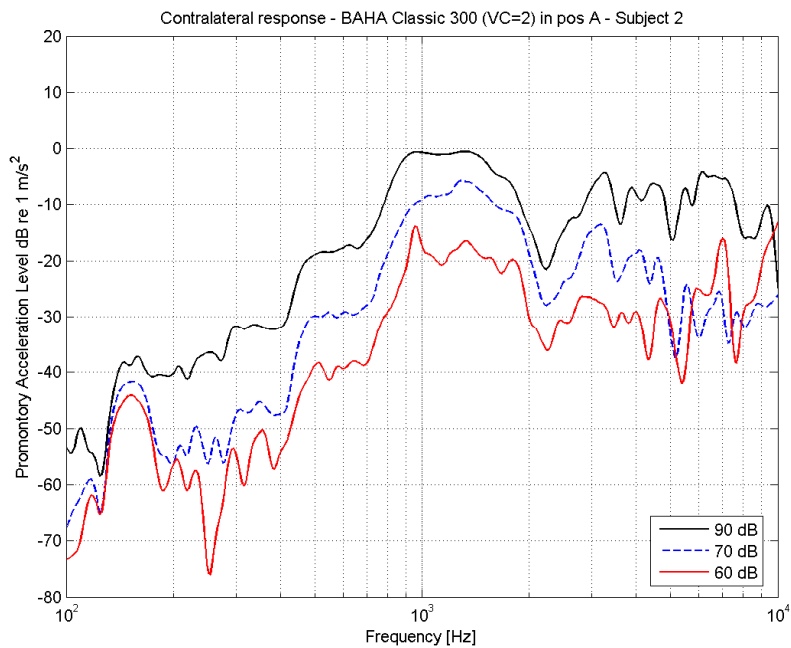


Figure 65: *Contralateral promontory acceleration response for the BAHA Classic 300 at 60, 70 and 90 dB SPL on subject 2.*

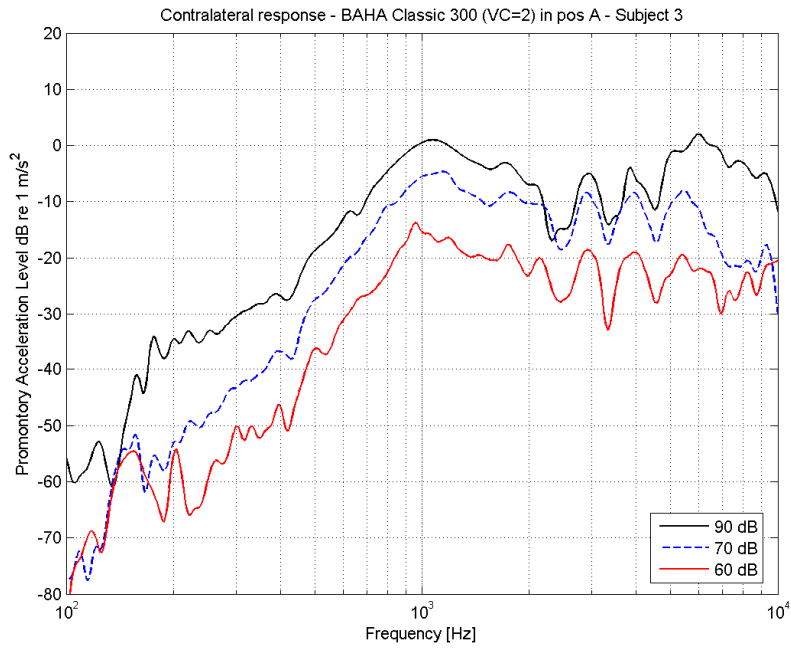


Figure 66: *Contralateral promontory acceleration response for the BAHA Classic 300 at 60, 70 and 90 dB SPL on subject 3.*

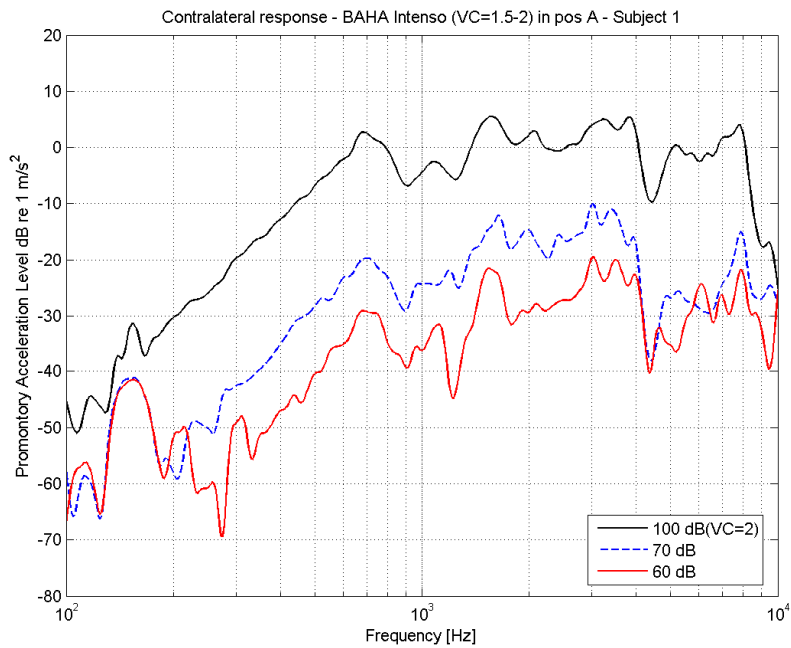


Figure 67: *Contralateral promontory acceleration response for the BAHA Intenso at 60, 70 and 100 dB SPL on subject 1.*

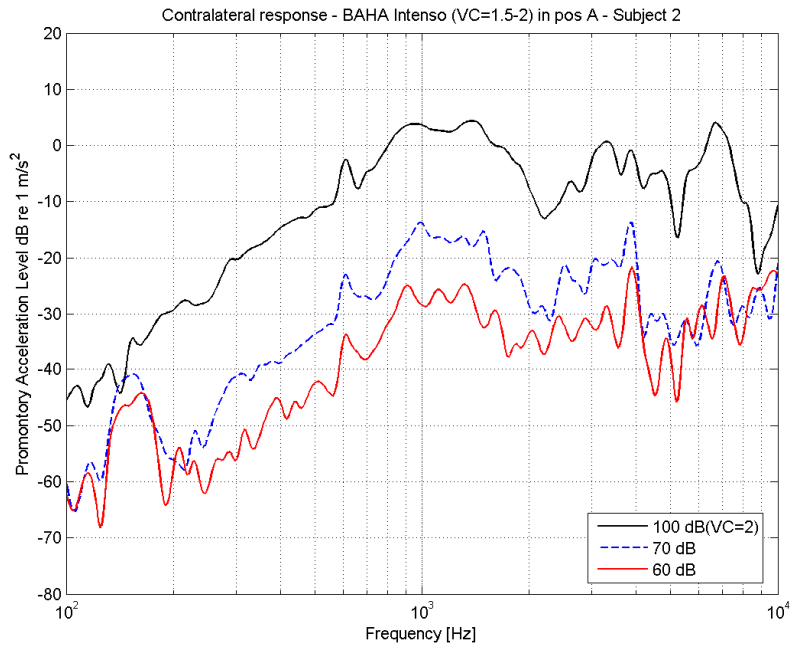


Figure 68: *Contralateral promontory acceleration response for the BAHA Intenso at 60, 70 and 100 dB SPL on subject 2.*

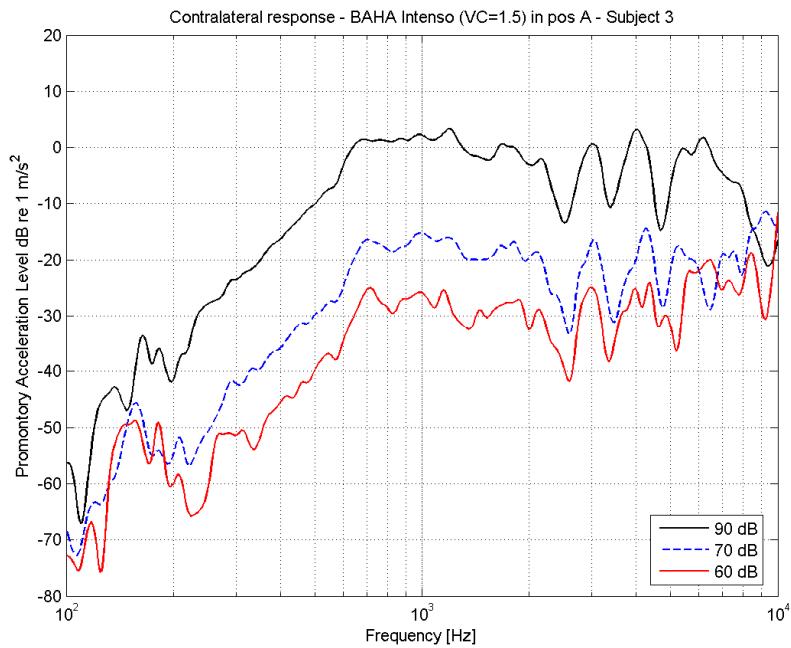


Figure 69: *Contralateral promontory acceleration response for the BAHA Intenso at 60, 70 and 100 dB SPL on subject 3.*

A comparison of the MPO responses for the BCI, the BAHA Classic 300 and BAHA Intenso can be seen in Figure 70 to 75. The MPO responses are presented for the three subjects separately, as goes for the ipsilateral and contralateral responses.

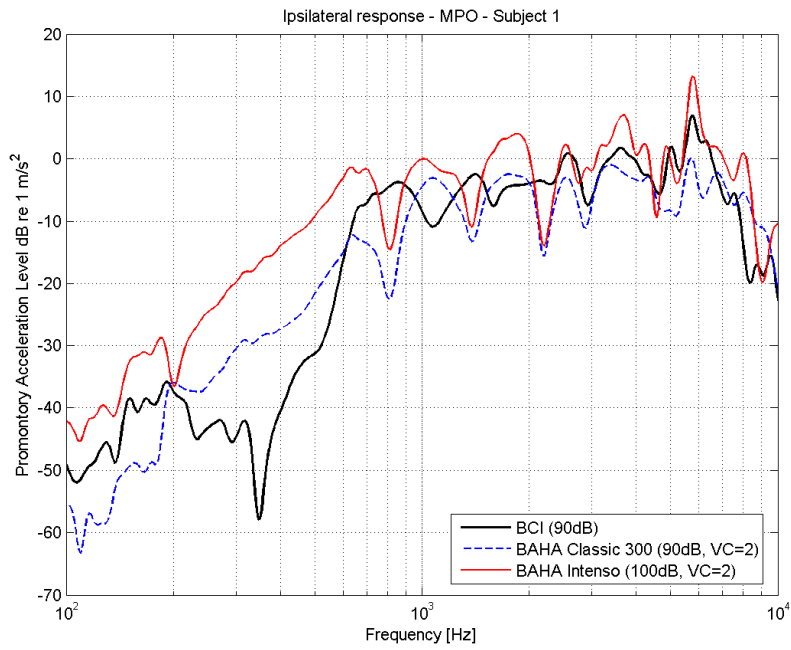


Figure 70: Comparison of the ipsilateral MPO for the BCI, BAHA Classic 300 and BAHA Intenso on subject 1.

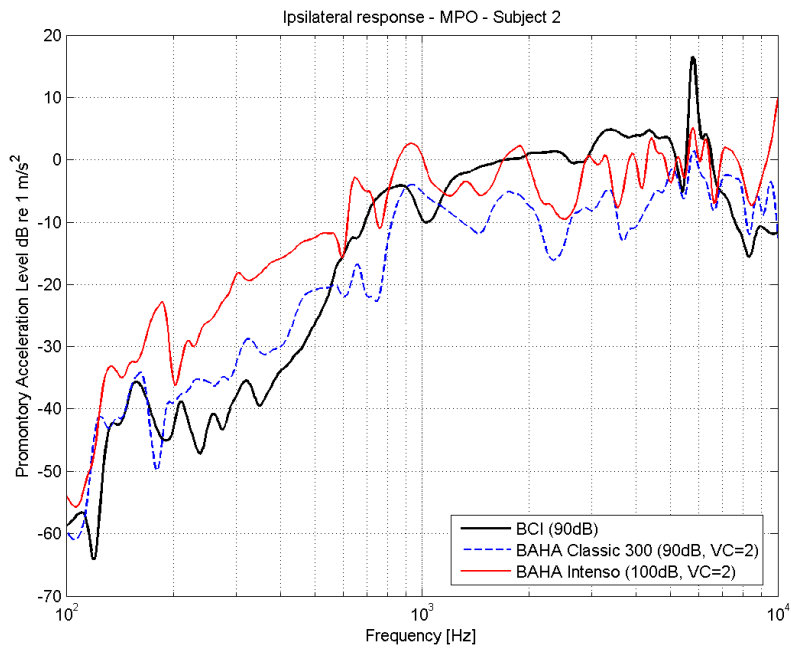


Figure 71: Comparison of the ipsilateral MPO for the BCI, BAHA Classic 300 and BAHA Intenso on subject 2.

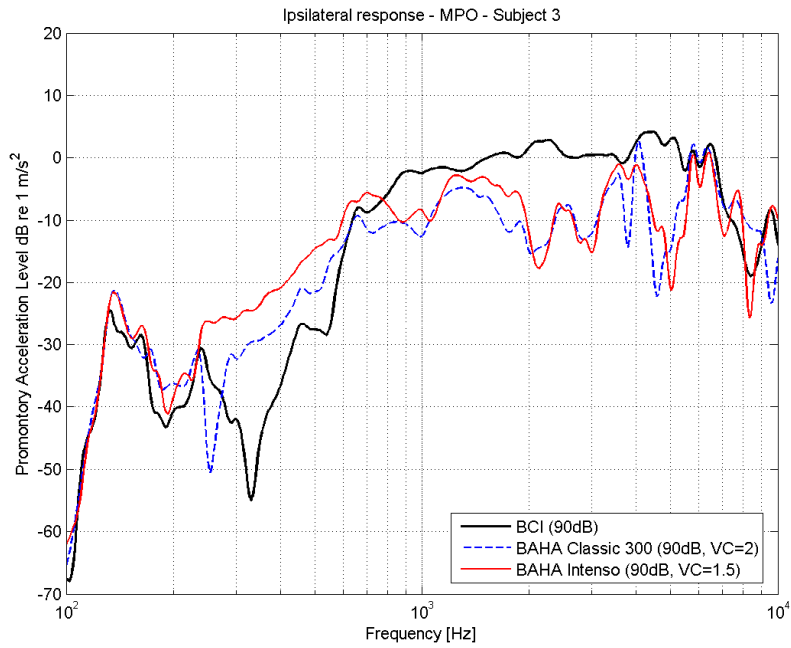


Figure 72: Comparison of the ipsilateral maximum power output for the BCI, BAHA Classic 300 and BAHA Intenso on subject 3.

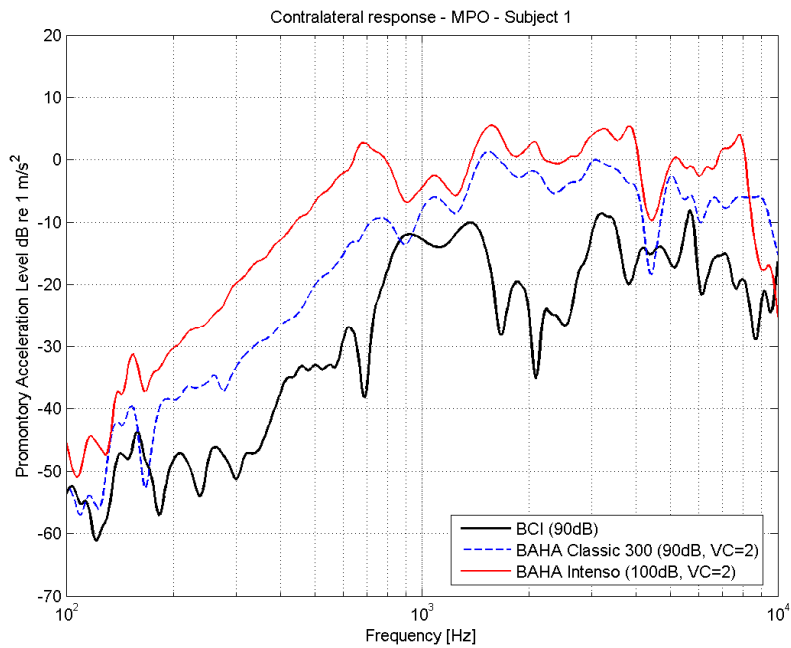


Figure 73: Comparison of the contralateral maximum power output for the BCI, BAHA Classic 300 and BAHA Intenso on subject 1.

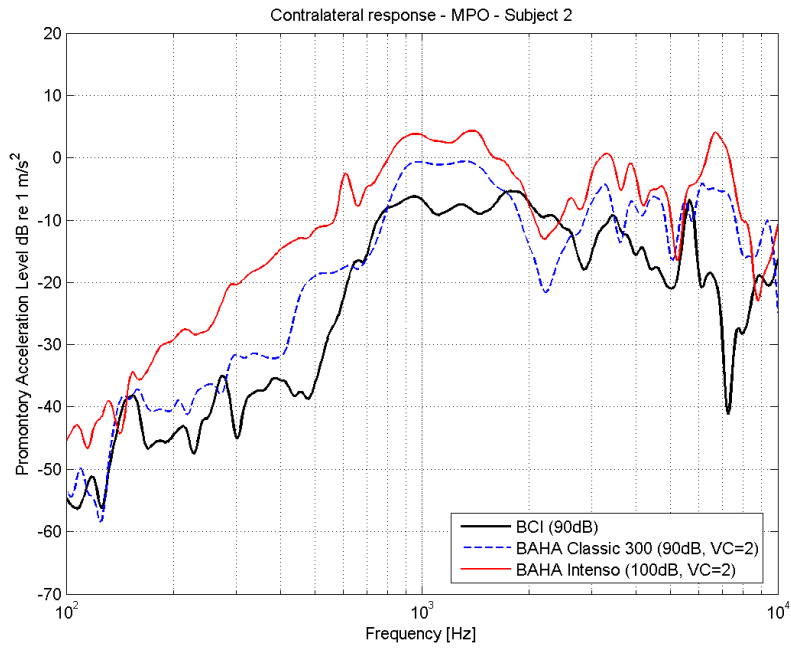


Figure 74: Comparison of the contralateral MPO for the BCI, BAHA Classic 300 and BAHA Intenso on subject 2.

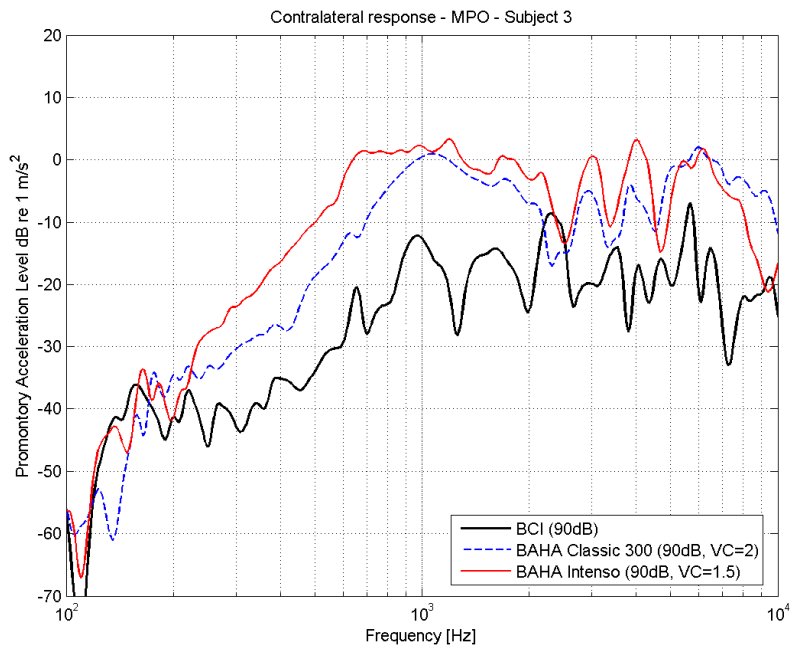


Figure 75: Comparison of the contralateral MPO for the BCI, BAHA Classic 300 and BAHA Intenso on subject 3.

To summarize the data from the figures above, the MPO differences between the BCI and the BAHA Classic 300 as well as the BCI and the BAHA Intenso are presented in Figure 76 to

79. In these figures, the differences are calculated based on an average MPO response over the three subjects for each of the devices.

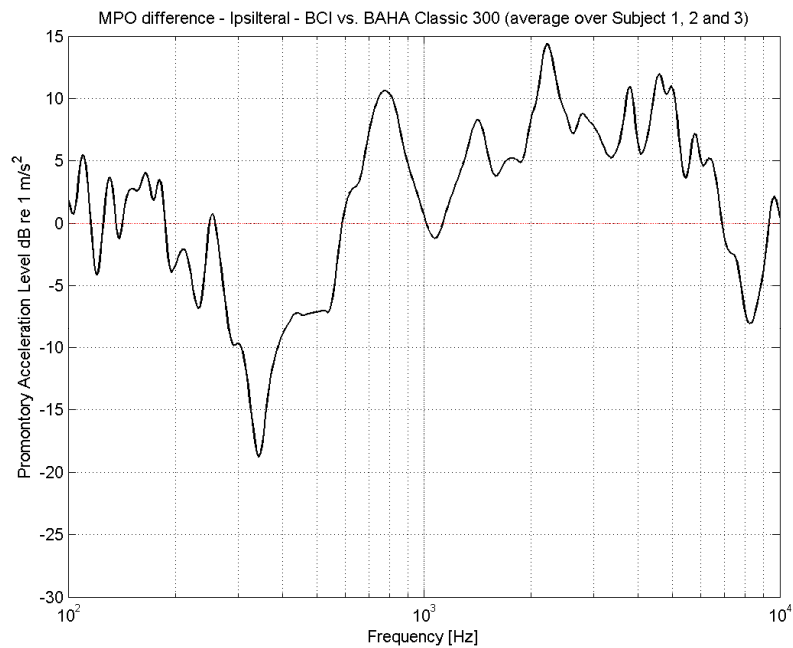


Figure 76: Difference in ipsilateral MPO comparing the BCI to the BAHA Classic 300. The curve is averaged over the three subjects.

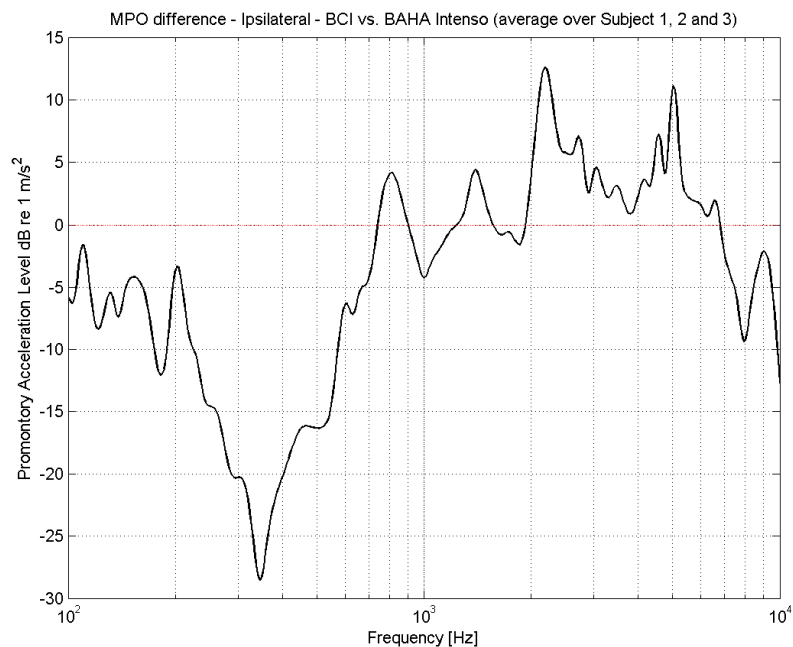


Figure 77: Difference in ipsilateral MPO comparing the BCI to the BAHA Intenso. The curve is averaged over the three subjects.

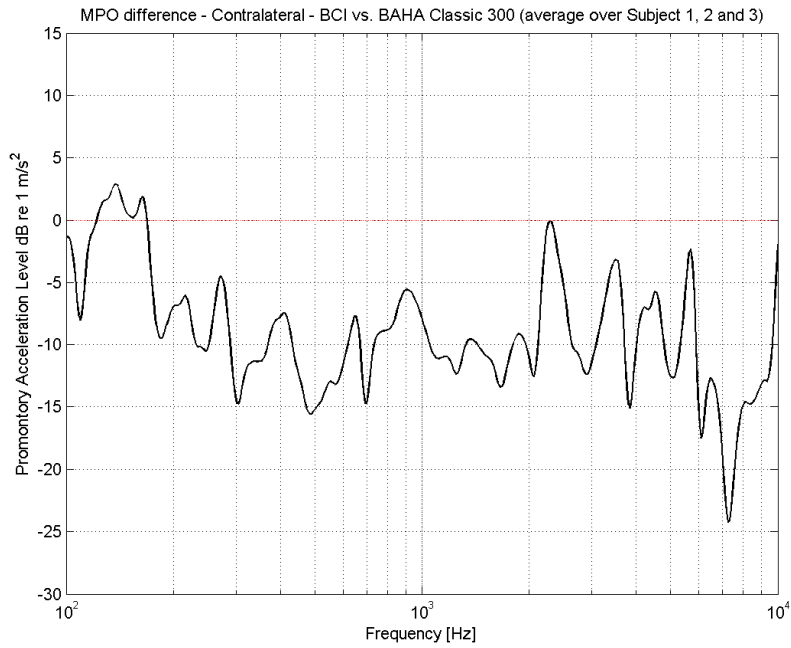


Figure 78: Difference in contralateral MPO comparing the BCI to the BAHA Classic 300. The curve is averaged over the three subjects.

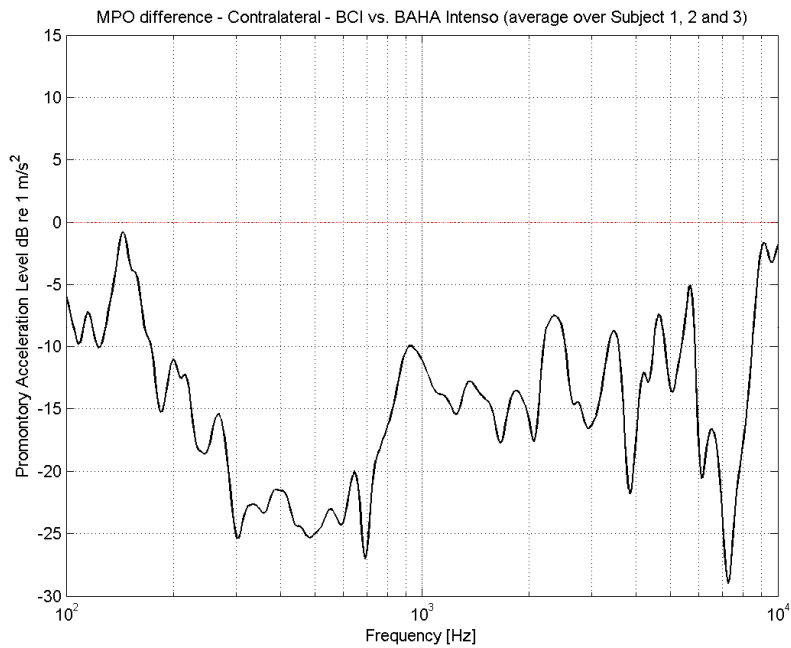


Figure 79: Difference in ipsilateral MPO, comparing the BCI to the BAHA Intenso. The curve is averaged over the three subjects.

To compare the transmission of vibrations ipsilaterally versus contralaterally, and investigate the effect of attachment position, these responses are plotted together in Figure 80 to 88 for

the BCI, the BAHA Classic 300 and the BAHA Intenso and presented for each of the three subjects.

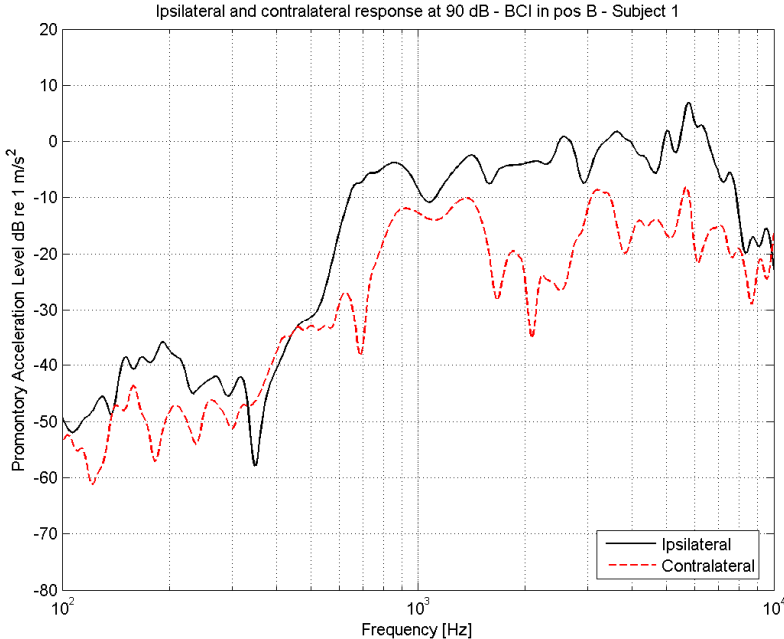


Figure 80: Comparison of the ipsilateral versus the contralateral promontory acceleration response for the BCI on subject 1.

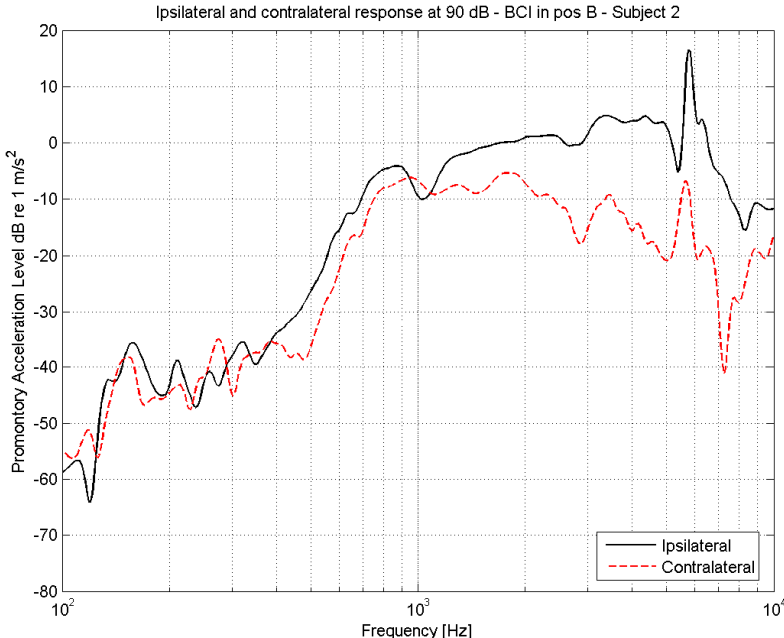


Figure 81: Comparison of the ipsilateral versus the contralateral promontory acceleration response for the BCI on subject 2.

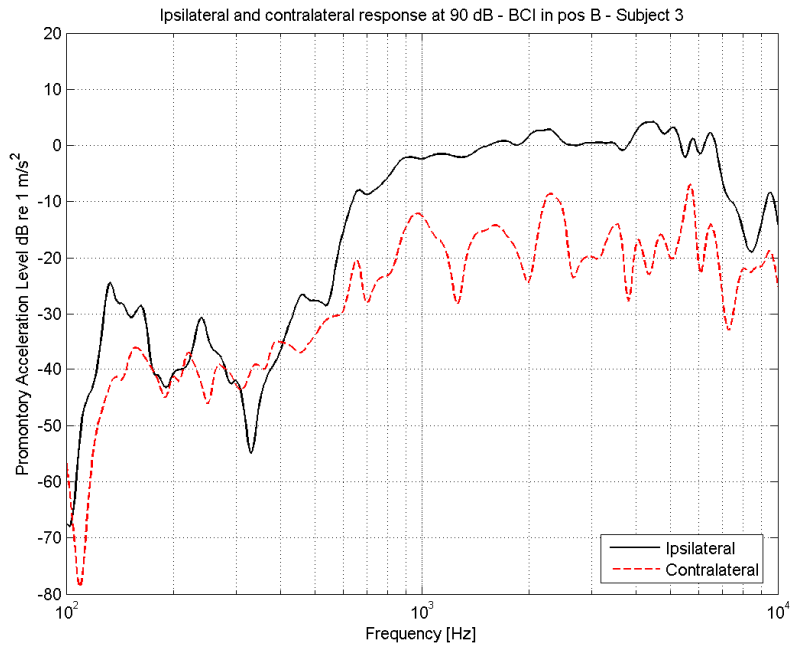


Figure 82: Comparison of the ipsilateral versus the contralateral promontory acceleration response for the BCI on subject 3.

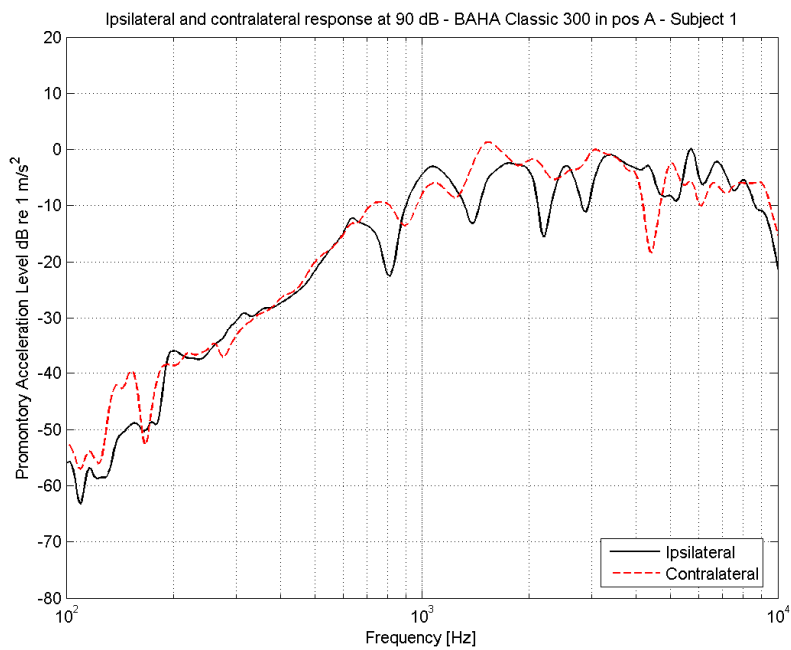


Figure 83: Comparison of the ipsilateral versus the contralateral promontory acceleration response for the BAHA Classic 300 on subject 1.

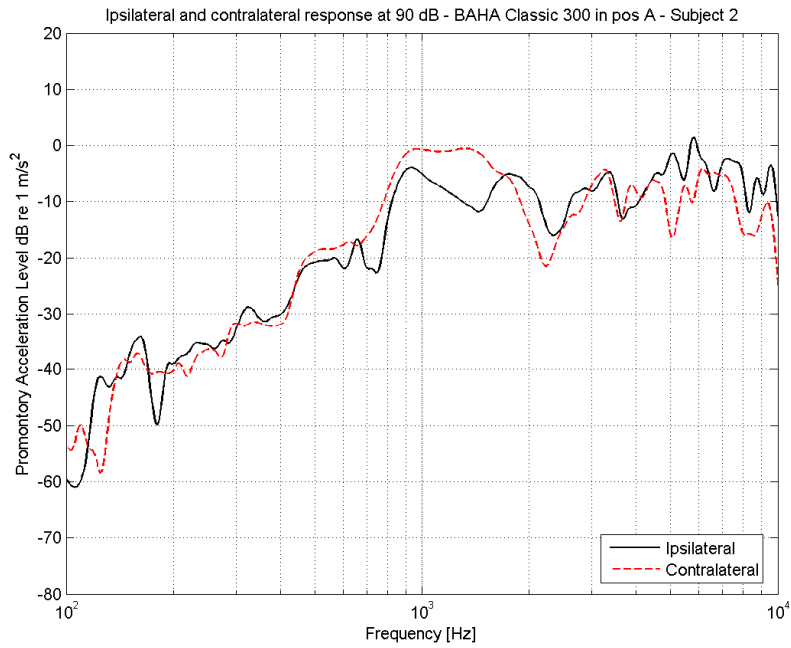


Figure 84: Comparison of the ipsilateral versus the contralateral promontory acceleration response for the BAHA Classic 300 on subject 2.

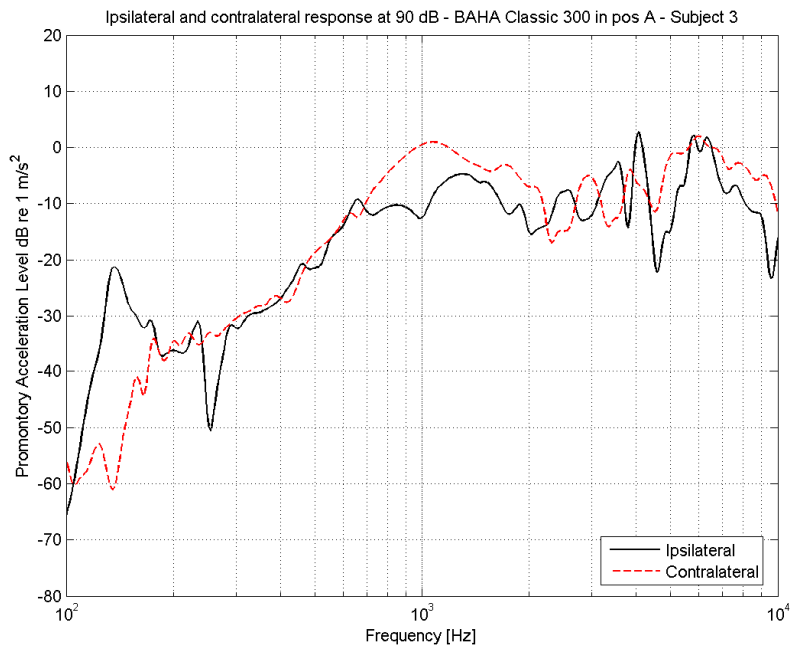


Figure 85: Comparison of the ipsilateral versus the contralateral promontory acceleration response for the BAHA Classic 300 on subject 3.

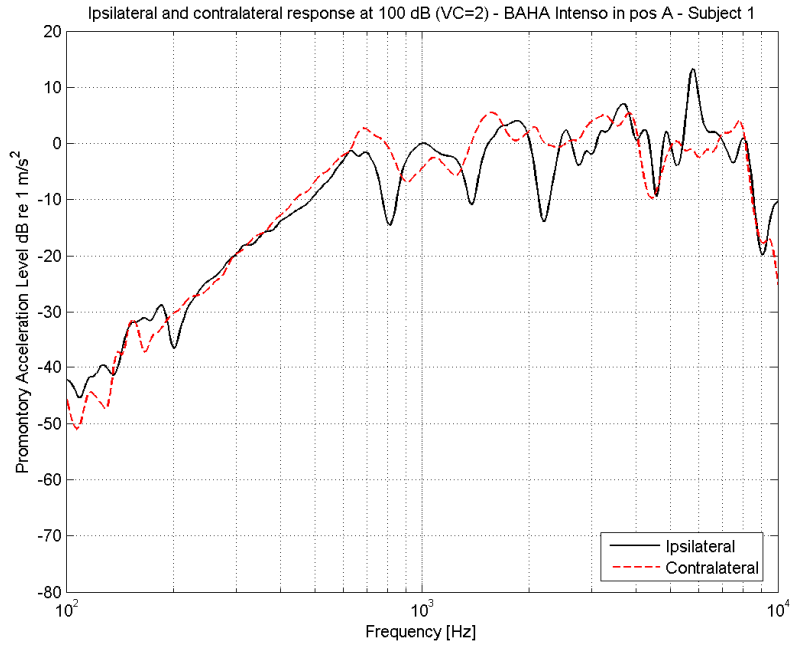


Figure 86: Comparison of the ipsilateral versus the contralateral promontory acceleration response for the BAHA Intenso on subject 1.

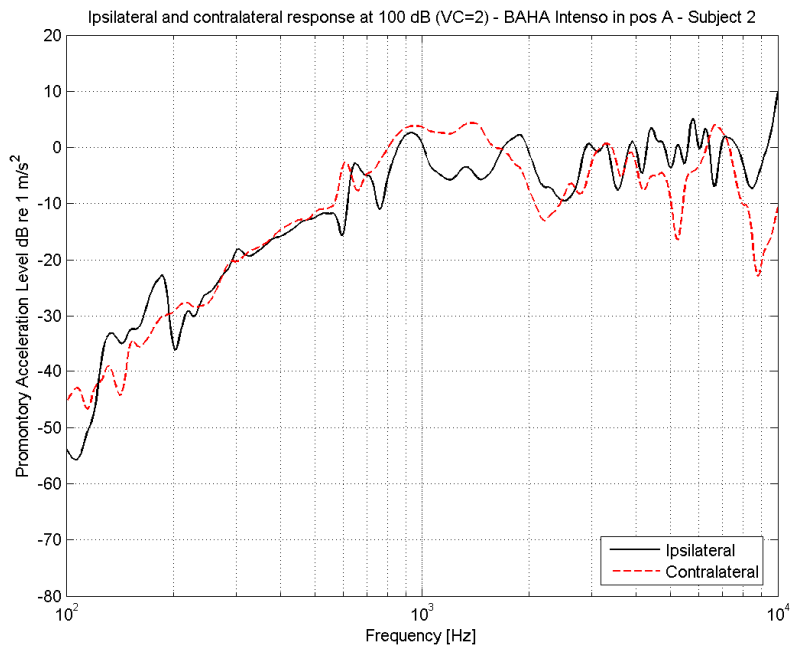


Figure 87: Comparison of the ipsilateral versus the contralateral promontory acceleration response for the BAHA Intenso on subject 2.

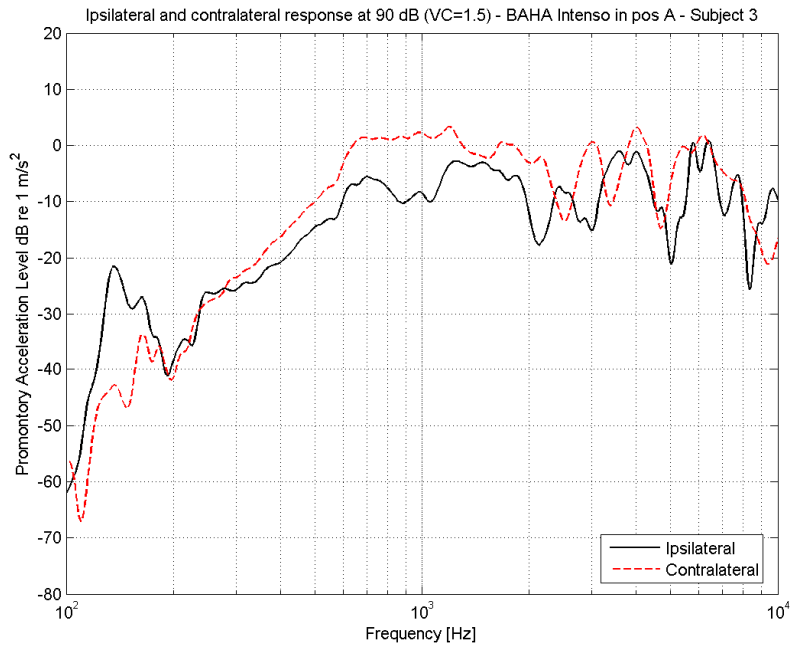


Figure 88: Comparison of the ipsilateral versus the contralateral promontory acceleration response for the BAHA Intenso on subject 3.

The figures above, representing ipsilateral versus contralateral frequency response, are also summarized in Figure 89 to 91 below, where the difference between the ipsilateral and the contralateral responses are presented, averaged over the three subjects and plotted together with their respective standard deviation.

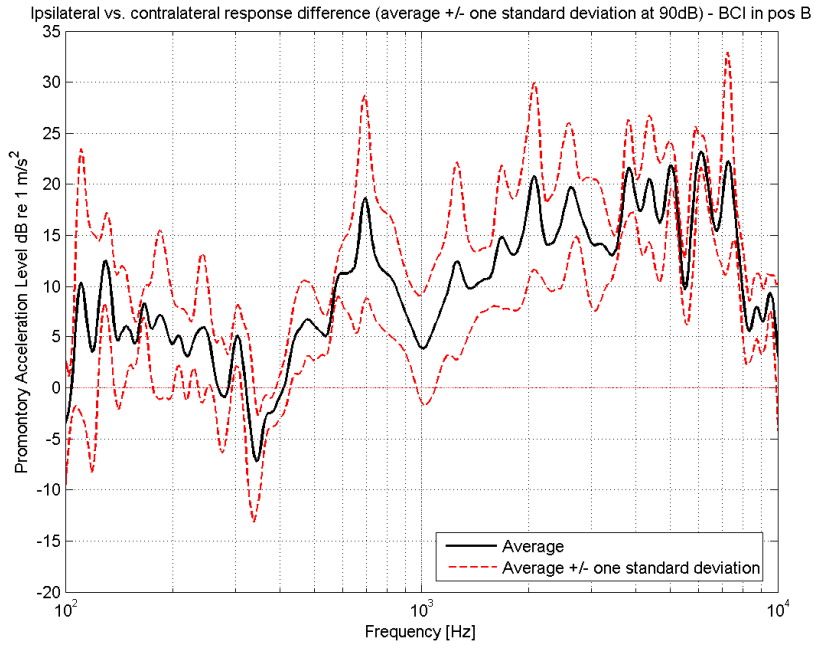


Figure 89: Difference in ipsilateral versus contralateral promontory acceleration response for the BCI in position B. The curve is averaged over the three subjects and presented together with its standard deviation.

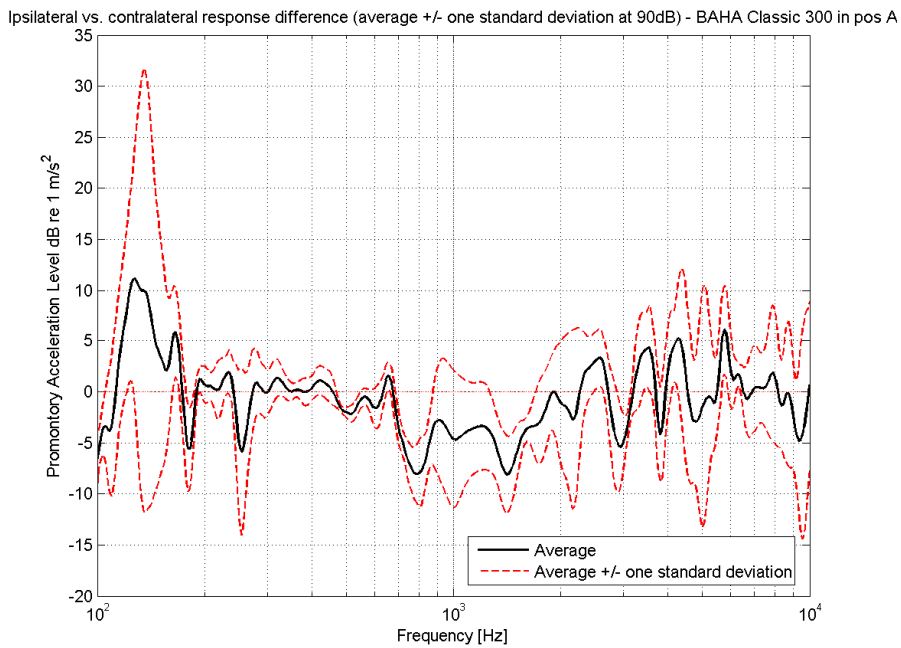


Figure 90: Difference in ipsilateral versus contralateral promontory acceleration response for the BAHA Classic 300 in position A. The curve is averaged over the three subjects and presented together with its standard deviation.

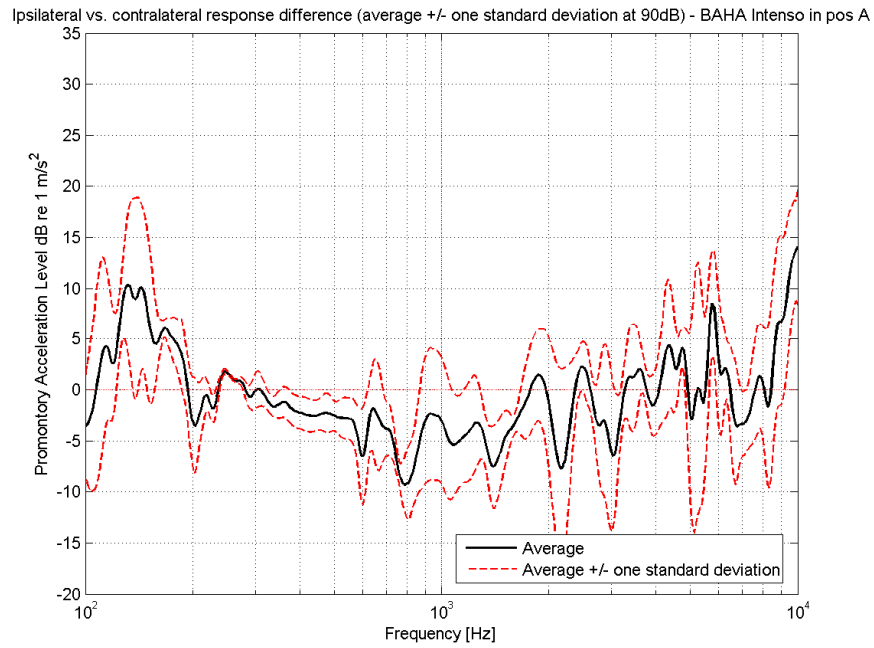


Figure 91: *Difference in ipsilateral versus contralateral promontory acceleration response for the BAHA Intenso in position A. The curve is averaged over the three subjects and presented together with its standard deviation.*

6 Discussion

The discussion is divided into subsections following the structure of the result section, discussing the results obtained from the Skull simulator measurements, the dry skull measurements and the cadaver head investigations.

6.1 Electrical impedance measurements

Electrical impedance measurements were carried out on both the Skull simulator and the dry skull to study variations in impedance relating to the object to which the transducer is attached. Seen from Figure 23 to 26, these measurements did not differ remarkably, hence no impedance measurements were obtained during the cadaver head investigations.

Comparing the impedance phase angles for the different transducers it can be seen that for high frequencies both of the BEST transducers stays close to 80° , whereas the BAHA transducers reaches a maximum of approximately 55° and then drops off. This indicates lower energy consumption for the BEST transducers for high frequencies considering the fact that a 90° phase angle implies a purely inductive behaviour and in this state no active power is consumed. The difference in phase angle can be explained by the BEST transducers' laminated iron core in the BEST, minimizing frequency dependent losses due to eddy currents and magnetic hysteresis.

A comparison of the impedance magnitudes shows that the BAHA Intenso has the lowest impedance, followed by both the BEST transducers and finally the Baha classic 300. These characteristics will also affect the transducers' power consumption and will be of importance when later comparing the results from the frequency response measurements.

6.2 Force output from Skull simulator

In general, the transducers' resonance frequency is designed to amplify the frequency range of human speech. This interval is believed to range from 400 to 500 Hz up to 5 to 6 kHz. As an interval for comparison, the bandwidth of today's telephone communication is 300 Hz to 3400 kHz. For lower frequencies, the presence of unwanted noise increases and hence the

amplification for these frequencies is kept low. This can be seen to be a common factor for all of the transducers [14].

From Figure 28 it can be seen that the maximum force output peak shifts in frequency between the transducers. The Baha Intenso is the most powerful transducer in the frequency range 100 Hz to 2 kHz, whereas the C-BEST is stronger between 2 kHz and 4 kHz. The location of the output force peak depends on the resonance frequency of the transducer. The resonance frequency of the C-BEST is designed higher up in frequency than the BEST90, resulting in an improved force output in the frequency range from 800 Hz up to 5 kHz, seen in Figure 29.

Relating the transducers' force output levels to the earlier discussed impedance measurements it can be seen that the BAHA Intenso, having the lowest impedance, generates the highest force output. A lower impedance results in a higher driving current and analogously a higher power consumption. By taking the transducers' respective input impedances (Z_{in}) into account when comparing the force output, the efficiency of the transducers can be compared. Figure 92 below presents the squared output force from the Skull simulator divided by the transducers' respective active power consumption, according to Eq.(10). The $(F_{skull})^2$ can be interpreted as the mechanical power out put ($P_{out,mech}$) to a normalized mechanical load ($Z_{load} = 1$), see Eq.(11). The figure is generated from the same data used for Figure 23 to 28.

$$\frac{F_{skull}^2}{P_{In}} = \left\{ P_{Active} = \frac{U_{in}^2}{|Z_{in}|} \cdot \cos(\theta) \right\} = \frac{F_{skull}^2}{U_{in}^2} \cdot \frac{|Z_{in}|}{\cos(\theta)} \quad (10)$$

$$P_{out,mech} = \frac{F_{skull}^2}{Z_{load}} = F_{skull}^2 \quad (11)$$

When the active power consumption is taken into account, it also includes an efficiency measure of the transducers. As seen in Figure 92 the superior force output of the BAHA Intenso, apparent in Figure 28 due to the lower impedance, is now changed as the high output had a cost high input power consumption. Also, the C-BEST's resonance peak at 3 kHz, seen in Figure 28, now appears even more distinct. This is because C-BEST here operates in a resonance region (all transducers are always more efficient in their resonance regions).

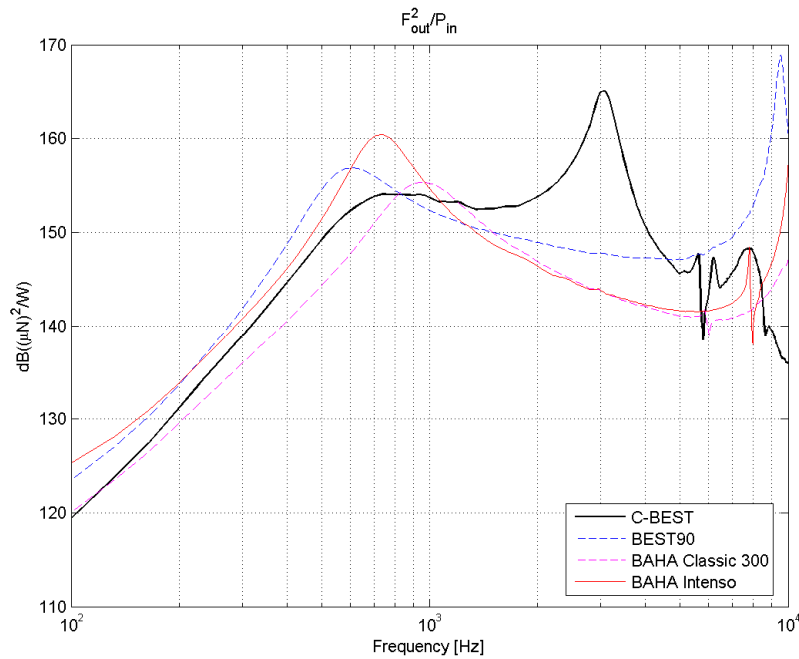


Figure 92: A quality of measure for the transducers presented as the squared force output from the Skull simulator divided with the transducer's respective active power consumption.

6.3 Frequency response from electrical stimulation on dry skull

To evaluate the attachment position of the transducers, the difference in frequency response between the BEST positioned in A and B is studied in the dry skull. From Figure 34, it can be seen that stimulation closer to the cochlea results in a higher ipsilateral promontory acceleration level from approximately 800 Hz and up. However, the results from the contralateral measurements in Figure 35 are inconclusive due to large variations concerning both stimulation positions.

Similar results are also apparent in Figure 32 to 33, where the differences in ipsilateral and contralateral frequency responses for all of the transducers are plotted with the C-BEST as reference. Regarding the ipsilateral measurements, the C-BEST is the most powerful transducer in the frequency range from 950 Hz up to 6 kHz. Compared to the BAHA Classic 300 and the BAHA Intenso, the C-BEST shows an approximately 5 – 10 dB higher promontory acceleration response. It can also be noticed that the C-BEST shows a 5 – 10 dB higher promontory acceleration response than the BEST in the entire frequency range from 100 Hz to 10 kHz. Even though the C-BEST and the BEST are not identical transducers, they

are still built around the same platform and this result indicates that promontory acceleration level benefits from stimulation closer to the cochlea.

Since the C-BEST is attached to the skull using a metal bar, pressing the transducer against the bottom surface of the recess, the possibility of the metal bar affecting the measurements was investigated. In Figure 93, measurements conducted both with and without the metal bar attachment are shown, showing negligible effect of the metal bar. However, both measurements are conducted using bone cement, keeping the transducer in place.

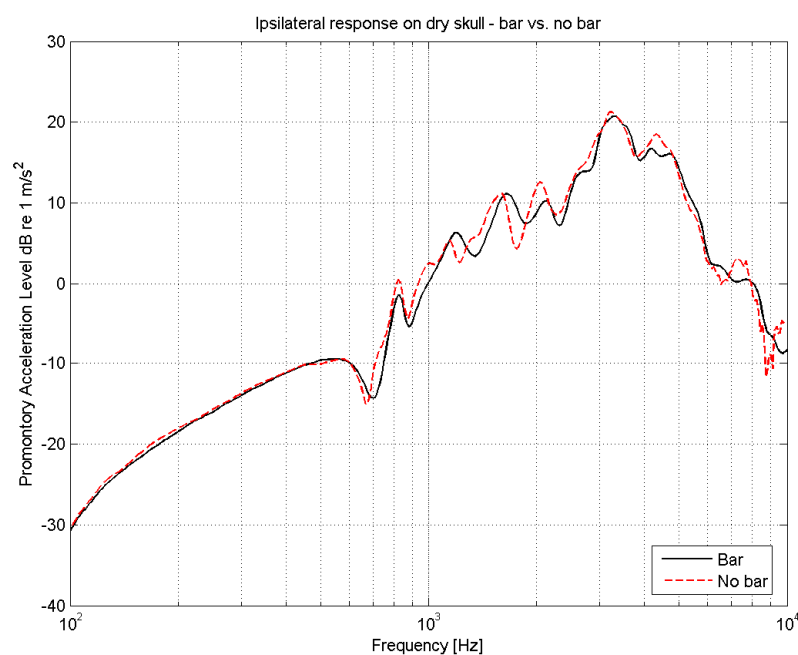


Figure 93: Influence of the metal bar used for attachment of the C-BEST.

6.4 Frequency response from acoustical stimulation on dry skull

All acoustical measurements involving the BCI are carried out using the MED-EL inductive link. Studying the difference between the electrical measurements with the C-BEST and the acoustical MPO results for the BCI, the loss in the inductive link can be seen. Figure 94 below shows a decreased promontory acceleration level of approximately 10 to 15 dB due to the inductive power transfer.

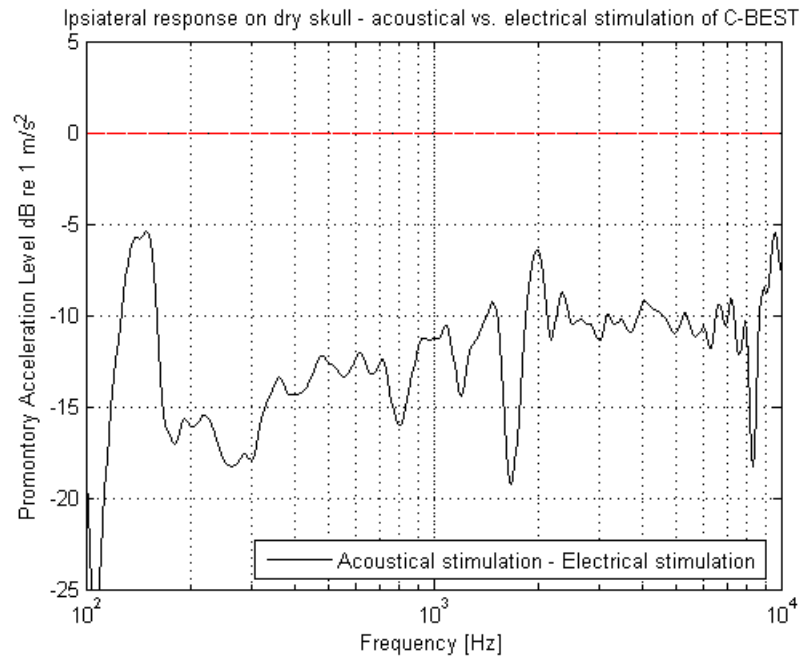


Figure 94: *Difference in ipsilateral promontory acceleration level between electrical and acoustical stimulation of the C-BEST, corresponding to the loss in the inductive energy transfer link across the skin.*

During the acoustical measurements, recurring problems with acoustical feedback for the BAHA Classic 300 and the BAHA Intenso was noticed, giving a howling sound with increasing amplitude. This implied that the use of full on gain for these transducers were not possible. The problem may be a result of that the amplification is optimized to give as high amplification as possible for full-on gain without the system oscillating, analogously the open-loop gain is designed close to unity. With objects in the vicinity the microphone, which is the case in the laboratory, reflecting sound waves from the speaker can cause the margin before oscillation criteria be exceeded, hence generating the howling sound [15]. To overcome this problem, the volume setting for the BAHA Classic 300 had to be set to 2. The feedback problem was never noticed for the BCI system, hence giving the possibility of maybe using a higher default volume setting.

Both the ipsilateral and contralateral frequency response measurements for the BCI and the BAHA Classic 300, Figure 36 to 39, seem to be linear up to 70 dB. When the sound pressure level is increased to 90 dB, both devices appear to operate in saturation, hence allowing comparison of the transducers' MPO.

When comparing the BCI and the BAHA Classic 300 on the dry skull, in terms of ipsilateral MPO response, the BAHA Classic 300 shows a higher response in the frequency range from 120 Hz to 1 kHz.

For higher frequencies similar response from both transducers are obtained. Regarding the contralateral measurements, the BAHA Classic 300 in general show a 5 to 10 dB higher frequency response than the BCI, well in accordance with the loss in the inductive link.

It should be mentioned that the dry skull seem to underestimate the promontory acceleration level at low frequencies as compared to the cadaver measurements discussed in the next section.

6.5 Frequency response from electrical stimulation on cadaver

The results from the electrically stimulated transducers included in the cadaver head investigation, indicates less variation in ipsilateral frequency response among subjects for the C-BEST in position B than for the BEST in position A. This result can be a consequence of that the C-BEST is attached to more compact bone than the BEST, resulting in that the exact attachment position for the C-BEST is of less importance.

Regarding the variation in contralateral frequency response among subjects, large variations can be observed for both the C-BEST and the BEST. Some of the variations associated with the C-BEST can be explained by varying antiresonances among the subjects, by comparing the electrical and acoustical results. Looking at Figure 44, the dip at 1.2 kHz for subject 3 can also be seen clearly in Figure 63, for the acoustical measurements. The huge dip reaching from approximately 1.4 up to 3 kHz for subject 1 in Figure 44, can also be found similar in Figure 65. Due to that no acoustical measurements were performed for the BEST, no such comparison could be made for this transducer.

Similar to the dry skull measurements, the C-BEST shows an increased acceleration level at the promontory for all of the three subjects in the frequency range from 500 Hz up to 9 kHz compared to the BEST, verifying the benefit of the of stimulating closer to the cochlea.

Electrical stimulation of the C-BEST and the BEST also enables a comparison of the anchoring positions A and B, considering only the physiological aspect of the skull. Since the C-BEST and the BEST are based around the same platform, but C-BEST have a high

frequency resonance at 3 kHz, and therefore with this in mind can be treated as basically the same transducer.

Figure 95 below covers two different approaches for this investigation. The leftmost plot shows the ipsilateral versus contralateral promontory acceleration level difference, when stimulation is applied to position A respective position B. These curves are completely independent of which transducer is used. The rightmost plot however, presents the difference in stimulation position, A versus B, treating the ipsilateral and contralateral responses separately. Here the difference in performance between BEST and C-BEST (see Figures 28 and 29) will influence the results. Both plots show the averaged curves over the three subjects.

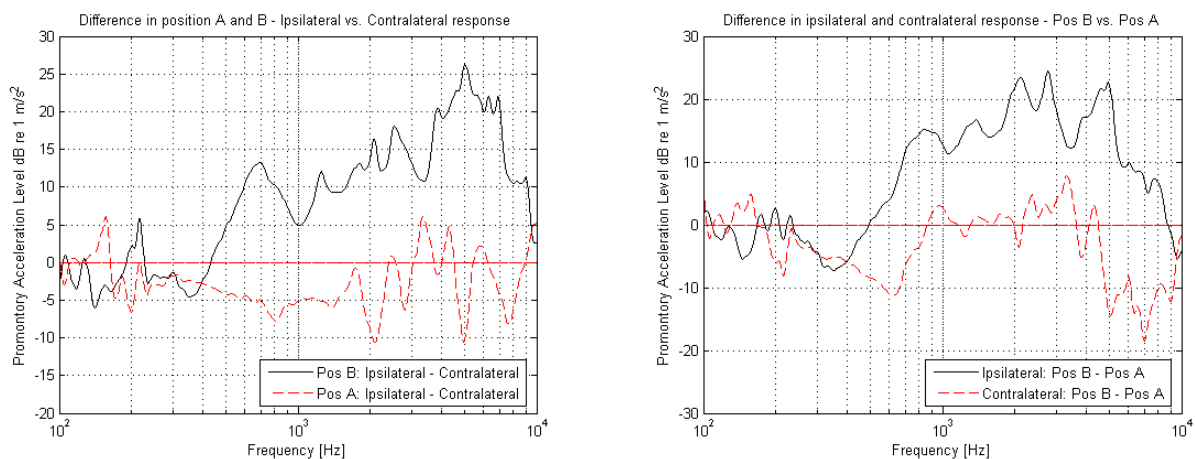


Figure 95: Comparison of anchoring position A and B, considering only the physiological aspect of the skull.

The result confirms previous assumptions, that stimulation closer to the cochlea, position B, results in a higher ipsilateral promontory acceleration response than stimulation in the traditional BAHA position, position A.

Since the traditional titanium screw anchoring was abandoned in favour for the flat surface attachment of the C-BEST, it was desirable to achieve a smooth attachment surface. For this purpose bone cement was used to mimic the process of the regrowth of bone in the area of the implant. However, measurements conducted with and without the use of bone cement, ipsilaterally and contralaterally, showed no direct advantage of using bone cement, as shown in Figure 96 below.

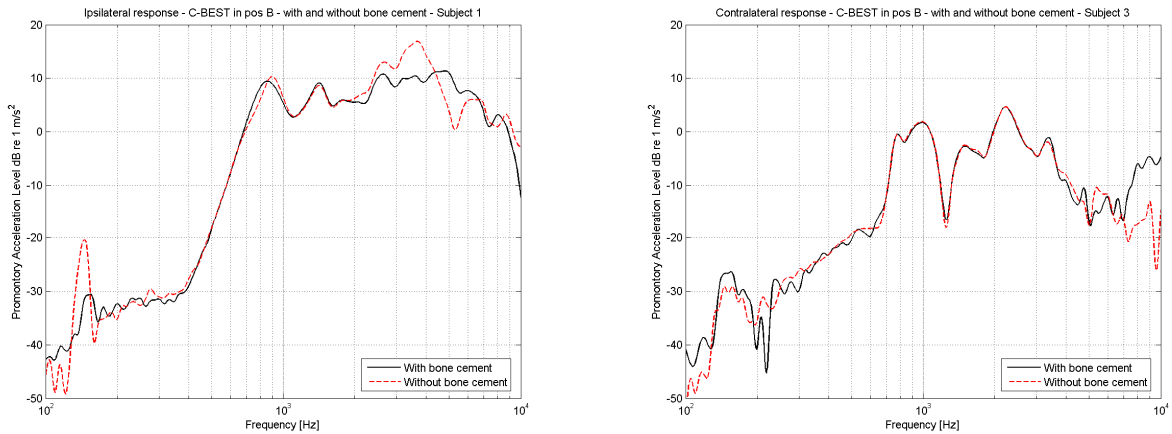


Figure 96: The influence of the bone cement used to create a smooth attachment surface when anchoring the C-BEST. Measurements were conducted both with and without the bone cement on two of the subjects and the both the ipsilateral and contralateral responses were studied.

To assure that the recess, made for attachment of the C-BEST, had no influence on the measurements dealing with the transducers anchored the titanium screw in position A, due to absence of bone tissue, repetitive measurements were conducted for the BEST both before and after the recess was made. Results from these measurements are shown in Figure 97. These measurements validates that the absence of bone tissue due to the recess have only minor effect the other measurements on the ipsilateral side whereas the effect is negligible on the conralateral side.

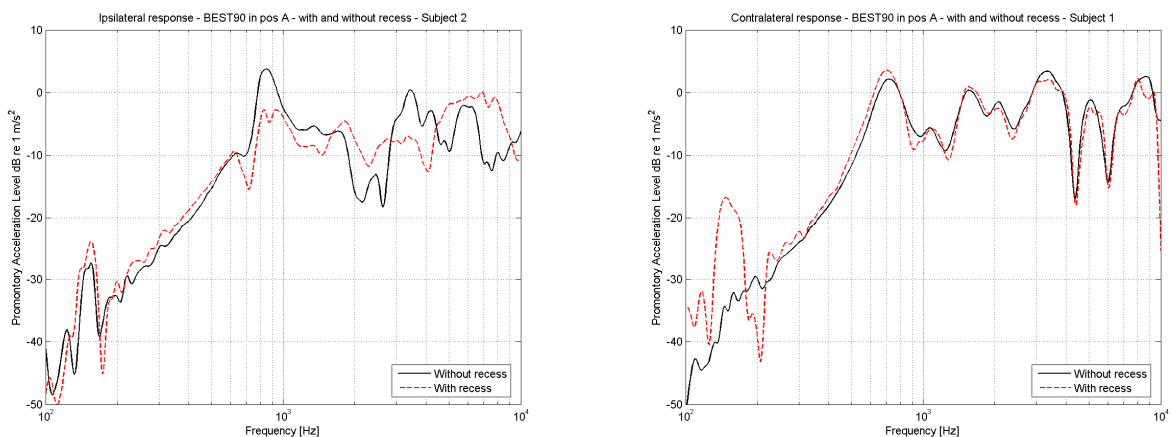


Figure 97: Measurements conducted both before and after the recess for the C-BEST was made.

6.6 Frequency response from acoustical stimulation on cadaver

The first observation regarding the acoustical measurements at Sahlgrenska, was the effect of the complex acoustical environment when a constant SPL was desired. The hard surfaces in the examination room did not only set demands on the equipment regulating the sound

pressure, but did also contribute to the presence of acoustical interference at certain frequencies. Acoustical interference can contribute to an increase in frequency response without being noticeable in the SPL curves, making it hard to trace back in the post-processing of the data. The demanding measurement environment is however visualized by comparing the sound pressure level regulation in the room at Sahlgrenska with the more controlled laboratory room at Chalmers, presented in Figure 98 below.

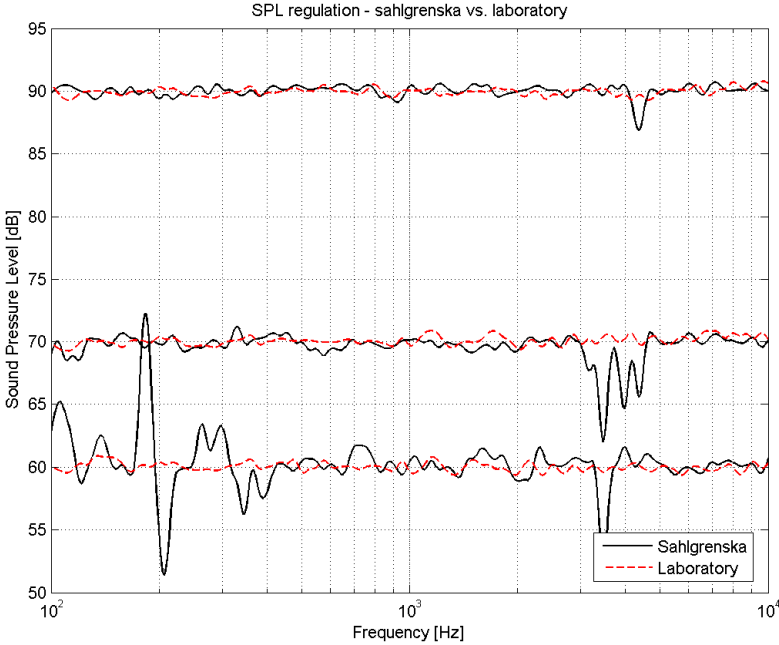


Figure 98: Measured sound pressure levels for regulation of the acoustical stimulation of the transducers, both at Sahlgrenska and in the laboratory, showing the demanding acoustical environment at the hospital.

The background noise in the room at Sahlgrenska was also measured to assure that the influence of the room acoustics had a negligible impact on the measurements. In Figure 99 these measurements presented, showing that the noise level is well below the bottom stimulation level, 60 dB SPL.

In the same figure, the background noise level in the laboratory at Chalmers is also included for comparison.

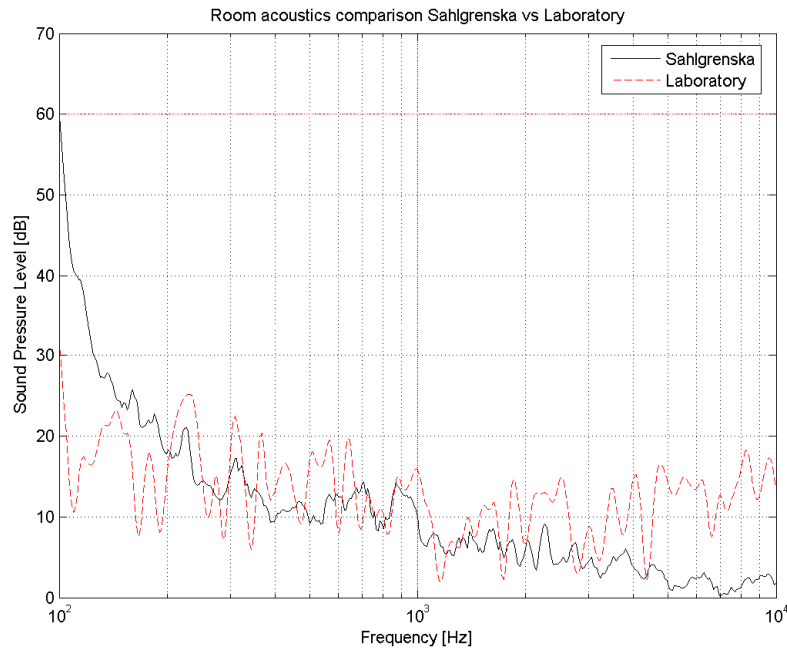


Figure 99: Measured background noise at Sahlgrenska and in the laboratory.

Another measurement conducted prior to the actual measurements on the cadavers at Sahlgrenska was the calibration of the reference microphone. This measurement was also repeated after all measurements were conducted, for validation. Both calibrations can be seen in Figure 100.

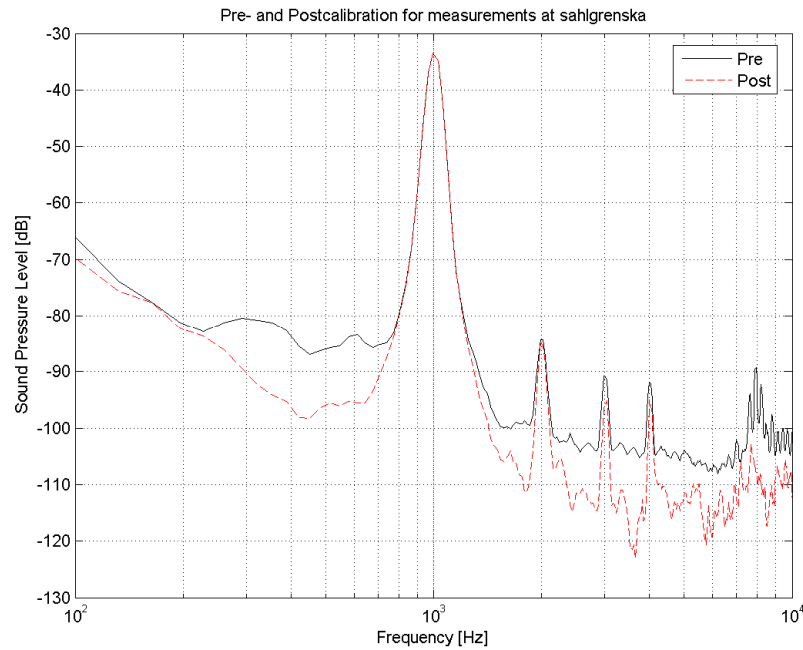


Figure 100: Calibration of the condenser microphone was performed both before and after the actual measurements at Sahlgrenska, to assure proper regulation of the sound pressure levels.

Similar to in the laboratory measurements, problems with acoustical feedback was noticed for both the BAHA Classic 300 and the BAHA Intenso. The volume control settings had to be kept at a maximum of 2 (total range 0-3) to avoid this problem. Again, no such behaviour was noticed for the BCI. This might imply that the BCI has larger stability margins before oscillation i.e. the open-loop has greater margin to unity gain. A redesigned driving unit might thus allow further amplification when used in combination with the C-BEST attached to position B.

The cadaver head investigation involved measurements performed on three subjects in order to achieve same statistical information but more subjects need to draw statistically based conclusions. By comparing deviations between subjects a more realistic understanding of the generic differences in the performance of the devices are obtained.

Comparing the BCI and the BAHA Classic 300 in terms of ipsilateral maximum power output, Figure 76, the BCI shows a fluctuating but on the average 5-10 dB higher promontory acceleration level than the BAHA Classic 300 in the frequency range 600 Hz to 7 kHz. The same comparison with the BAHA Intenso, Figure 77, shows an also fluctuating 0 -5dB higher promontory acceleration level in the frequency range between 700 Hz and 7 kHz. The

contralateral frequency response differences, Figure 78 to 79, show a significantly lower response for the BCI compared to both the BAHA Classic 300 and the BAHA Intenso.

Further, from Figure 89, comparing ipsilateral and contralateral frequency response for the BCI averaged over the three subjects, it can be seen that the contralateral frequency response is significantly lower than the ipsilateral response. For the BAHA Classic 300 and BAHA Intenso, Figure 90 and 91, it is just the opposite, the contralateral response is higher than the ipsilateral response in the frequency range from approximately 300 Hz up to 3 kHz. To have a low contralateral response comparing with ipsilateral response is not only unappreciated, it profits the ability of binaural hearing described in the hearing physiology chapter. As long as the ipsilateral response is sufficiently high and normal hearing in the contralateral ear.

Combining the electrical and acoustical results, a generally smoother ipsilateral frequency response is obtained from stimulating in position B than in position A. This implies that stimulation closer to the cochlea means less sensitivity to antiresonances in the skull. On the other hand, position A has a superior contralateral transmission ability compared to position B, making stimulation in position A well suited for patients suffering from for example single sided deafness.

Comparing the ipsilateral frequency responses for the BCI, Figure 52 to 54, with similar measurements from previous year's master thesis [16], at that time with the BCI attached to position B using the titanium screw snap coupling, similar results can be seen. This observation motivates the replacement of the titanium screw attachment with a flat surface attachment for the BCI. The surgical procedure involved with the implantation of the BCI would here by result in a lowered risk of complications, due to that it is implanted not so deep into the temporal bone with a lower risk of damaging the facial nerve and the vestibular organ.

The results from this master thesis indicate that a transcutaneous implantable bone conducted hearing aid (BCI) can be a realistic alternative to today's percutaneous BAHA systems. Furthermore, an additional study is made in parallel with this master thesis, concentrating on the inductive link supplying the C-BEST. With an improved inductive energy transfer, the BCI has the qualifications of being a very strong competitor to today's existing systems.

7 Conclusion

- The BCI had 5-10 dB higher ipsilateral MPO promontory acceleration level than the Classic 300 in the range 700-7k Hz.
- The BCI had approximately 0 - 5 dB higher ipsilateral MPO promontory acceleration level than the Intenso 700-7k Hz.
- The contralateral MPO promontory acceleration levels are considerably lower for the BSI than for the BAHA Classic 300 and BAHA Intenso.
- For the BAHA Classic 300 and the BAHA Intenso the contralateral response is the same or higher than the ipsilateral response for frequencies from 700-5k Hz
- The results in this study indicates that the screw attachment used in a previous studies can be replaced with a flat surface attachment under static pressure which has a lower profile and is safer to install.
- It was shown that any bone cement for creating a smooth attachment surface between the pneumatized bone bed was not needed.
- It was experienced that the BCI was not suffering from any feedback problems for the preset gain whereas both the BAHA Classic 300 and the BAHA Intenso could not be used at full on gain (volume 3) because of feedback.
- The responses from the electrical stimulations indicate that the C-BEST have an improved high frequency response as compared with the BEST that was verified on Skull simulator measurements.

8 References

Literature, written papers and internet sources

- [1] Reinfeldt S. (2006) Bone conducted soundtransmission for communication systems, Lic Thesis. Chalmers University of Technology, Guthenburg, ISSN 1403-226X
- [2] Siemens Hearing Instruments, Binaural Vs. Bilateral, Retrieved September 03, 2008 from http://www.siemens-hearing.com/hearing_instruments/products/acuris_binauralVsBilateral_p.aspx
- [3] Håkansson B. (2003) The balanced electromagnetic separation transducer – A new boneconduction transducer, J. Acoust. Soc. Am. 113(2)
- [4] Andersson A. and Östli P. In vitro investigations of a mastoid anchored transcutaneous bone conduction hearing system, Master Thesis at Chalmers University of Technology, Gothenburg, EX089/2007.
- [5] VIBRANT MED-EL. Technology & Capabilities Description, Retrieved August 10, 2008 from <http://www.vibrant-medel.com/Shared/PDF/Professional/Info/Technology.pdf>
- [6] Cochlear. BAHA Intenso, Retrieved September 03, 2008 from <http://www.cochlear.co.uk/Products/2279.asp>
- [7] Cochlear. Introduction to BAHA, Retrieved July 08, 2008 from <http://www.cochlear.co.uk/Products/1755.asp>
- [8] Agilent Technologies (2008). Agilent 35670A Dynamic Signal Analyzer Product Overview, Retrieved July 2, 2008 from <http://cp.literature.agilent.com/litweb/pdf/5966-3063E.pdf>.
- [9] Agilent Technologies (2007). Agilent I/O Hardware Family Datasheet, Retrieved July 12, 2008 from <http://cp.literature.agilent.com/litweb/pdf/5989-1889EN.pdf>

- [10] Media Collage. Condenser Microphones, Retrieved July 15, 2008 from:
<http://www.mediacollege.com/audio/microphones/condenser.html>
- [11] Håkansson B. and Carlsson P. (1989) Skull simulator for Direct Bone Conduction Hearing Devices. Chalmers University of Technology, Gothenburg.
- [12] Ostell, How do you determine implant stability? Retrieved August 20, 2008 from
<http://www.osstell.com/filearchive/2/2528/Low%20Ostell%201.pdf>
- [13] Ostell, Clinical Manual. Retrieved August 20, 2008 from
http://www.osstell.com/filearchive/2/2540/ID_25006-0_Clin_Manual.pdf
- [14] Adin H. (2002) Ringsimulator, Retrieved July 20, 2008 from www.diva-portal.org/diva/getDocument?urn_nbn_se_liu_diva-1098-1__fulltext.pdf
- [15] Nils W. (2006) COUNTERACTING ACOUSTIC DISTURBANCES IN HUMAN SPEECHCOMMUNICATION Retrieved August 1, 2008 from
[http://www.bth.se/fou/forskinfornsf/0/343efb30a0905236c125715d002ec160/\\$FILE/Westerlund_diss.pdf](http://www.bth.se/fou/forskinfornsf/0/343efb30a0905236c125715d002ec160/$FILE/Westerlund_diss.pdf)
- [16] Magnus S. and Maria S. Percutaneous vs transcutaneous bone conduction hearing systems - Cadaver head investigations and heat aspects, Master Thesis at Chalmers University of Technology, Gothenburg, EX086/2007.

Appendix A

8.1 Data acquisition using Labview

Labview is a graphical programming environment supporting access to instrumentation hardware. The program is divided into two main components, the Front Panel, representing the graphical user interface, and the Block Diagram, where functions and components are wired together in the form of graphical blocks. In this thesis Labview 8.5 was used to develop an application communicating with the Agilent 35670A to facilitate the process of transferring measured data from the instrument to the computer using the instrument's GPIB port.

The user interface, or the application's Front Panel, is shown in Figure 101 including a graph for visualization of the transferred data to ensure that it matches the desired trace of the instrument. It also includes a prompt for saving the received data to a text document and a menu for selecting which trace to be transferred.

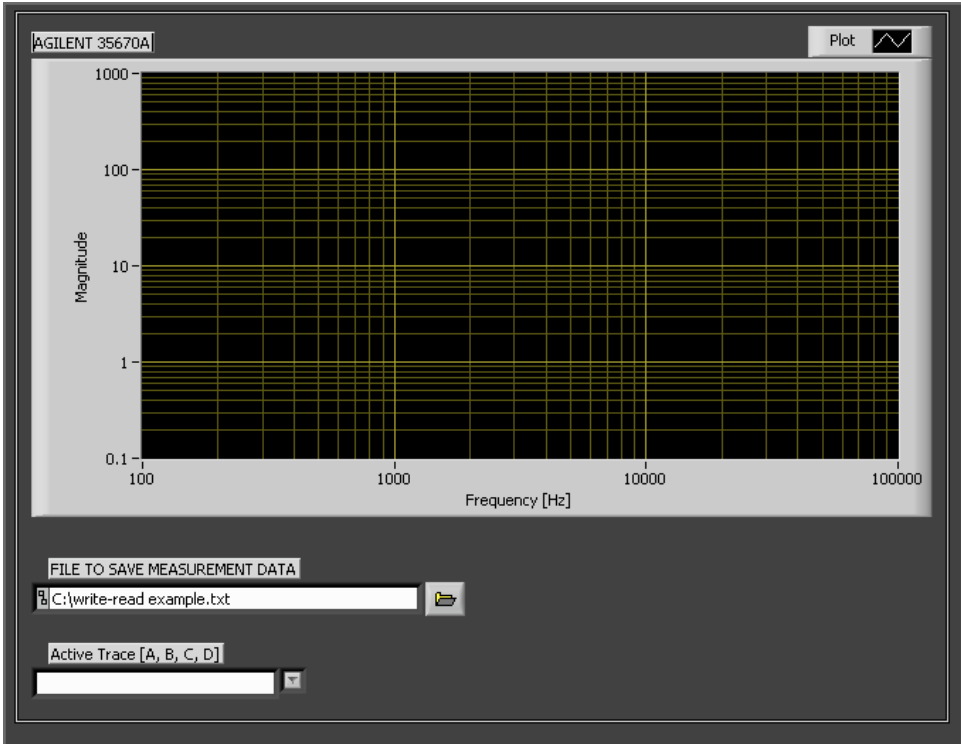


Figure 101: Front Panel

Figure 102 shows the first frame in a stacked programming structure. The structure is sequentially executed and this frame executes the first GPIB interaction command. The command FORM ASC is sent to GPIB address 11 to tell the instrument to send data in ASCII format. This frame also includes some blocks of purely esthetic nature, to control the coloring of the front panel.

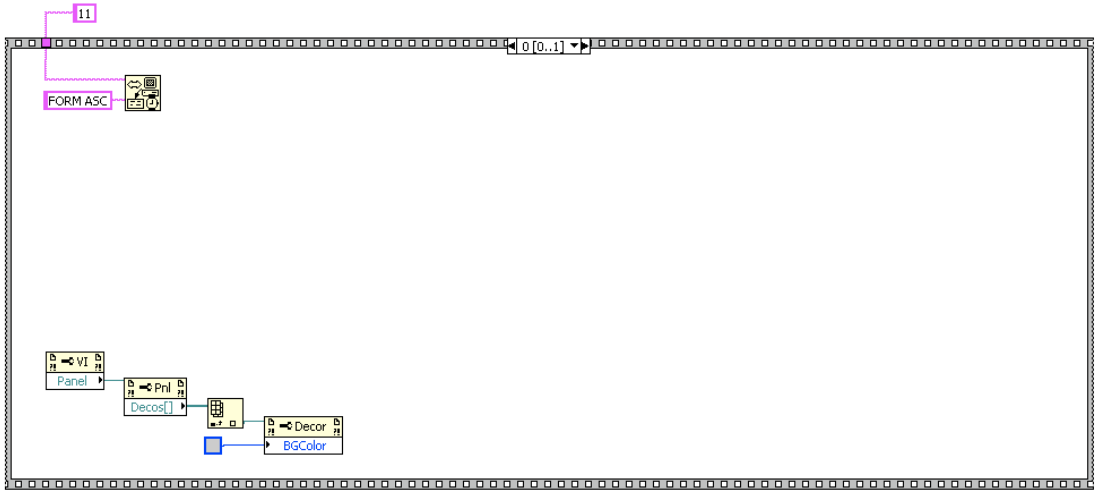


Figure 102: Block diagram view 1.

The second frame of the outer programming structure, shown in Figure A.3, also includes an interior sequential structure. By using an interior sequential structure, objects requiring accessibility from multiple sequences can be placed outside this interior structure. The first frame of the interior sequential structure asks the instrument for the data on the x-axis by sending the command CALC:X:DATA? to GPIB address 11. Reading a string from the same GPIB address then transfers the x-axis data, as shown in Figure 104.

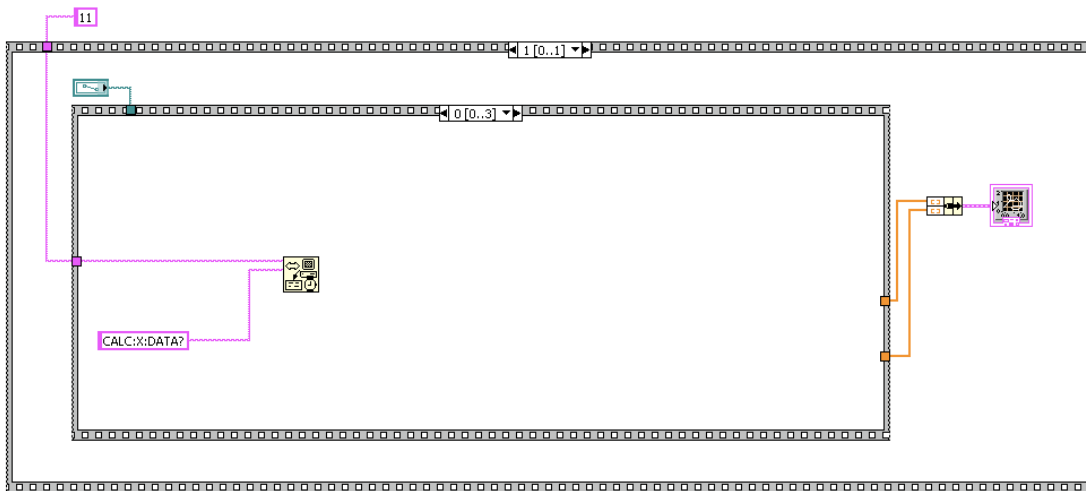


Figure 103: Block diagram view 2.

The data is then manipulated by replacing all commas with a blank space before saving the data to the location specified in the Front Panel. This facilitates the importing process when the data is used together with for example MATLAB . The received data is simultaneously processed in a while-loop structure, extracting the numbers from the string and adding them into an array of numbers format. This array is then sent outside the interior sequence to represent the x-values shown on the Front Panel. This process is shown in Figure 104.

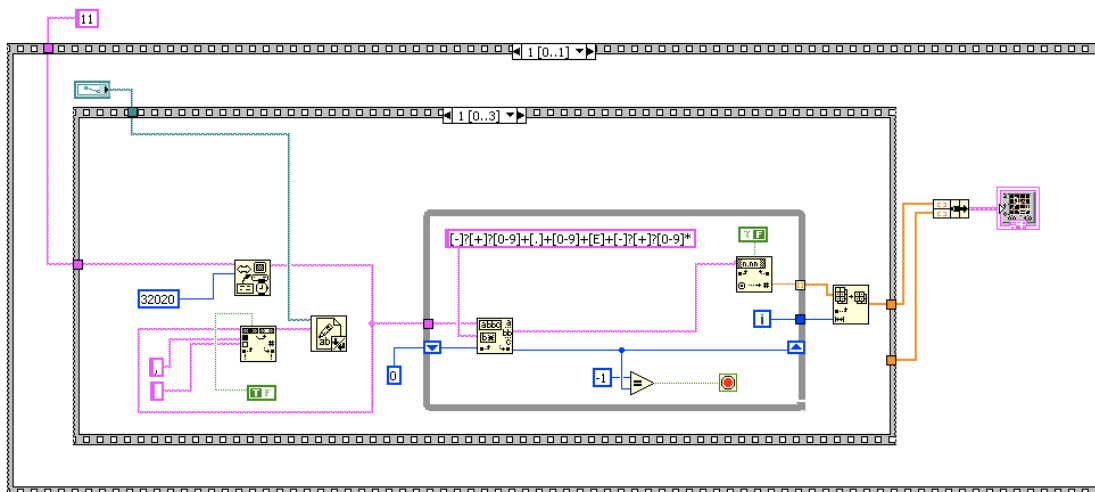


Figure 104: Block diagram view 3.

The purpose of the frame presented in Figure 105 is two things. The first is to separate the now transferred x-values from an upcoming set of y-values. This is done by opening the existing file, containing all the x-values, and changing the position of the current file mark to the end of the document, preventing the x-values from being overwritten by the new set of y-

values. This frame also sends a query command for the y-values for one of the instrument's four traces, specified by the user on the Front Panel. The command used for requesting the y-values is `CALC<n>:DATA?`, where `<n>` is the user specified trace number (1 to 4) corresponding to trace A to D on the instrument.

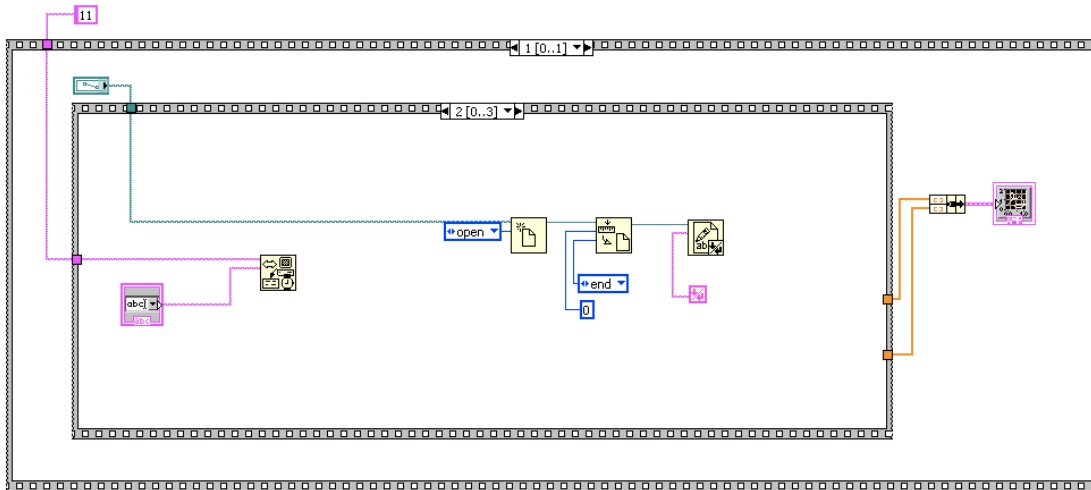


Figure 105: Block diagram view 4.

The next frame, shown in Figure 106, has the same functionality as Figure 104, but now considering the y-values. The data is collected as a string, manipulated by replacing commas with blank spaces and saved by appending the data to the existing file containing the x-values. As before, the data is added to an array of number format and sent outside the interior sequence. The y-values are then combined with the x-values to form a bundle, which is sent to the xy-graph to be visualized on the Front Panel.

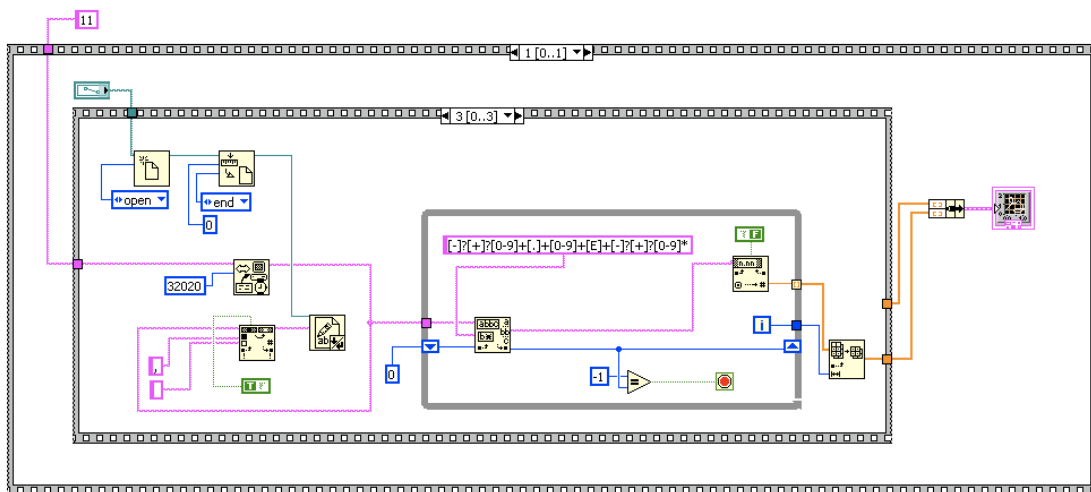
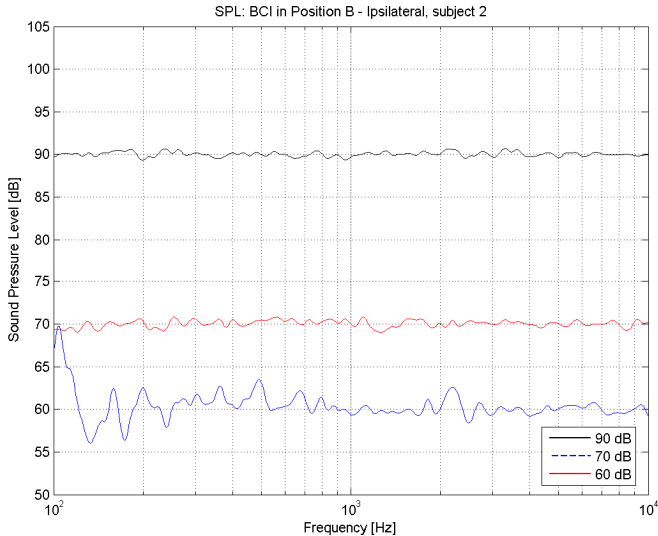
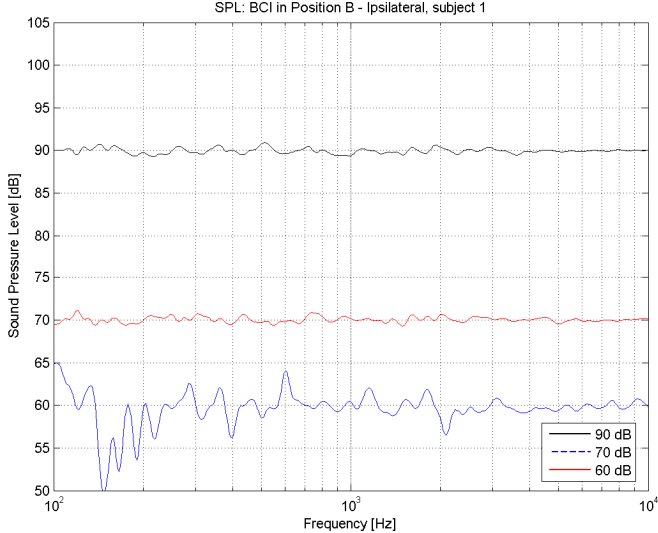
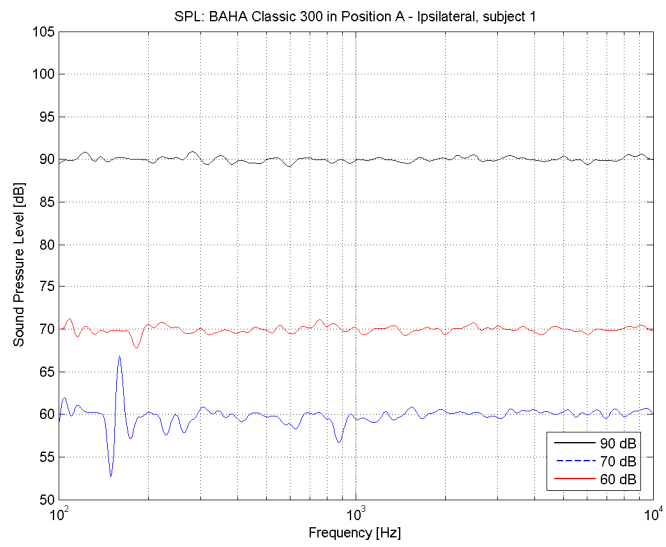
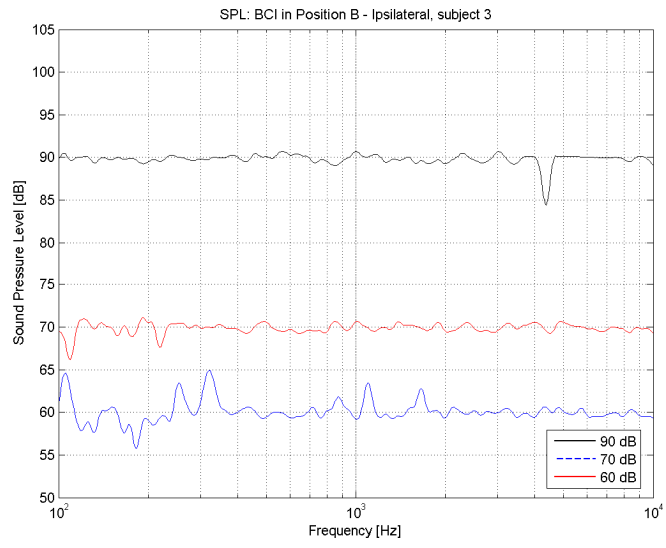


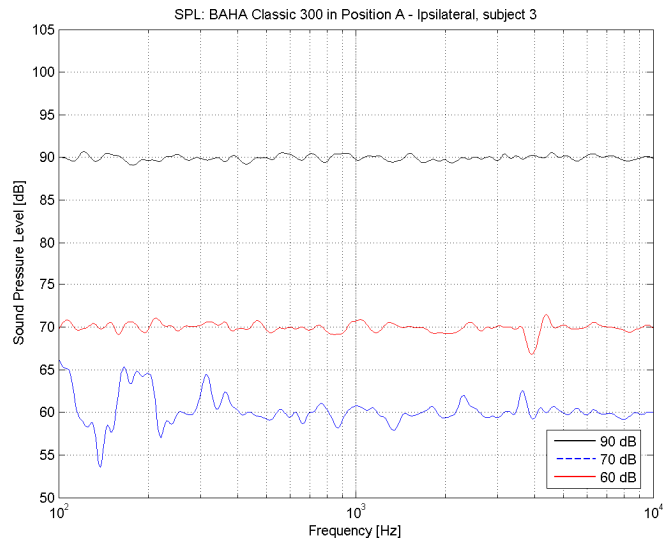
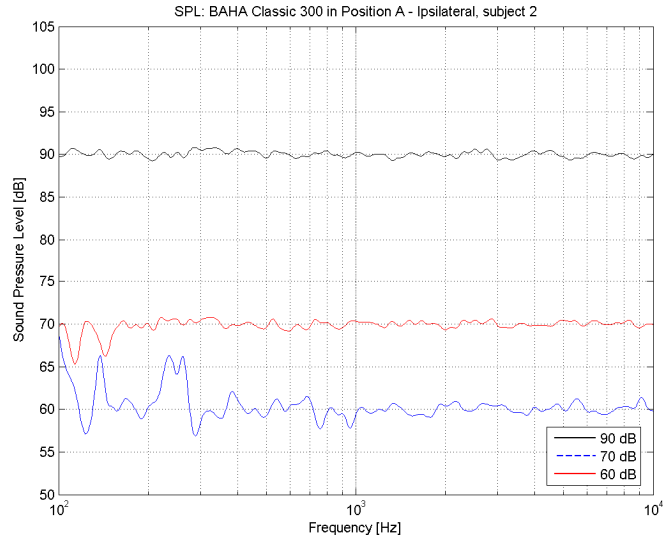
Figure 106: Block diagram view 5.

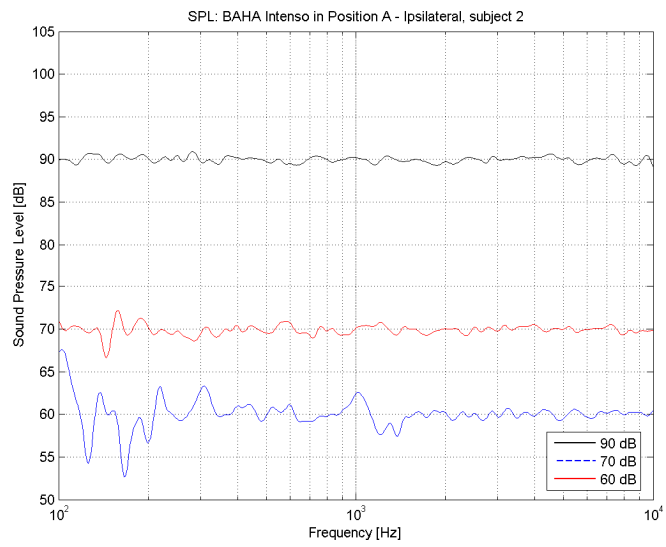
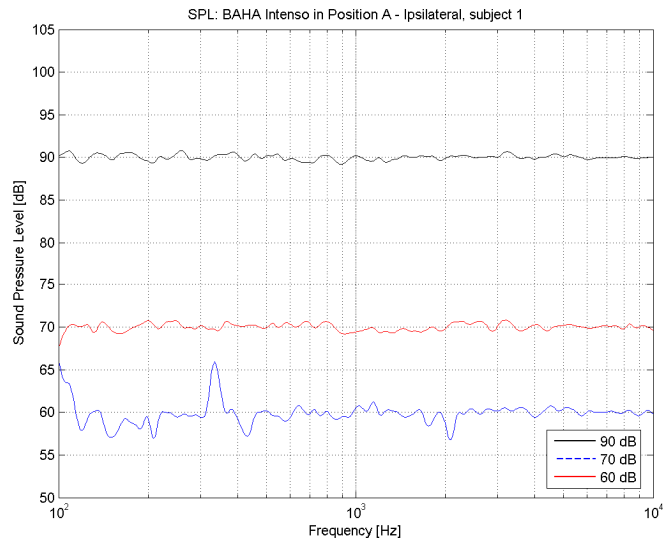
From the steps above, the measured data from any of the instrument's four traces can be transferred directly to the computer with no need of using the instrument's floppy drive. But one undesirable quality of the Agilent 35670A is that it returns more x-data points than y-data points, resulting in an uneven data array. This results in that the general loading command in MATLAB-command, "load('filename')", can not be used. Instead the command "textread('filename')" is used to import only the first 400 x- and y-data values, considering that a resolution of 400 lines is used.

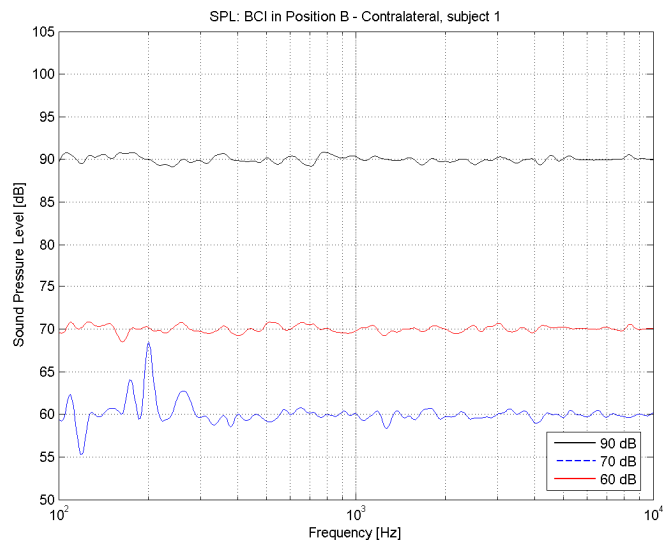
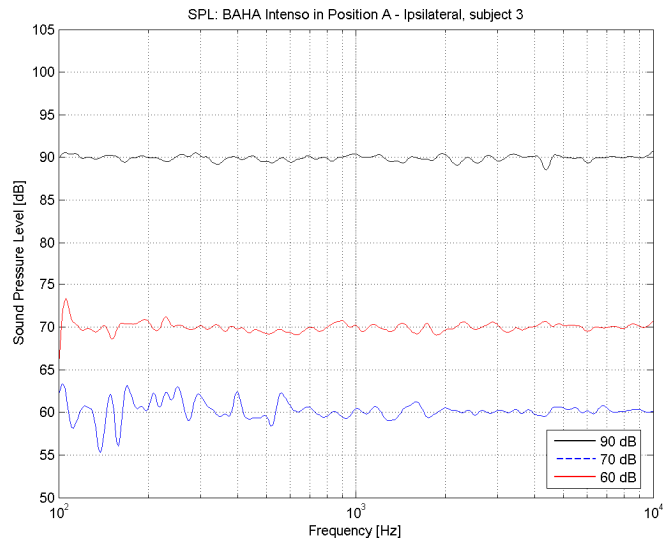
9 Appendix B

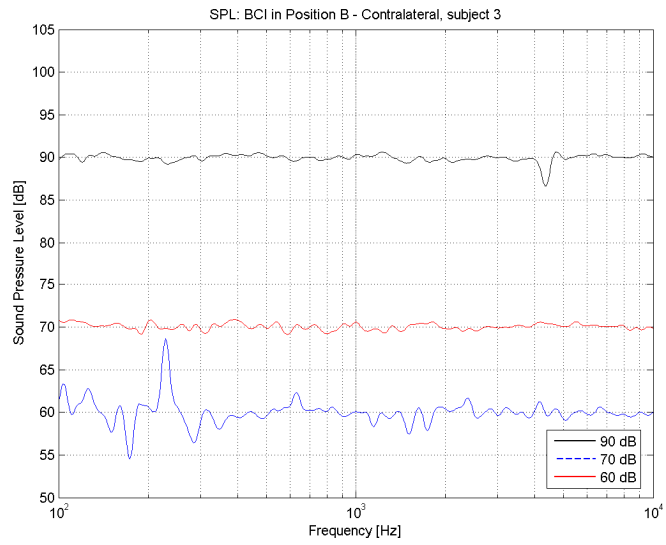
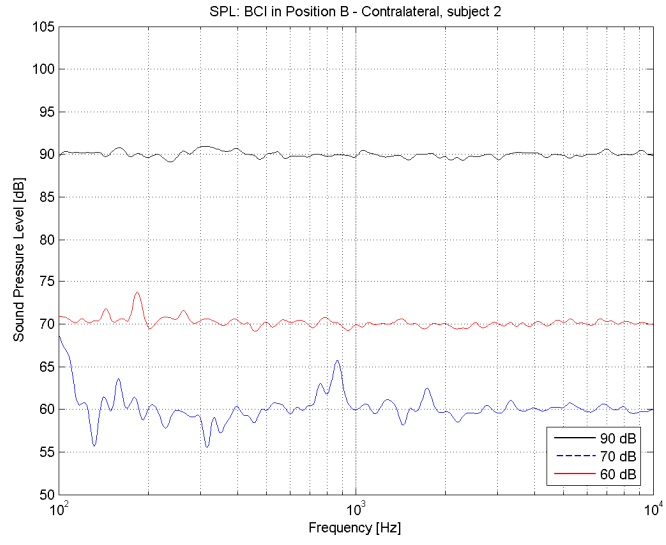


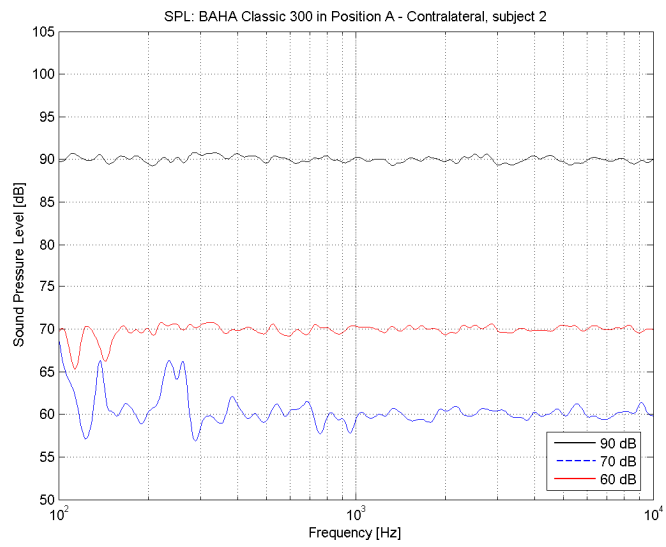
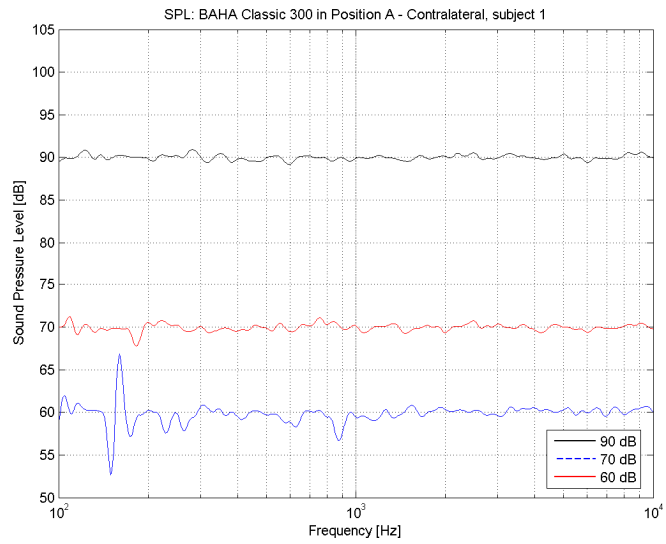


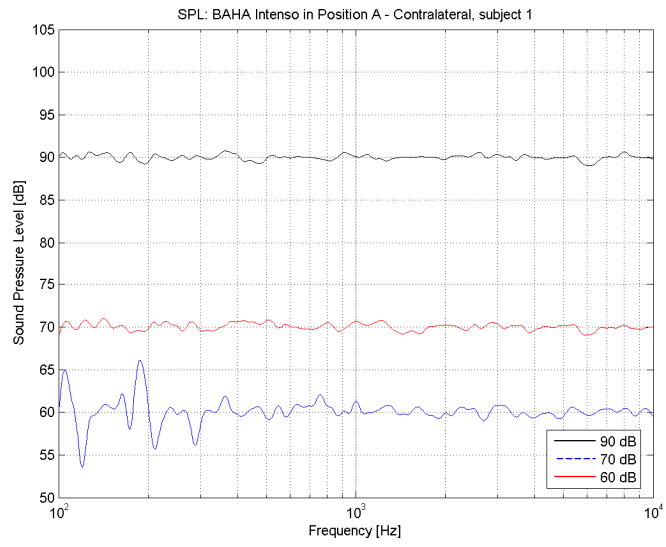
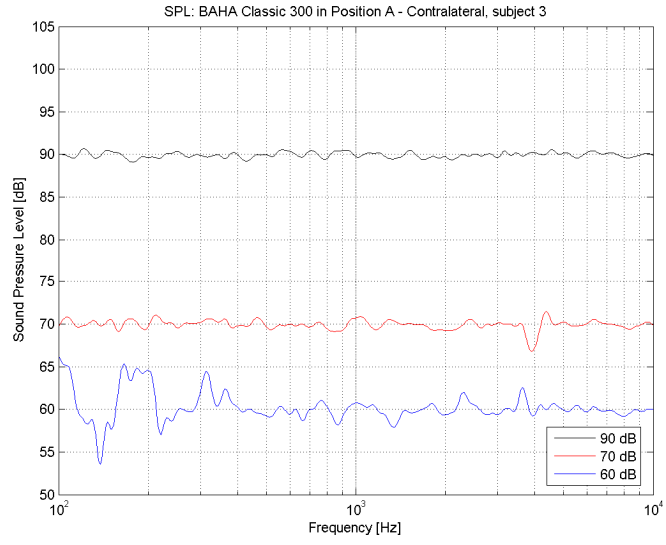




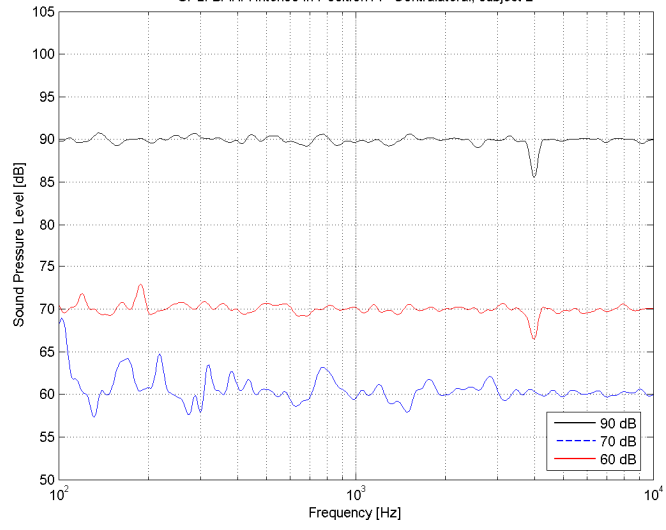








SPL: BAHA Intenso in Position A - Contralateral, subject 2



SPL: BAHA Intenso in Position A - Contralateral, subject 3

